



University of
Stavanger

Faculty of Science and Technology

MASTER'S THESIS

Study program/ Specialization:

Petroleum Geosciences Engineering

Spring semester, 2015

Open

Writer:

Abder Dahman

.....
(Writer's signature)

Faculty supervisor: Chris Townsend

External supervisor(s):

Thesis title:

The Vouraikos Valley: an example of rift segmentation in the Corinth Graben, Greece

Credits (ECTS): 30

Key words:

Greece
Peloponnesus
Gulf of Corinth
Vouraikos Valley
Normal Faults
Transfer Faults
Syn-rift Deposits

Pages: 88

+ enclosure: 88

Stavanger, 15/06/2015

Copy Right

By

Abder Dahman

2015

The Vouraikos Valley: an example of rift segmentation in the Corinth Graben, Greece

By

Abder Dahman, Bsc

Master thesis

Presented to the Faculty of Science and Technology

The University of Stavanger

The University of Stavanger

June 2015

Acknowledgements

I wish to express my sincere thanks to my supervisor Chris Townsend for the guidance in the field work and the support throughout this thesis. I am also grateful to my co-supervisor Alejandro Escalona for all the encouragement. I would like to thank my field partner Rizky Amanda Syahrul.

I place on record, my thanks to the sponsors of the field trips; Total and Lundin.

Finally I would like to take this opportunity to express my gratitude to my family and friends for all the support this semester.

Abstract

The Vouraikos Valley: an example of rift segmentation in the Corinth Graben, Greece

Abder Dahman

The University of Stavanger

Supervisor: Chris Townsend

The Gulf of Corinth is recognized as one of the most active rift systems in the world, the study area covers an onshore rift section on the southern flank of the gulf, the northern part of Peloponnesus. The area comprises inactive faults in the south and currently active faults on the north. The rift initiated 5 Ma, and has undergone several acceleration in the extension rate, northward fault migration, uplift and erosion. The deeply cut NNE Vouraikos Valley provide an exceptional study area of early rifting, sun-rift infill and normal faulting. North dipping faults with an overall east-west trend, dipping $40-50^{\circ}$, these normal fault has been described as continuous faults, traced from tip to tip point across the Vouraikos Valley, but fault investigation in the valley proved the opposite, there are several faults that terminates in the valley, such as Kerpini- and Dhoumena Fault that shows several hundreds of meters of fault displacement on the west, though on the east valley side there are no evidence for these major faults are crossing. Further faults show stepping in the valley and vertically displacement of the basement rock. However the northernmost faults, Mamosia Pirghaki-, Dhervini- and East Eliki Fault shows no sign of stepping in the valley, but these faults may all be currently active and these may yet to be further displaced. Transfer fault has been assigned the study area to explain the abrupt discontinuity of the faults across the valley, high angle fault underlying the valley structure, allowing the extension to be transferred between two adjacent normal fault that are undergoing differential displacement and strain. A three dimensional structural model of the area is presented to illustrate how the fault blocks interact with each other and shows the effect of transfer faults.

Table of Contents

Chapter 1	1
1.1 Introduction.....	1
1.2 Geological Framework.....	4
1.3 Previous Work.....	5
1.4 Fault Interaction.....	11
Chapter 2	13
2.1 Field Observation.....	13
2.2 Chelmos Fault.....	15
2.3 Kalavrita Fault.....	15
2.4 Roghi Mountain.....	16
2.5 Kerpini Fault.....	16
2.6 The West Basement Inlier.....	17
2.7 East Vouraikos.....	24
2.8 Souvardho Fault.....	24
2.9 Toriza Fault.....	25
2.10 East Basement Inlier Fault.....	26
2.11 Megha Spileo Fault.....	26
2.12 Dhoumena Fault.....	30
2.13 Dhoumena Fault 1.....	30
2.14 Dhoumena Fault 2.....	31
2.15 Psili Rachi.....	31

2.16 The Horst.....	35
2.17 Megha Spileo Fault 1 and 2.....	35
2.18 Tilted Basement.....	40
2.19 Mamousia Pirghaki Fault.....	40
2.20 Dhervini Fault.....	40
2.21 Eliki Fault.....	43
Chapter 3.....	47
3.1 Structural Interpretation.....	47
Chapter 4.....	56
4.1 3D Model Construction.....	56
4.2 Faults.....	56
4.3 Transfer Faults.....	61
4.4 Problem and Solution.....	62
Chapter 5.....	66
5.1 Discussion.....	66
5.2 Reconstruction of Cross-sections.....	67
5.3 East Section.....	70
5.4 West Section.....	73
5.5 Evolution History of the Study Area.....	75
Chapter 6.....	79
6.1 Conclusion.....	79
References.....	80

CHAPTER 1

1.1 Introduction

The Gulf of Corinth is located in the central Greece, separating the Peloponnesus peninsula in the south from the continental Greece in the north (fig. 1). The Gulf has a WSW-ENE trending graben structure, and is still active in the new evolving Aegean plate. This extension in the Aegean plate, as well as in the west Anatolian plate is a result of the different convergence rates between the NE subduction of the African plate, relative to the disrupted Eurasian lithosphere (Yaltrik et al., 1998; Matinod et al., 2000; Bozkurt, 2001), (fig. 2). Within the Aegean-Anatolian system the Corinth rift is described as the most active rifts by Armijo et al, (1999), and lately described as one of the most active rifts in the world by Ford et al, (2013). However, the relative role of each phenomenon is not yet fully understood, such as the period between the main Hellenic compression and the current faults extension, the link between regional Aegean extension and the N-S extension in the Corinth Graben and the uplift of the northern part of the Peloponnesus peninsula.

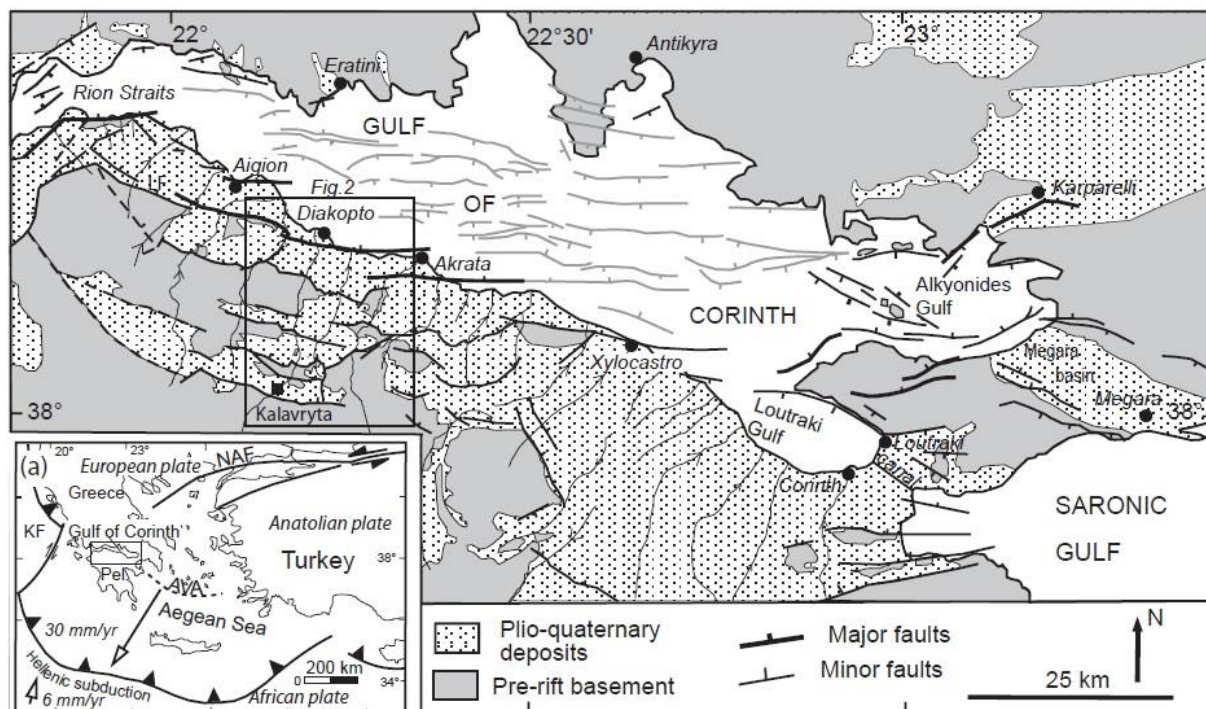


Figure 1 – a) Tectonic map of the Aegean region showing main plates and plate boundaries and the location of the Gulf of Corinth. b) Tectonic map of the Corinth rift showing principal faults, based on the work of Lyon-Caen et al. (2004), Moretti et al. (2004), Flotte´ et al. (2006), Ford et al. (2007a), Rohais et al. (2007a), Bernard et al. (2006), with boxed study area (Kalavrita-Diakopto).

The study area of this thesis is a valley structure called the Vouraikos Valley that is one of several NNE-SSW trending valleys on the southern margin of the Gulf of Corinth. The Vouraikos valley is approximately 20 km long, stretching from the village of Kalavrita to the coast city of Diakopto (boxed area in fig. 1). A series of dominantly north dipping normal faults occur on both sides of the valley. These normal faults are generally inactive early faults in the south and currently active faults of the Corinth rift in the north. The earlier inactive faults have been uplifted and deeply cut by erosion and provide a rare and exceptional study area of early rifting, syn-rift infill and normal faulting.

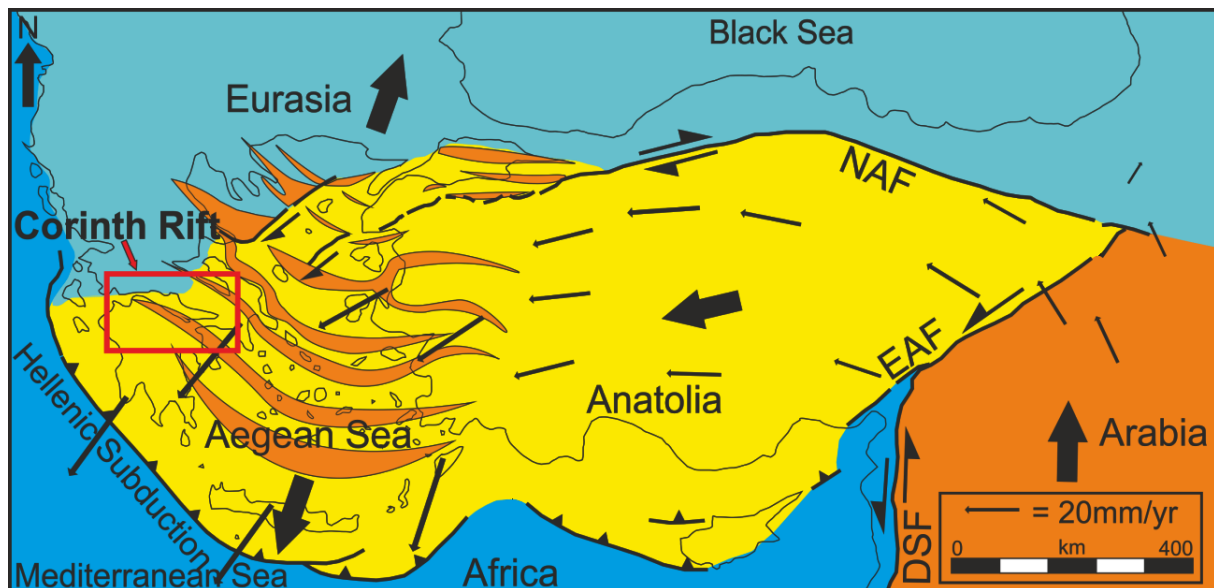


Figure 2 – Westward propagation of the North Anatolian Fault (NAF) into the northern Aegean plate, modified after Armijo et al., (1999).

The outcrops on the sides of the valleys are extremely well exposed with up to 1000 m of topographic relief. The preserved syn-rift deposits help in constrain the tectono-stratigraphic evolution of the Gulf; there has been for instance several extensively studies and mapping of the southern flank of the Gulf the last decades, e. g. Doutsos et al., (1988); Ori, (1989); Doutsos and Piper, (1990); Doutsos and Poulimenos, (1992); Flotté et al., (2005) and Ford et al., (2013). However a detailed structural and stratigraphic study of the outcrops is lacking, the geometry and orientation of the fault system and relationship between the different segments of the margin are still not completely understood, in spite of the excellent exposure, they are still a major challenge and open to interpretation.

The purpose of this thesis is to do a detailed study and examine the fault geometry in the Vouraikos Valley and evaluate the evidence of a transfer fault existing in the Valley. In addition, an evaluation of fault segmentation and syn-rift deformation was conducted so we can gain a better insight into the fault evolution, sediment transportation and accumulation, and further it will provide a better understanding in seismic study and interpretation of

subsurface structures, for example graben structures in the North Sea. The result is going to be presented as a 3D geological model with mapped fault, unconformity between the basal carbonates and the clastic sediments and the general bedding of the sediments, a sketched evolution history will also be presented to help explain the development of the graben.

1.2 Geological Framework

The active rift is WNW to ESE oriented gulf, about 100 km long (Ford et al., 2013). The extension rate and geometry is related to a combination of back-arc extension due to the NE subduction of the African plate at the Hellenic Trench (McKenzie, 1972, 1978; Doutsos et al., 1988), in addition the lateral propagation of the Anatolian plate along the dextral North Anatolian Fault (Armijo et al., 1999; Jolivet, 2001). The Corinth rift is the most active in the Aegean-Anatolian plate system with a general E-W to NW-SE trending rifts that lie between the tip of the SW propagating North Anatolian Fault and the dextral Kephallonia Fault to the west (Armijo et al., 1999), (Fig. 2). The rifting of the Corinth is estimated to have started in the Pliocene, ca. 5 ma. This dating is mainly based on the micro-paleontological dating, Ford et al., (2013). Radiometric dating presented coherent ages as well; $2,62 \pm 0,8$ and $4 \pm 0,4$ Ma, Collier and Dart (1991).

The faults offshore from south to north flank of the gulf included the East Eliki Fault record an accumulation heave of 3,4 km, a value of 6,4 – 7,7 km was taken as a minimum total extension according to Ford et al., (2013). A similar estimation (5-13 km) was presented by Bell et al., (2011). The estimation of Ford et al., (2013) gave a long –term extensional rate of 1,3 - 1,5 mm a⁻¹ over a 5 Myr of rifting. However the present day extensional rate is recorded to be 10-16 mm a⁻¹ (Davis et al., 1997, Clarke et al., 1998, Briole et al., 2000, Avallone et al., 2004, Bernard et al., 2006). If the current extensional rate is to be applied to the 5 Myr of rifting history, it would result 50-80 km of a total rift extension. The response is several extensional rate changes; this has been reported by Leeder et al., (2008). Our study area has experienced the following extensional rates; 0.6 - 1 mm a⁻¹ (5 - 1,8 Ma), 2 - 2,5 mm a⁻¹ (1,5 - 0,7 Ma) and 3,4 - 4,8 mm a⁻¹ (0,7 - 0,5 Ma). So the Corinth Rift records a significant increase in extensional rate during the rifting history. Yet there is still uncertainty regarding the displacement of East Eliki Fault and the age of onshore faults and offshore fault.

Along the southern margin of the Corinth rift, north Peloponnesus, early rift sediments and normal faults have been uplifted to more than 1000 m altitude and deeply dissected by north flowing river through time, resulting several NNE to SSW valleys with well exposed

extensional half-graben structures (Doutsos and Poulimenos, 1992), bounded by north dipping normal faults, these valleys are an exceptional natural laboratory for the study of the early rift history in.

The lithology exposed can basically be divided in two groups; the pre-rift basement composed of Mesozoic pelagic carbonates and the overlying non-marine syn-rift deposits dated to Pliocene to recent time. The marine basement unit has not been detailed mapped, this unit is complex and highly deformed and this is again related to the continental collision and overthrusting during the middle Mesozoic. Furthermore description of Collier and Jones (2004) is that the thrust sheets strike perpendicular to the younger rift faults, these Mesozoic internal structures are not mapped, but are recognized to play a role in controlling, for example, the segmentation of the rift.

The overlying non-marine deposits are built up by several events, but can be simplified to three sections, the first one is composed of alluvial to lacustrine formations, what characterize this section is the massive pebble and cobble conglomerates within it. This section is up to 800 m thick and is dipping south, the clast composition suggest that these early rift sediments derived from the uplift and erosion of the footwall. The second section is fluvial formation composed of conglomerate-sandstone, and the third and upper section is a significant progradational alluvial fan formation and Gilbert-type fan deltas, in this phase a large volume of coarse sediments where transported through the rift from the south (Jackson et al., 1982; Doutsos et al., 1988; Collier et al., 1992; Doutsos and Poulimenos, 1992; Dart et al., 1994; Collier and Jones, 2003; Ford et al., 2013).

1.3 Previous work

There have been several extensive studies of the Corinth Rift during the last decades covering different geological aspects (e.g. Ori 1989; Doutsos and Piper 1990; Armijo et al., 1996; Sorel 2000; Collier and Jones 2004; Bell et al., 2008; Ford et al., 2013).

Doutsos and Piper (1990) proposed that the normal faults are of listric structure, however most researchers disagree and argue that there is not enough evidence and favor a model of a planar faults (e.g. Westaway 2002; Moretti et al., 2003; Rohais et al., 2007; Ford et al., 2013). In 1992 Doutsos and Poulimenos suggested that the surface of southernmost normal fault were linked to a low angle fault at deeper crustal level (>7km deep). Sorel (2000), Flotté and Sorel (2001) and Flotté (2002) again suggested an underlying major north dipping crustal detachment fault, the “Khelmos (or Chelmos) detachment” (>100 km long), figure 3.

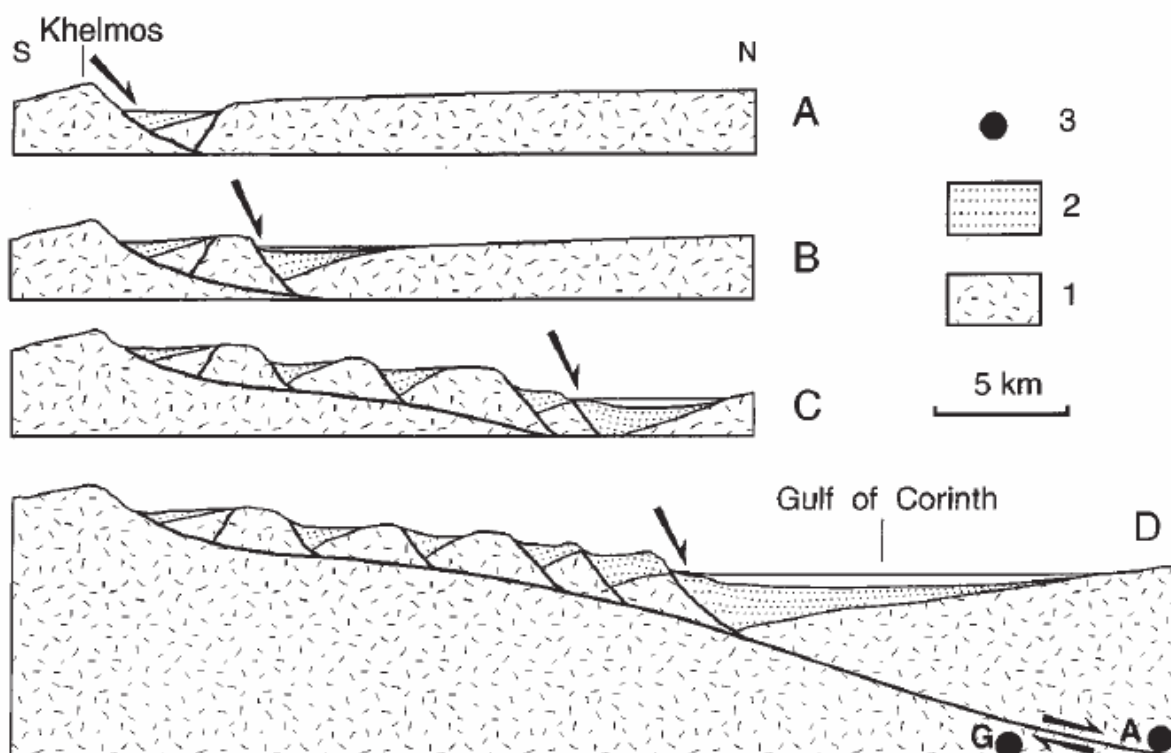


Figure 3 - Evolution and development of the Gulf of Corinth during 4 steps. A) Early rift along the active Chelmos fault. D) Present day showing the progression of the Chelmos detachment fault. Modified after Sorel (2000)

The northern part of Peloponnesus is undergoing both extension and uplifting but at a different rate, in its eastern and western part (Pirrazoli et al., 2004; Ford et al., 2013). There are various suggestions to the driving mechanisms behind it that led to a considerable debate on whether the Corinth is symmetrical or asymmetrical. Brooks and Forentinos (1984) describe the Corinth as an asymmetrical half-graben structure, almost two decades later

Stefatos et al., (2002) propose the same description but more complex, a composite of asymmetrical graben structures that is north dipping on the east and south dipping on the west part of northern Peloponnesus. Moretti et al., (2003) do not agree with this description and suggest that the graben structures here are symmetrical. However the majority of all the researchers of the Corinth agree on the proposal that the fault activity has shifted from south to north Peloponnesus with time.

There is also a vast variety on descriptions of the syn-rift structures and sedimentology of the inactive faults of the rift domain. Ori (1989) is among the first to present a detailed division of the onshore syn-rift succession. Collier and Jones (2004) presented an interpreted field map of the fault and sediments distribution around the three river valleys, The Vouraikos, Ladhopotamos and Kratis (fig. 4). The latest paper by Ford et al., (2013) presented a detailed field map of the same area including the Kerintis River to the west as well (fig. 5).

Both the interpreted field maps present five main north dipping fault systems, from the south, Kalavrita Fault, Kerpini Fault, Dhoumena Fault, Mamousia-Pirgaki Fault and Heliki Fault. In addition it is claimed that all the faults can be traced from tip point to tip point according to Ford et al., (2013) interpretation.

The Kalavrita Fault exposure is limited, but there is a noticeable topographic relief that suggest a major W-E fault. In Ford et al., (2013) map the fault stretches from Krathis River in the east and continues across the Vouraikos River, while in Collier and Jones (2004) geological map (fig. 4) the Kalavrita Fault is displayed over three kilometer in the Vouraikos River.

The Kerpini Fault is traced for 9,6 km in Ford et al., (2013) geological map, from the west it starts in the Kerintis River then it's displayed 850 m by left stepping in the Vouraikos River, the fault links eastward with Tsivoli Fault across a right stepping relay fault (Kastraki Fault) which is underlying the Ladhopotamos River. Collier and Jones (2004) interpretation of Kerpini Fault matches the latter description but excluded any linkage between Kerpini- and Tsivoli Fault. In the center of Kerpini Fault Block in Ford et al., (2013) geological map, pre-rift carbonate is exposed on both sides of the Vouraikos River (fig. 5), this exposed basement has been interpreted as a pre-rift inlier or a paleo-surface, while in the study of collier and Jones (2004) the same exposed basement is assigne faults to the uplifted basement outcrops (fig.4).

The Dhoumena Fault is traced for 13 km in the Ford et al., (2013) geological map, the fault is dextrally displayed by 600 meter by a cross-fault in the Vouraikos River and continues

through the Ladhopotamos River in the East (fig. 5). Jones and Collier interpretation terminate Dhoumena fault in the Vouraikos River Valley, in addition the Dhoumena Fault seems to bend on both maps close to Dhoumena village as possible stepping in the Dhoumena fault.

The Mamousia-Pirgaki Fault system is 25-28 km long and comprising three hard-linked segment according to Ford et al., (2013); Pirgaki, Mamousia and Voutsimos. Pirgaki and Mamousia are linked by Kerintis fault in the Kerintis River, between Vouraikos River and Ladhopotamos River the fault is bounded by several N-S cross-faults, and further to the east the fault connects perpendicular to the Voutsimos Fault in Krathis River in Ford et al. (2013) field map. The Mamousia-Pirgaki orientation in Collier and Jones (2004) matches the interpretation of Ford et al., (2013) but fault stepping is interpreted less angular.

The Eliki (or Heliki) Fault is the last onshore fault to the north, separating the uplifting of the Peloponnesus peninsula from the subsiding Gulf. The Eliki fault is divided between West and East in Ford et al. map and they overlap across the Kerintis River, and the same applies to Collier and Jones (2004) interpretation.

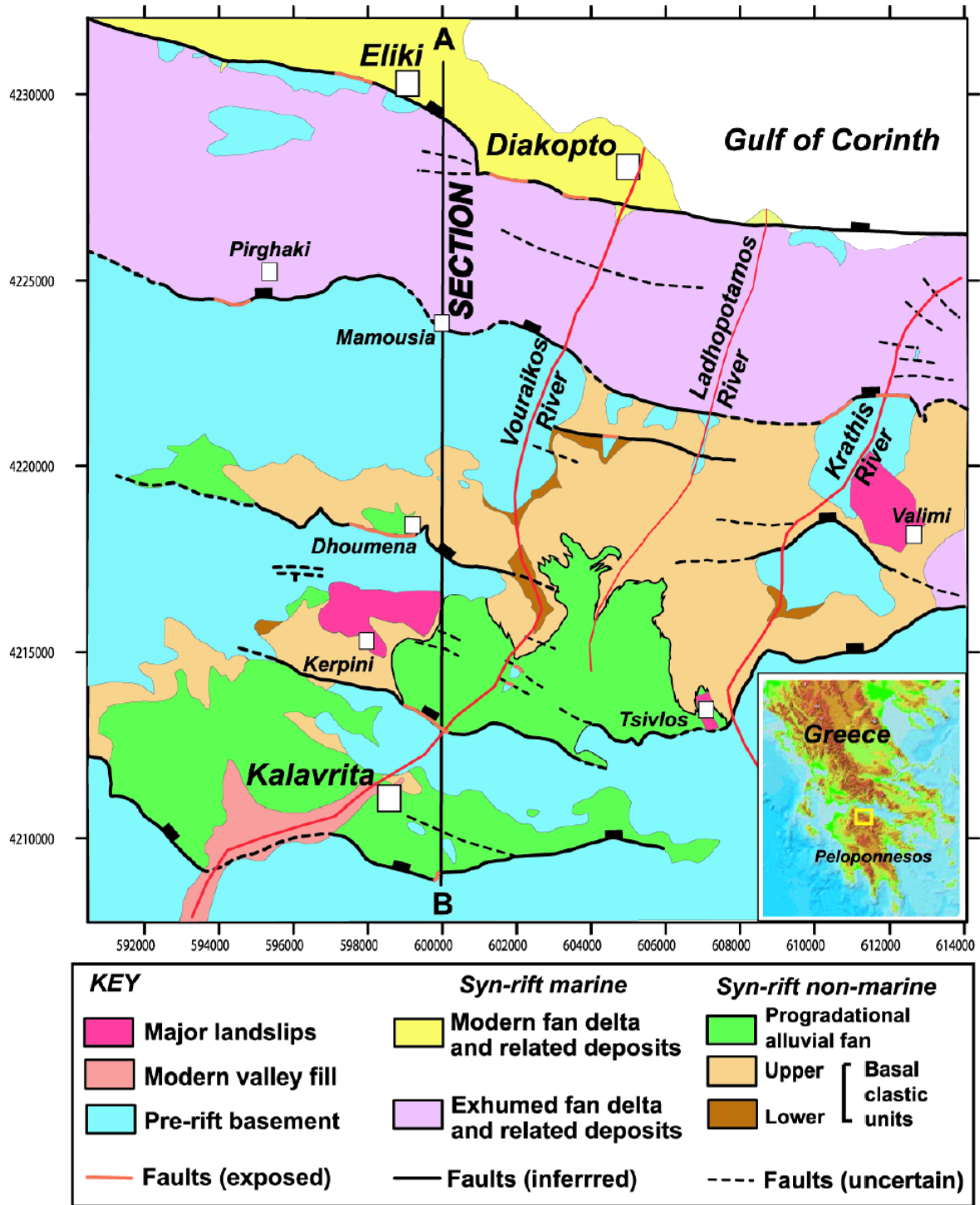


Figure 4 – Geological map of south flank of the Corinth Gulf, the area from Kalavrita to Diakopto, modified after Collier Jones (2004).

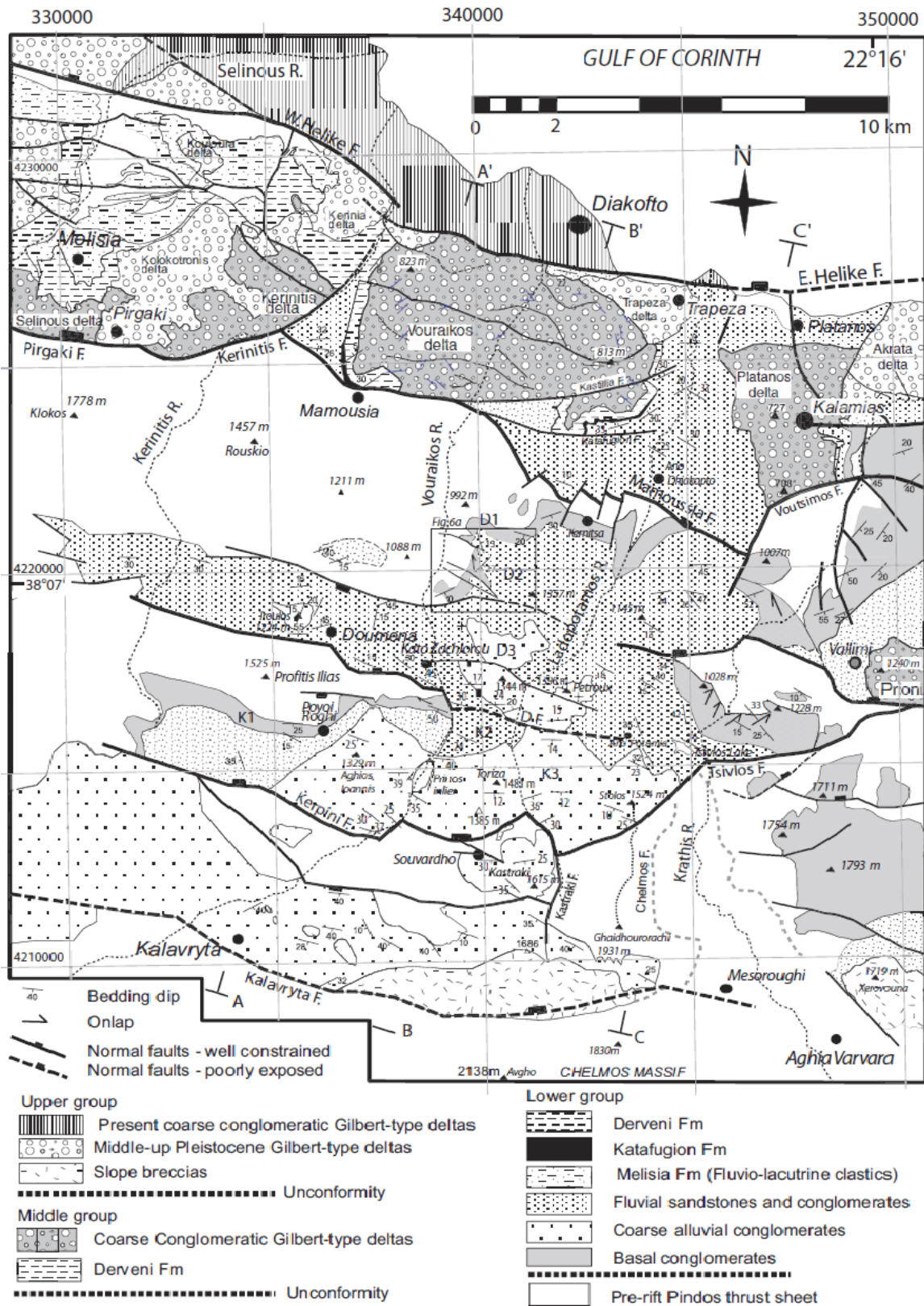


Figure 5 – Geological map of the south flank of Corinth Gulf, the area from Klavrita to Diakopto, modified after Ford et al., (2013).

1.4 Fault interaction

Rift zones are generally segmented at different scales; segments are the transient features in fault evolution in rift zones, as the faults grow and interact they may link to form larger structures (Macdonald and Fox, 1983; Pollard and Aydin, 1988; Dawers and Anders, 1995; Koukouvelas et al., 1999). There are mainly two types of interaction between two or a group of fault segments, the interaction may progress into a relay ramp (fig. 6 a) or accommodation zone which consists of wide area between extensional structures, such as normal faults, graben and extensional fractures (Peacock et al., 2000), (fig.6). This type of interaction is referred to as ‘soft linkage’ (Walsh and Watterson, 1991).

The second type of fault interaction is that the relay ramp becomes faulted, and the result is a Transfer fault (fig.6 b). Transfer fault is a sub-vertical and transtensive fault that dips at high angle and transfer two adjacent fault that are undergoing differential displacements and strains. The latter fault interaction represents a ‘hard linkage’ (Walsh and Watterson, 1991).

Both types of fault interaction are found in rift zones, they have been described for instance in the Rio Grande Rift (Sherman, 1978; Mack and Seager, 1995), the East African Rift System (Morley, 1988; Ebinger et al., 1989; Morley et al., 1990; Nelson et al., 1992), the Suez Rift (Moustafa, 1996), and the Reconcavo Graben (Milani and Davidson, 1988), fig. 7.

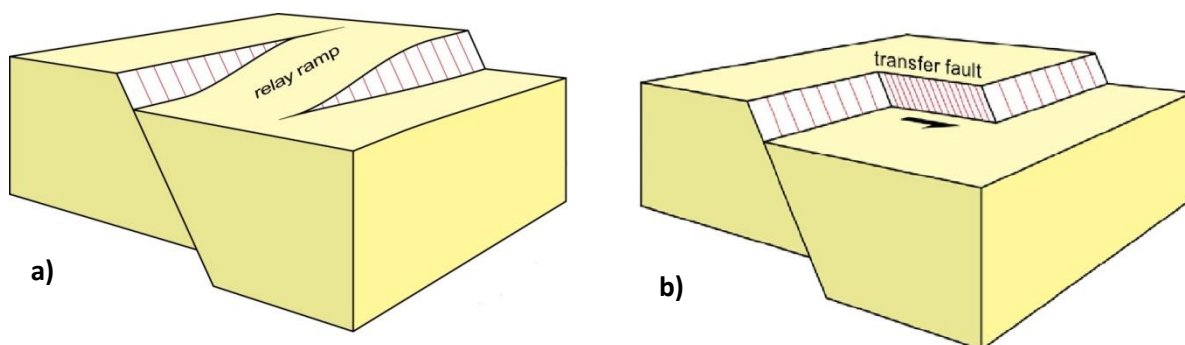


Figure 6 - Schematic sketch of transfer zones, a) relay ramp between two overlapping normal faults, b) extension transfer from a normal fault to another normal fault through a transfer fault, modified after Burn, J.P., *Tectonics – Extension systems*, 76-79.

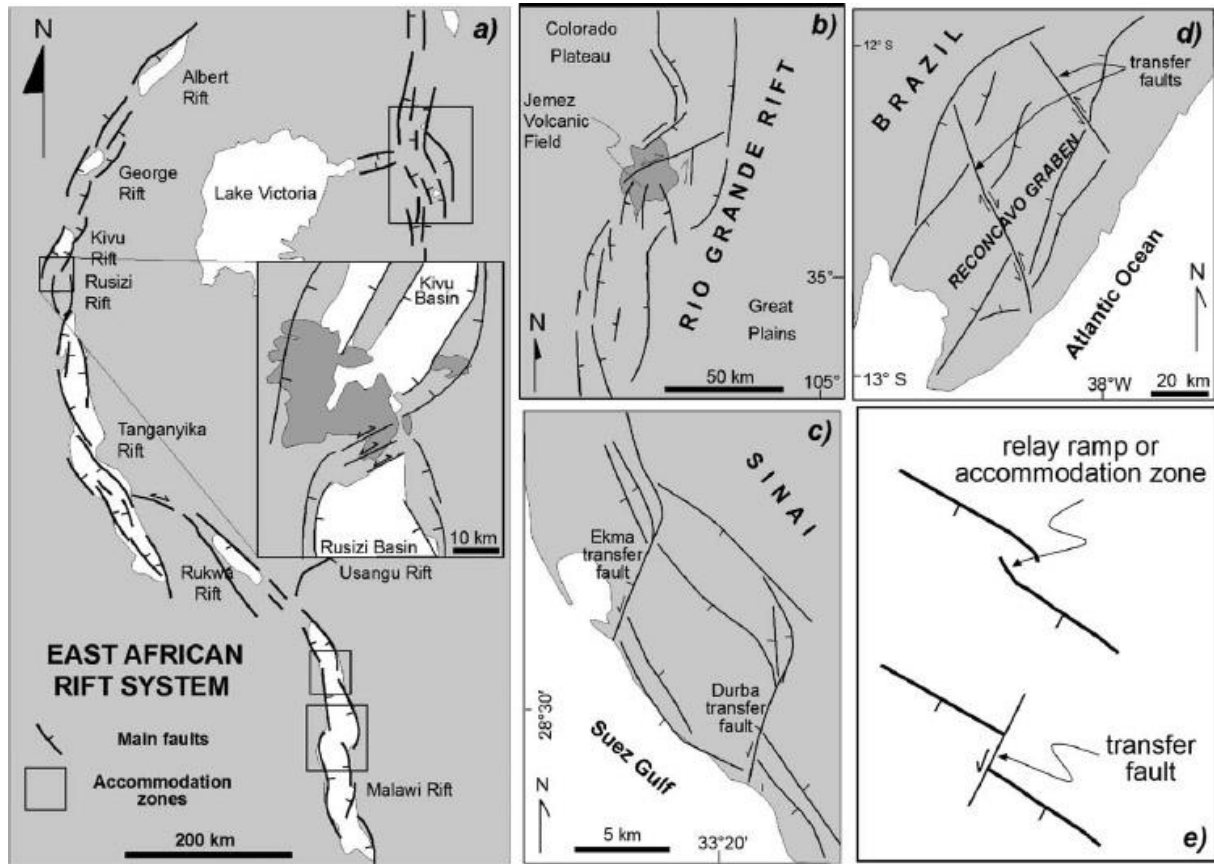


Figure 7- Types of interaction between extensional structures at various rift zones; a) Relay ramps in East African Rift System, modified after Ebinger (1989), b) Rio Grande graben, modified after Aldrich (1986), c) transfer faults in the Suez Rift, d) Atlantic margin of Brazil, e) schematic view of relay ramps and transfer fault in extensional domains.

CHAPTER 2

2.1 Field observation

This study is based on a five weeks fieldwork that was carried out in three separate time periods in the Kalavrita-Diakopto region (fig.1), the first week was a field trip and a part of a geological 3D modeling course. A geological map was compiled showing the main structural elements as faults and unconformities on a 15 x 25 km area. The second field trip was an independent and detailed mapping of the exposed structures on both Vouraikos valley sides. After processing the field data a third and final field trip was carried out for further mapping of the key areas in the Vouraikos. A special focus was aimed at the Roghi Mountain and its relationship with the rest of Kerpini fault-block and the horst structure on the north side of Dhoumena fault-block. Each exposed faults on the Vouraikos Valley was carefully measured and projected to the opposite side of the valley, the projected area was then investigated for any fault evidence and was assigned a likelihood of each structure crossing the valley accordingly.

The data collected from the field was done by measurement of strike and slip of faults, dip angle of sediments, lithology description, photos and GPS points. The post processing of the field data was processed further in 3D modeling on Petrel E&P 2014, satellite pictures and ArcGIS maps. A detailed geological map of the study area was presented with fault and sediment distribution (fig. 8).

For the two southern most faults, Chelmos Fault (CF) and Kalavrita Fault (KF) the interpretation is modified after the observation and analysis of Finnestad (2013) who presented a detailed study of these two faults.

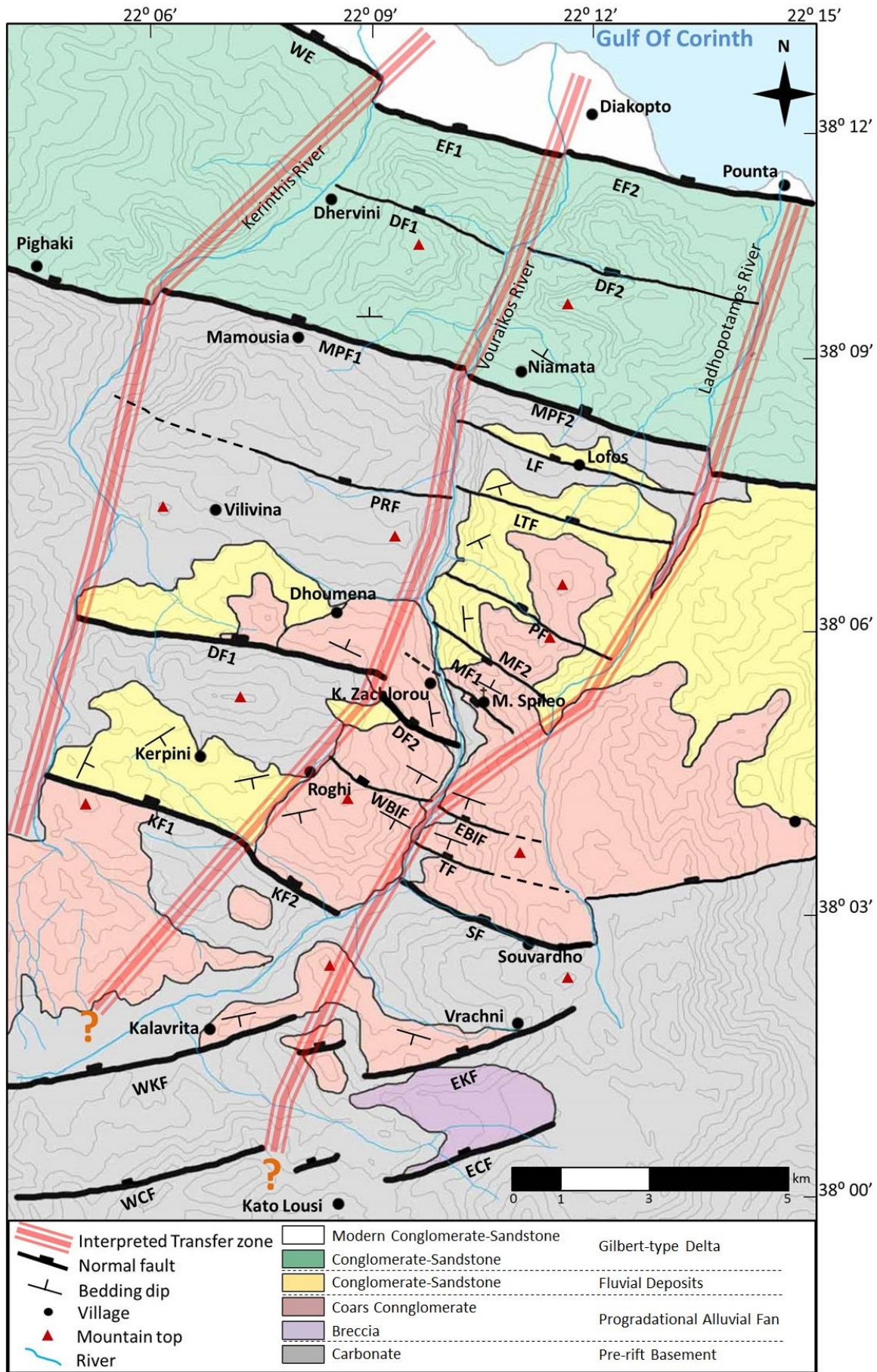


Figure 8 – Interpreted geological map generated from field observation and analysis of the study area, the map is the boxed area in Figure 1.

2.2 Chelmos Fault

The Chelmos Fault is the fault that is related to the north dipping crustal detachment, as mentioned in section 1.3. The Chelmos Fault is a normal fault dipping 45° and striking 85°NE , the fault can be traced for 13,5 km. it's comprised of three fault segments, relatively referred to as West Chelmos Fault (WCF) and East Chelmos Fault (ECF) with a minor fault step in between. The East Chelmos Fault is 6,5 km and is right stepping to West Chelmos Fault south-east of Kalavrita Village, fig. 8. The transfer zone between the three fault segments reveals a slope like feature that has similar dip as the faults, but the dip of the slope is almost perpendicular relative to the faults, the transfer zone resemble the characteristics of a relay-ramp, as explained in section 1.4.

The uplifted footwall block for both West- and East Chelmos Fault is consisting entirely of carbonate basement rock. For the East Chelmos Fault the hangingwall is made up by $20\text{-}25^{\circ}$ south dipping breccias, while the West Chelmos Fault has no preserved syn-rift sediments, only exposed carbonate basement rock, fig. 8.

2.3 Kalavrita Fault

The Kalavrita Fault can be traced for 14 km, from Ladhopotamos River in the east, crosses the Vouraikos River and dies out close to Maneseikos River in the west outside the study area. The Kalavrita Fault resembles the Chelmos Fault geometry; it comprises three fault segments; two extensive faults, West Kalavrita Fault (WKF) and East Kalavrita Fault (EKF) with a minor fault step in between, fig. 8.

The Kalavrita fault segments have a general dip of 45° and strikes 88°NE . The uplifted footwall of East Kalavrita Fault consists of carbonate basement overlain by breccia from E Chelmos Fault Block. The syn-rift succession is making up the hangingwall, 23° south dipping conglomerates unconformable overlying carbonate basement rock.

The East Kalavrita Fault right steps into the West Kalavrita Fault east of Kalavrita Village, fig. 8, the West Kalavrita Fault Block is much wider than the East Kalavrita Fault Block and comprises massive conglomerates together with some lacustrine deposits, and these sediments are unconformable overlying the basement and are dipping south with 22° , towards the fault plane. The rock exposed on the footwall is made up by carbonate basement from the West Chelmos Fault Block.

2.4 Roghi Mountain

The structural high of Roghi Mountain is controlled by three north dipping normal faults, from the south; Kerpini fault 2 (KF2), West Basement Inlier Fault (WBIF) and the Dhoumena Fault 2 (DF2), all the sediments that build up the Roghi mountain are south dipping into the fault plane, fig. 9.

2.5 Kerpini Fault

The Kerpini Fault can be traced for 7,2 km from The Vouraikos River on the East to The Kerinthis River in the West, fig. 9. The name Kerpini Fault was given due to its close location to the Kerpini Village, the Kerpini Fault shows an abrupt change in lithology and significant topography relief that support the existence of the fault, the fault plane is not well exposed, so a dip of 40-45°N was assigned, the strike of the fault is 120 SE. The Kerpini Fault has a clear step in the Roghi Valley, south of the Roghi village. The fault is described as two fault segments in this thesis, from the west; Kerpini Fault 1 (KF1) and Kerpini Fault 2 (KF2), fig. 9. In addition there is a sharp facies change across the Kerpini Fault block, the Roghi Mountain consists of south dipping alluvial conglomerates, immediately west of the Roghi Valley the sediments are much finer as it consists of south-east dipping fluvial conglomerates-sandstones, fig. 9. The basement carbonate is far more exposed and elevated west of Roghi Mountain and can be observed at the footwall of Dhoumena Fault 1 at a height of 1500 m, the highest carbonate basement was observed at 800 m at the footwall of Dhoumena Fault 2, south of Ano Zachlorou.

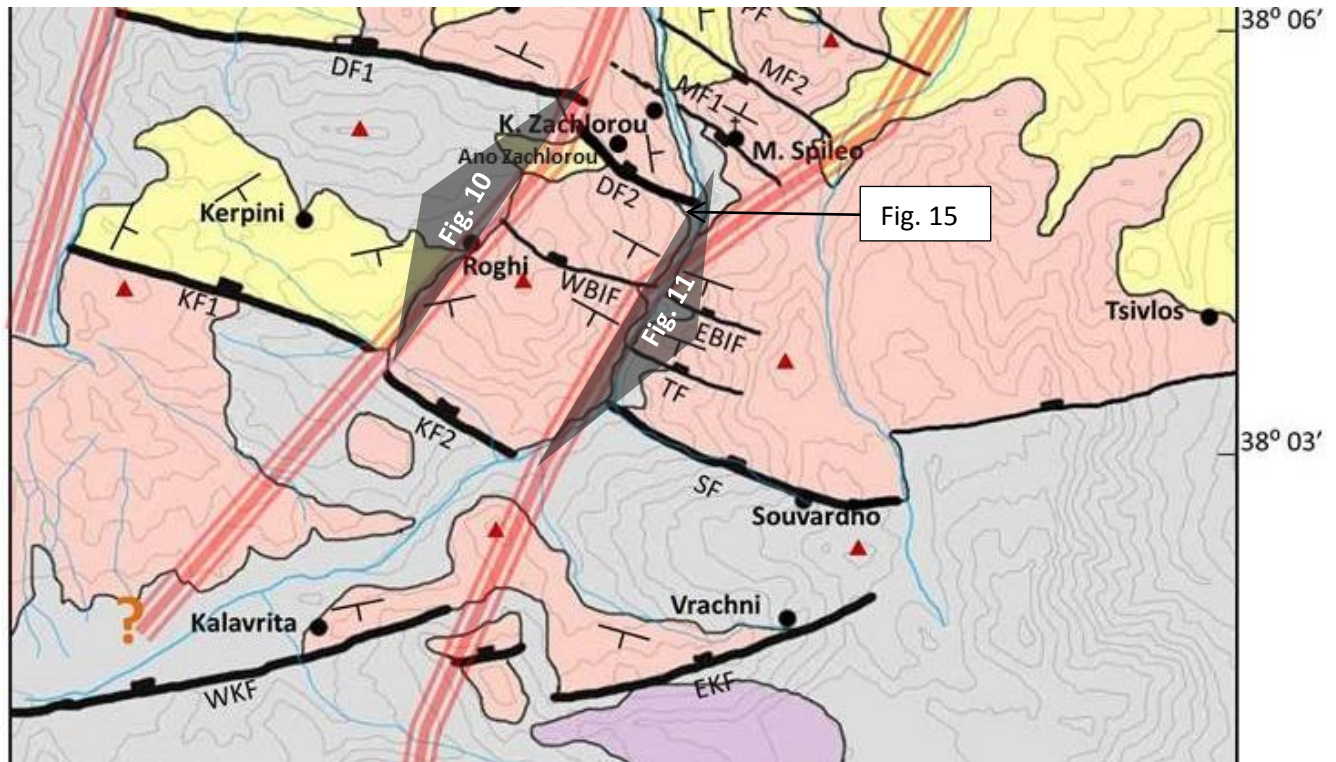


Figure 9 – Section of the geological map (fig. 8) to highlight the view of the profile pictures (fig 10, 11 and 15).

2.6 The West Basement Inlier Fault

The Roghi Mountain is highly eroded on the east and on west, within the valleys of Roghi and Vouraikos. Looking from the west (fig. 10), the mountain reveals two dip changes, the first sediments are dipping into kerpini Fault 2 with a dip 20° , close to the Roghi Village the sediment beds have a notable dip change from 20° to approximately $25-30^{\circ}$, the second dip change marks also a lithology change, from coarse conglomerates to finer conglomeratic-sandstone sediments. The finer sediments flatten out and onlaps onto the footwall of Dhoumena Fault 2 (fig. 10), the flat sediments are however not completely horizontal, but have a slightly south dipping angle of $5-10^{\circ}$.

When looking from the east (fig. 11), the structures observed on the west Roghi Mountain can be traced across the mountain. There is a dip change along the strike of the interpreted West Basement Inlier Fault (WBIF) that aligns with dip change on the west, the hangingwall of the fault is highly covered by late syn-rift fans, yet there was a clear observation of the “flat sediments” on the footwall of Dhoumena Fault 2 (fig 11). Closer investigation of West Basement Inlier Fault showed further structures that enforce the fault theory across Roghi Mountain; by following the railway in the Vouraikos along the Roghi Mountain from north to south a clear lithology change was observed from coarse conglomerate to basement carbonate, fig. 12. The basement carbonate was last observed at 670 m in the footwall of West Basement

Inlier Fault overlain by unconformable conglomerate (fig. 13). The basement outcrop was traced for 80 m before it ended unconformable with 20° south dipping conglomerates, fig. 14. A small outcrop of basement was observed further north on the hangingwall of West Inlier Fault partly covered by the late syn-rift fans, immediately on the footwall of Dhoumena Fault 2, fig 14 (marked on fig. 9).

Roghi West

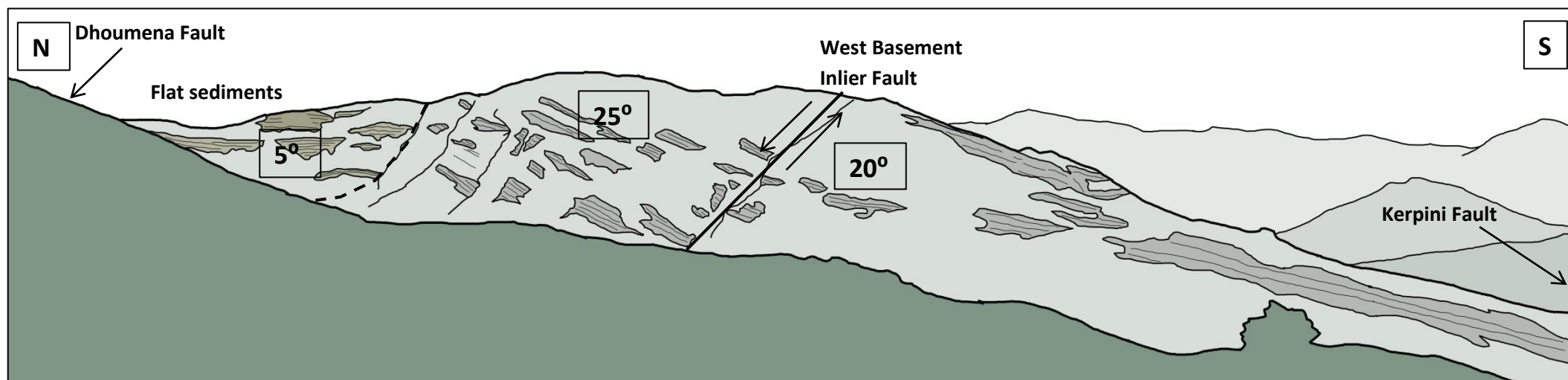


Figure 10 – Roghi Mountain, looking east, across the Roghi Valley.

Roghi West

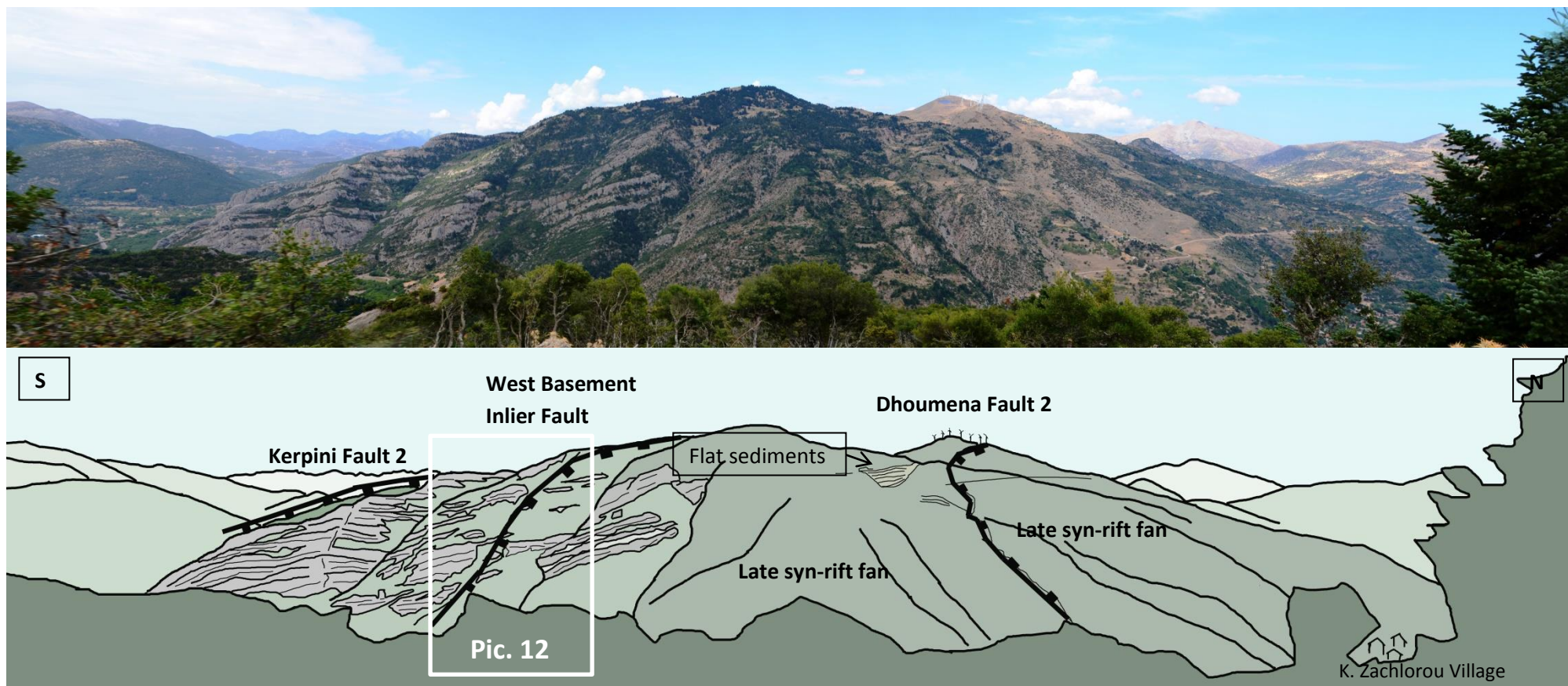


Figure 11 - Roghi Mountain, looking west across the Vouraikos River Valley.

West Basement Inlier Fault

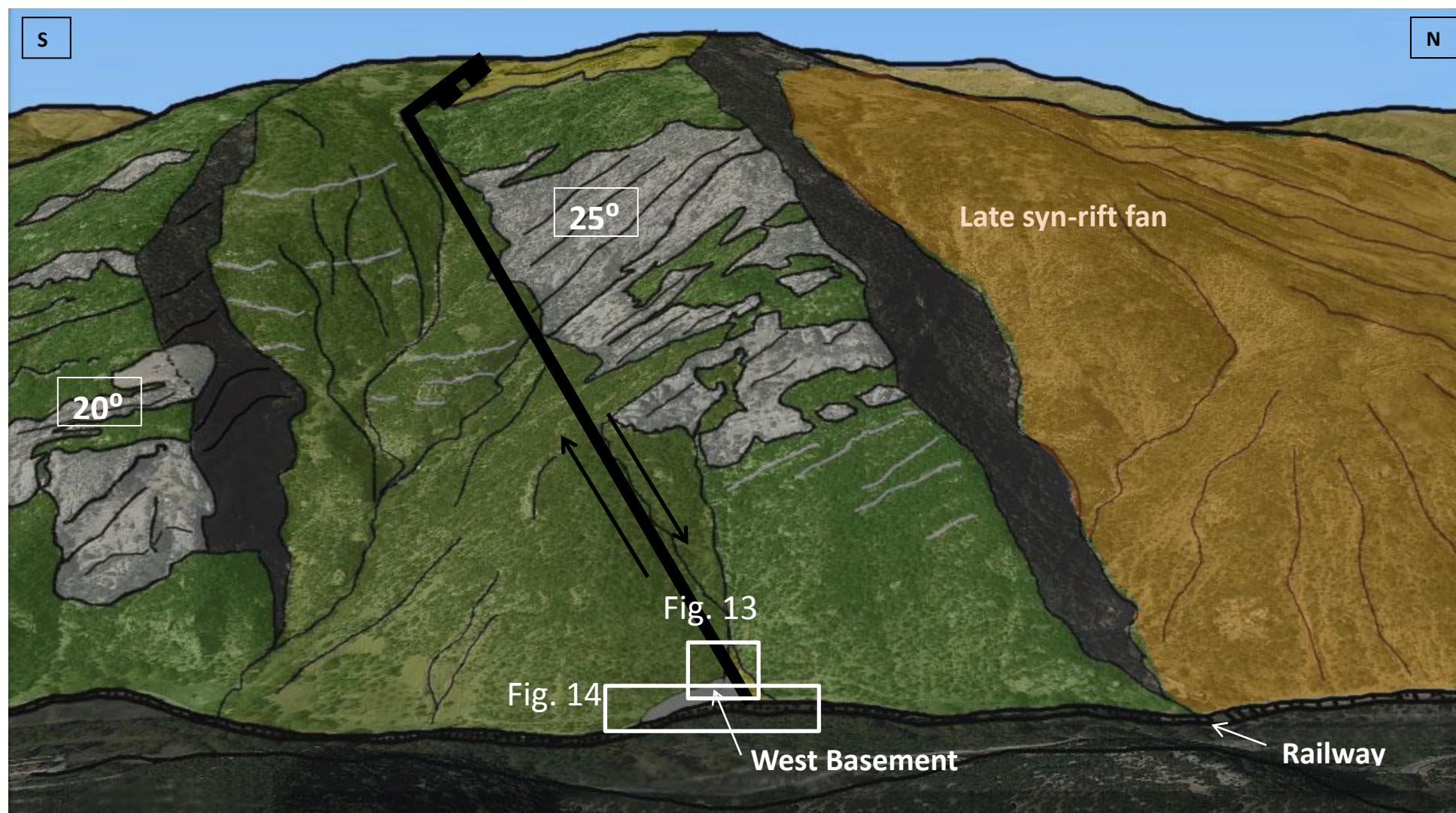


Figure 12 – West Basement Inlier Fault in Roghi Mountain, showing the dip change along the fault, the hanging wall is covered by late syn-rift fan. Uplifted basement in the footwall are marked and shown in figure 13 and 14.

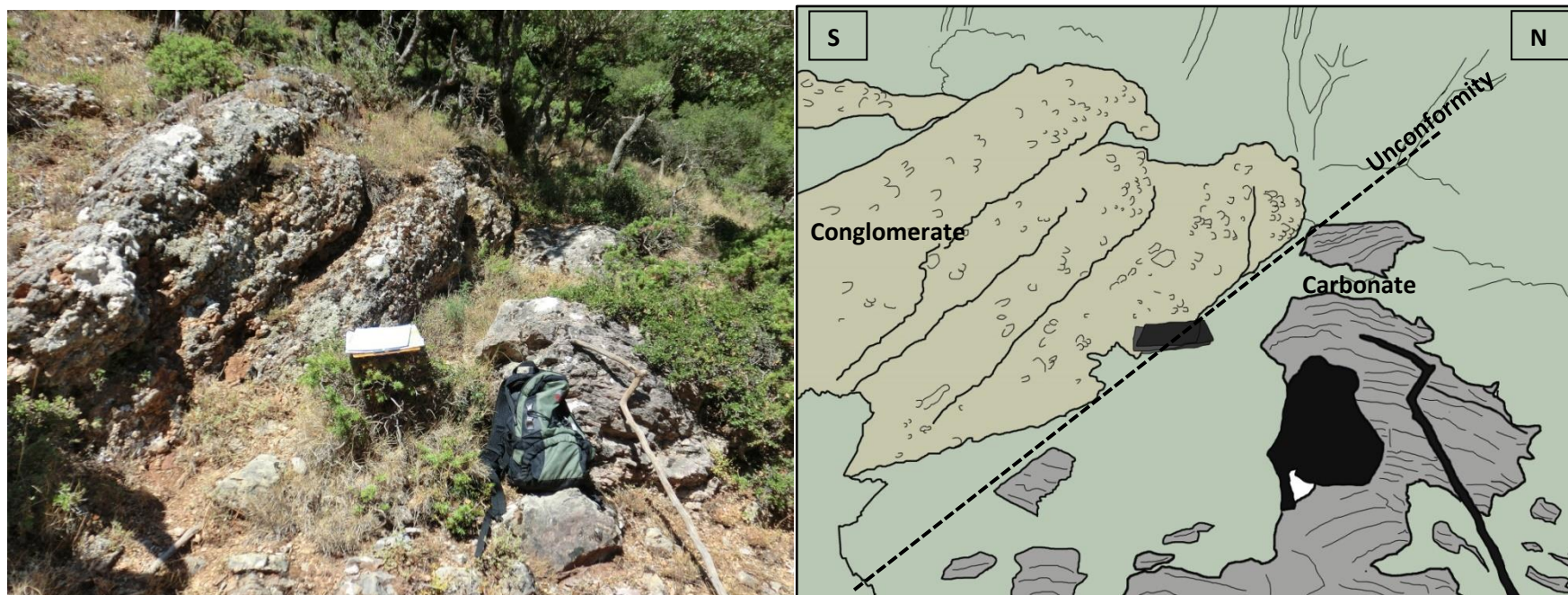


Figure 13 – Last observed basement on the West Basement Inlier Fault, carbonate overlain by unconformable conglomerates. .

Basement Carbonate Outcrop – West Basement Inlier Fault

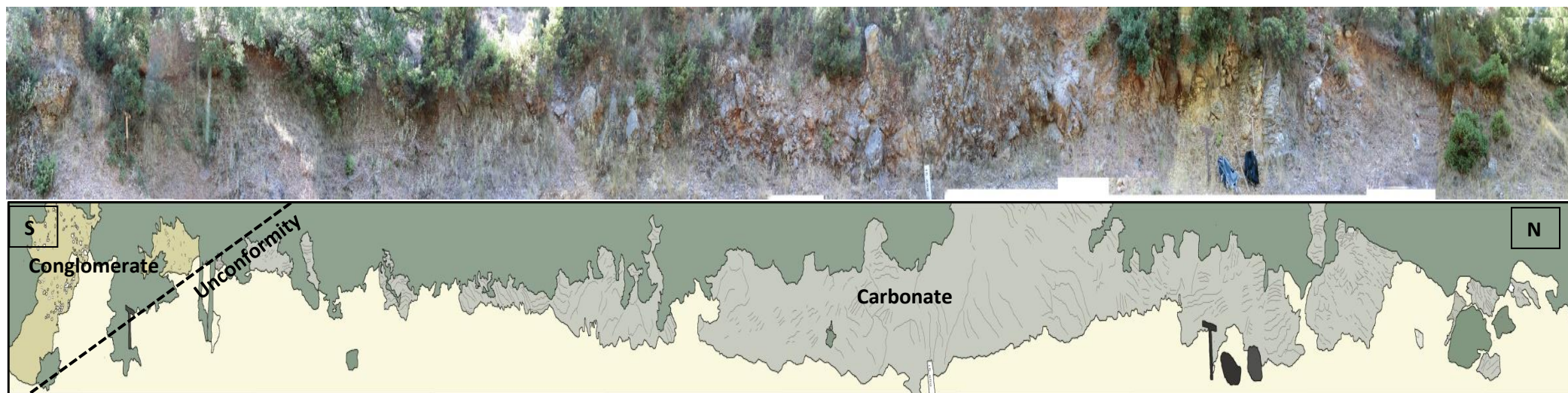


Figure 14 – Carbonate Basement outcrop along the railway in the Vouraikos River Valley with unconformable conglomerates.



Figure 15 – Uplifted basement in the footwall of Dhoumena Fault 2.

2.7 East Vouraikos

Looking to the east from the Roghi Mountain, the mountains revealed down stepping structure that are recognized at the uplifted footwalls. From the south the faults that are comprised are; East Kalavrita Fault (EKF), Souvardhou Fault (SF), Toriza Fault (TF), East Basement Inlier Fault (EBIF) and the antithetic Megha Spileo Fault 1 (MF1), fig. 16 and 17.

2.8 Souvardho Fault

East Kalavrita Fault (EKF) is followed by Souvardho Fault (SF), this fault has in many occasions been interpreted as a left stepping of Kerpini Fault across the Vouraikos, and have been referred to as East Kerpini Fault, however if the Kerpini Fault is stepping across the Vouraikos Valley, the stepping is 1500 m wide. In this thesis the fault is interpreted as a separate fault. The Souvardho Fault has been assigned the name due to its near location to the Souvardho village. The fault does not expose the fault plane, however a small outcrop expose a small outcrop of the fault contact with a dip of dip of 45° , the fault strikes is 110° SE. The

footwall of Souvardho Fault is consisting of carbonate basement which is for instance 400 m higher than the uplifted basement on the footwall of Kerpini fault 2. The hangingwall is build up by at least 700 m thick alluvial conglomerates underlying by carbonate basement which is back-tilted at 690 m along the car road in Vouraikos Valley making up the footwall of the following fault; the minor Toriza Fault.

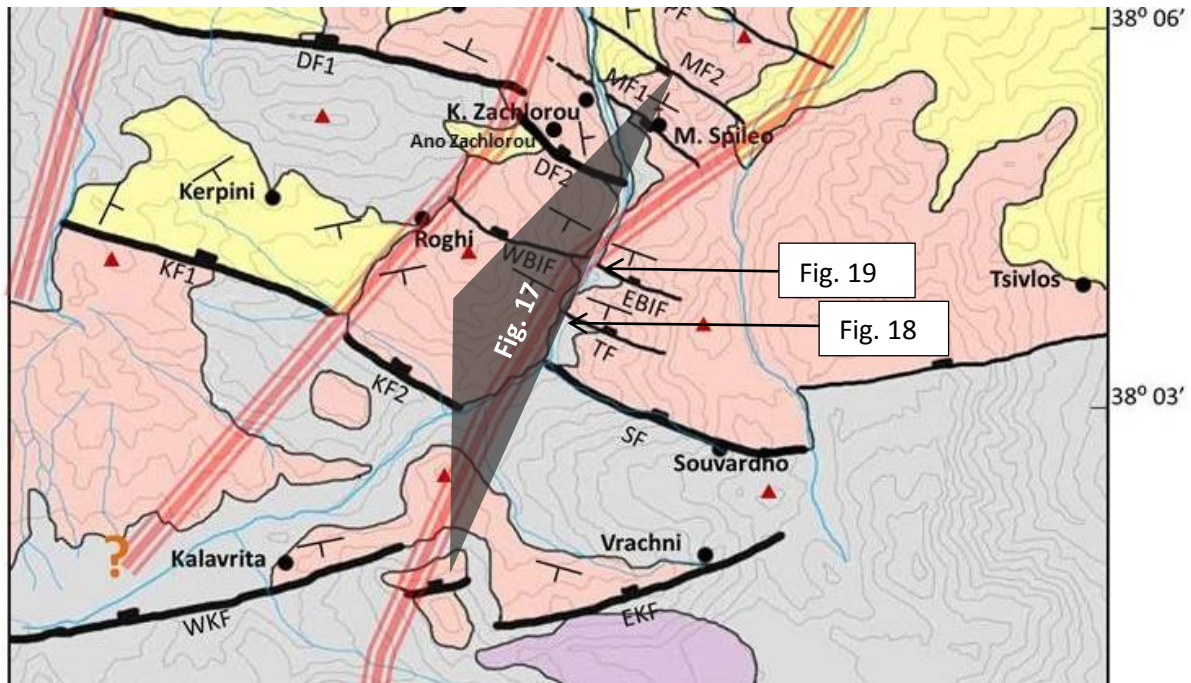


Figure 16– Section 1 of geological map, highlighting the panoramic profiles.

2.9 Toriza Fault

By following the car road in the Vouraikos Valley northwards; passing Souvardhou Fault, a small basement outcrop is exposed, this basement is interpreted as the uplifted and back-tilted basement in the hangingwall of Souvardhou Fault and as the footwall of Toriza Fault (TF), the basement outcrop ends against conglomerates with an angle of 50° , this is interpreted as the fault contact (fig. 18), as it aligns with the topographic relief and the hangingwall is overlain by onalpping sediment, that may have been deposited during the an active Toriza Fault (fig. 17). Toriza Fault could not be traced due to dense vegetation; the fault was assigned with a strike of 110SE, similar to the major Souvardhou Fault

2.10 East Basement Inlier Fault

Continuing north along the car road in the Vouraikos Valley passing Toriza Fault, another more extensive basement outcrop was observed, this outcrop could be traced for over 200 m along the road, the basement ended against unconformable conglomerates. This lithology transition is interpreted as East Basement Inlier Fault (EBIF), the hangingwall of Toriza Fault make up the Footwall of East Basement Inlier Fault, fig. 17. This fault aligns well with the West Basement Inlier Fault on the Roghi Mountain. These basements on each side of the Vouraikos Valley have not been recognized as fault in most of the earlier studies of this area, except by Collier and Jones (2004) that interpret these basements as minor faults or a collapse in Kerpini Fault 2 and Souvardhou Fault, see the geological map in figure 4. The uplifted basement was last observed at 780 m, approximately 100 m above the uplifted basement on the West Basement Inlier Fault. The unconformity might however be much higher, but the tracing was restricted by the protected National Park in this area; the last carbonate was observed at the National Park fence (fig. 19). The East Basement Inlier Fault is the last traced fault in the south east section of the Vouraikos, the northward area show little to no geological structures, as the area is covered by very dense vegetation.

2.11 Megha Spileo Fault

Megha Spileo monastery is located 2 km north of the East Basement Inlier Fault, facing the villages of Kato Zachlorou in the west, fig. 16. This monastery is built on a high angle south dipping normal fault, though the name of the Megha Spileo Fault. This fault is partly aligned with Dhoumena Fault 1 and overlap Dhoumena Fault 2, in the bending of the Vouraikos River, fig. 16. The Megha Spileo Fault will be further described at a later section.

East Vouraikos View

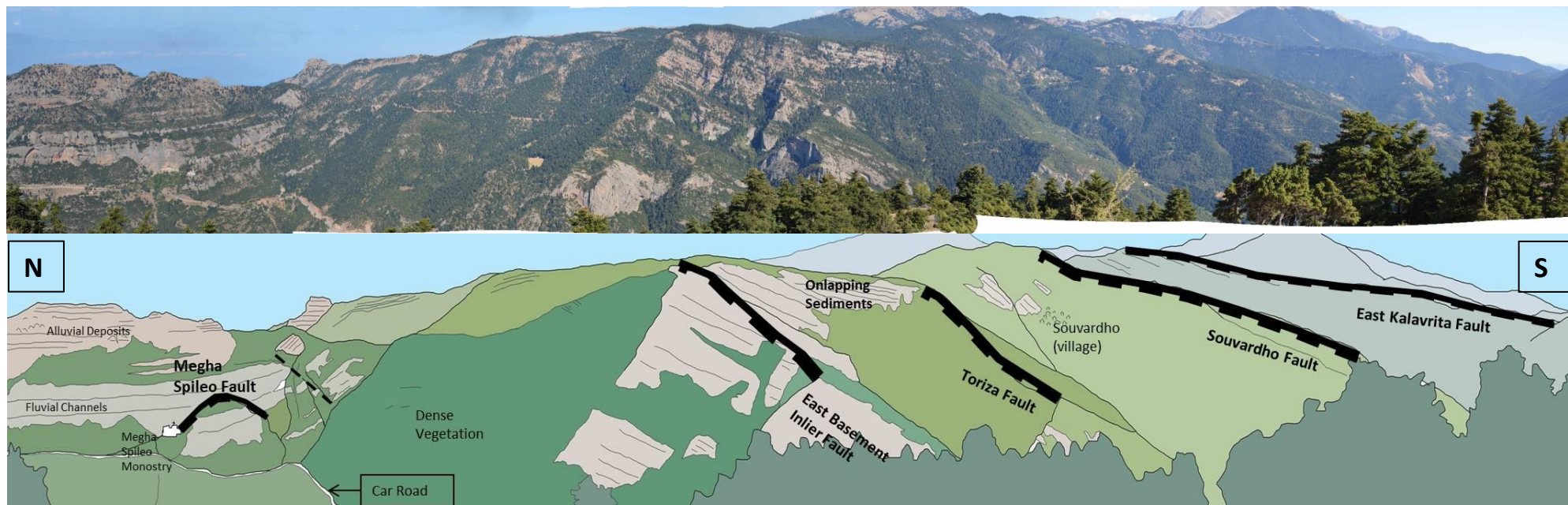


Figure 17 – South east section of Vouraikos Valley side, comprising Est kalavrita Fault, Souvardho Fault, Toriza Fault, East Basement Inlier Fault and the south dipping fault of Megha Spileo Fault 1, the north dipping faults and the south dipping fault are separated by a large and dense vegetated area.

Toriza Fault



Figure 18 – Toriza Fault contact and unconformity, along the car road.

East Basement Inlier Fault

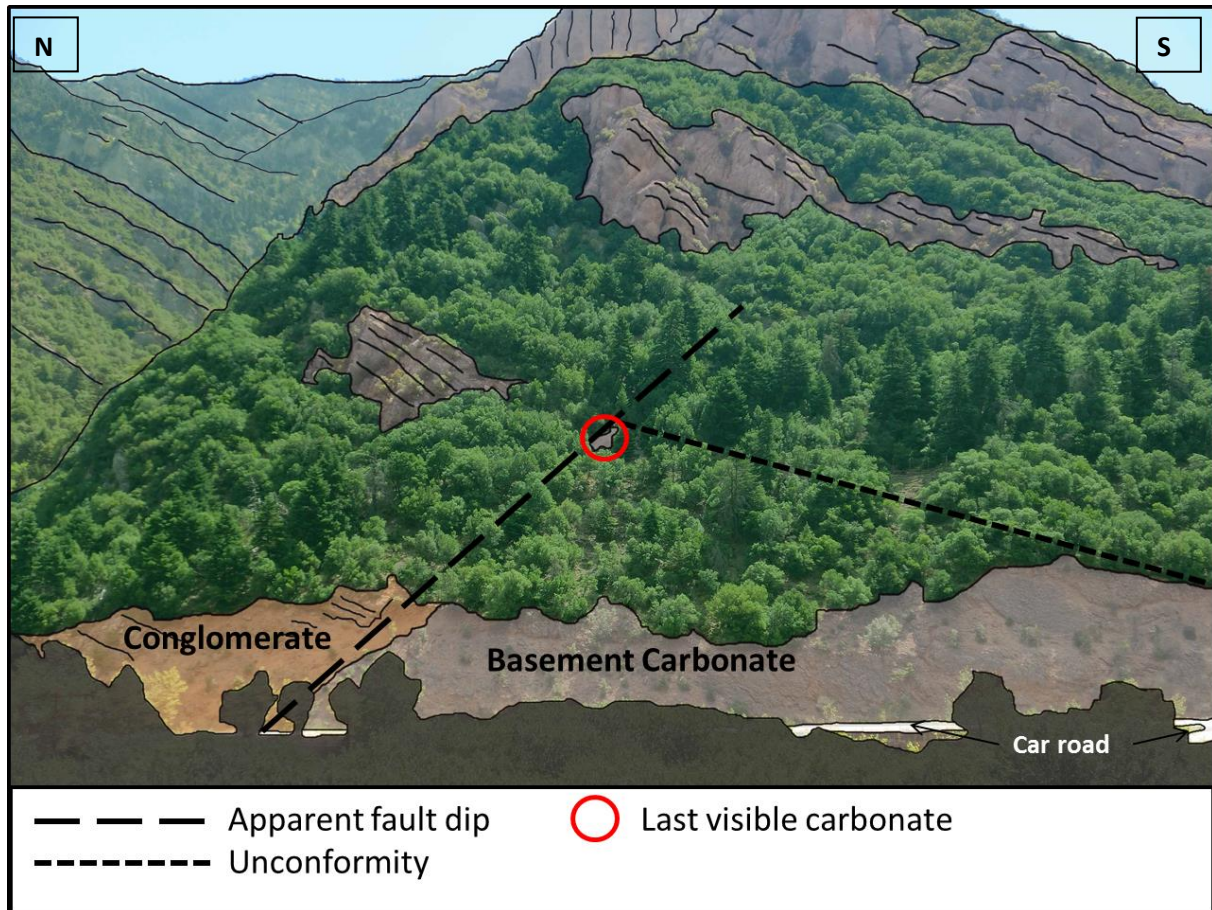


Figure 19 – East Basement Inlier Fault contact, the last observed uplifted basement and a possible unconformity.

2.12 Dhoumena Fault

The major fault following Kerpini Fault to the north is Dhoumena Fault on the east of the Vouraikos Valley, fig. 20. The Dhoumena Fault can be traced for 7,5 km from the Kerinthis River in the west to the Vouraikos River in the east, this fault comprises of at least two fault segments; Dhoumena Fault 1 (DF1) and Dhoumena Fault 2 (DF2). The fault is right stepping in the same alignment with the Roghi Valley where the Kerpini Fault is stepping, fig. 20.

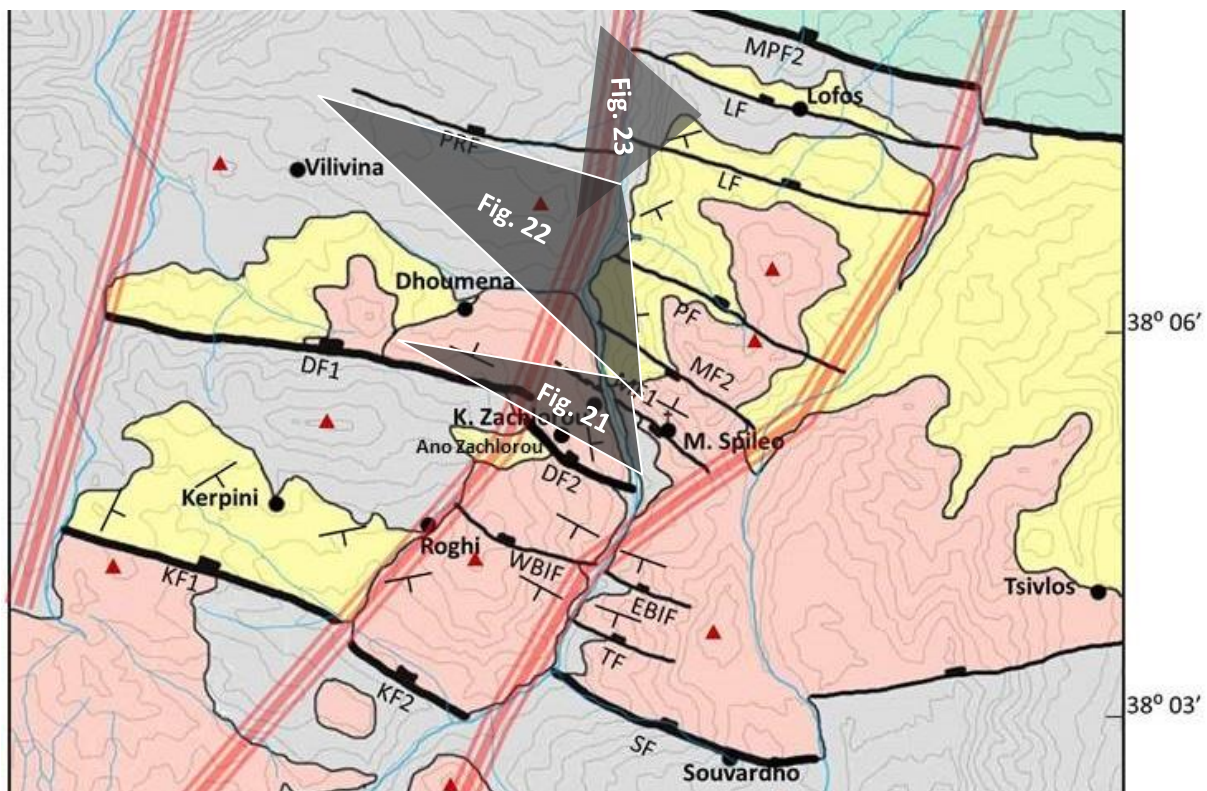


Figure 20 – Section 2 of the geological map, highlighting the panoramic profiles.

2.13 Dhoumena Fault 1

The footwall of Dhoumena Fault 1 is the fault block of Kerpini Fault 1, the carbonate basement is uplifted to 1500 m in the west close to Kerinthis River, decreasing to 1300 m close to the stepping in the fault. The hangingwall of Dhoumena Fault 1 is made up of fine fluvial sediments such as marl, silts and sandstones overlain by debris flow alluvial fans, that are fed by Dhoumena Footwall or Kerpini Fault Block 1 (Kolbeinsen, 2013), the rest of the fault block is exposed carbonate basement uplifted to 1100 m making up the footwall of Psili

Rachi Fault, fig. 21. The fault plane of the Dhoumena Fault is perfectly exposed, and has a slope that measures a dip of $44-48^{\circ}$, and has a strike of 110°SE .

2.14 Dhoumena Fault 2

Dhoumena Fault 2 is right stepping relative to Dhoumena Fault 1, and is overlapping and passing in front of Megha Spileo Fault 1. The footwall of Dhoumena Fault 2 is the hangingwall of the West Basement Inlier Fault, the uplifted basement can be observed here close to Ano Zachlouro village at approximately 800 m (fig. 21), several hundred meters below the uplifted basement on the footwall of Dhoumena Fault 1. The hangingwall of Dhoumena Fault 2 is defined by similar late syn-fans described by Kolbeinsen (2013) in section 1.14. By standing on the hangingwall of Litha Fault close to the Vouraikos Valley it's possible to demonstrate how well the stepping of Dhoumena along the Roghi Valley is in addition well aligned with the north Vouraikos section, Fig. 22.

2.15 Psili Rachi

Psili Rachi Fault (PRF) footwall is the tilted Dhoumena Fault Block 1, both the hangingwall and the footwall is made up by exposed carbonate basement rock. Psili Rachi Fault has a strike of 110°SE and the fault has a dip of 50° . The fault surface is exposed in the Vouraikos Valley, fig. 23. Psili Rachi Fault is nearly aligned with Litha Fault across the valley to the east, but the uplifted basement on Psili Rachi Fault is roughly 100 m higher than the uplifted basement on Litha Fault across the Vouraikos. Psili Rachi is the last fault observed on the west section before the major Mamousia Pirghaki Fault.

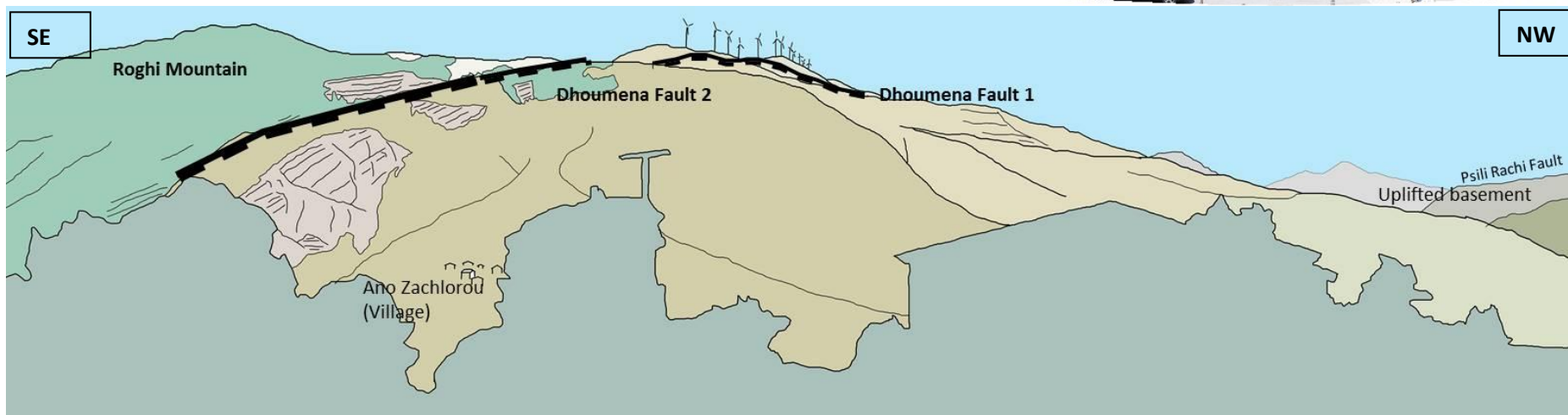


Figure 21 – Dhoumena Fault Blocks 1 and 2; covered by late syn-rift fans.

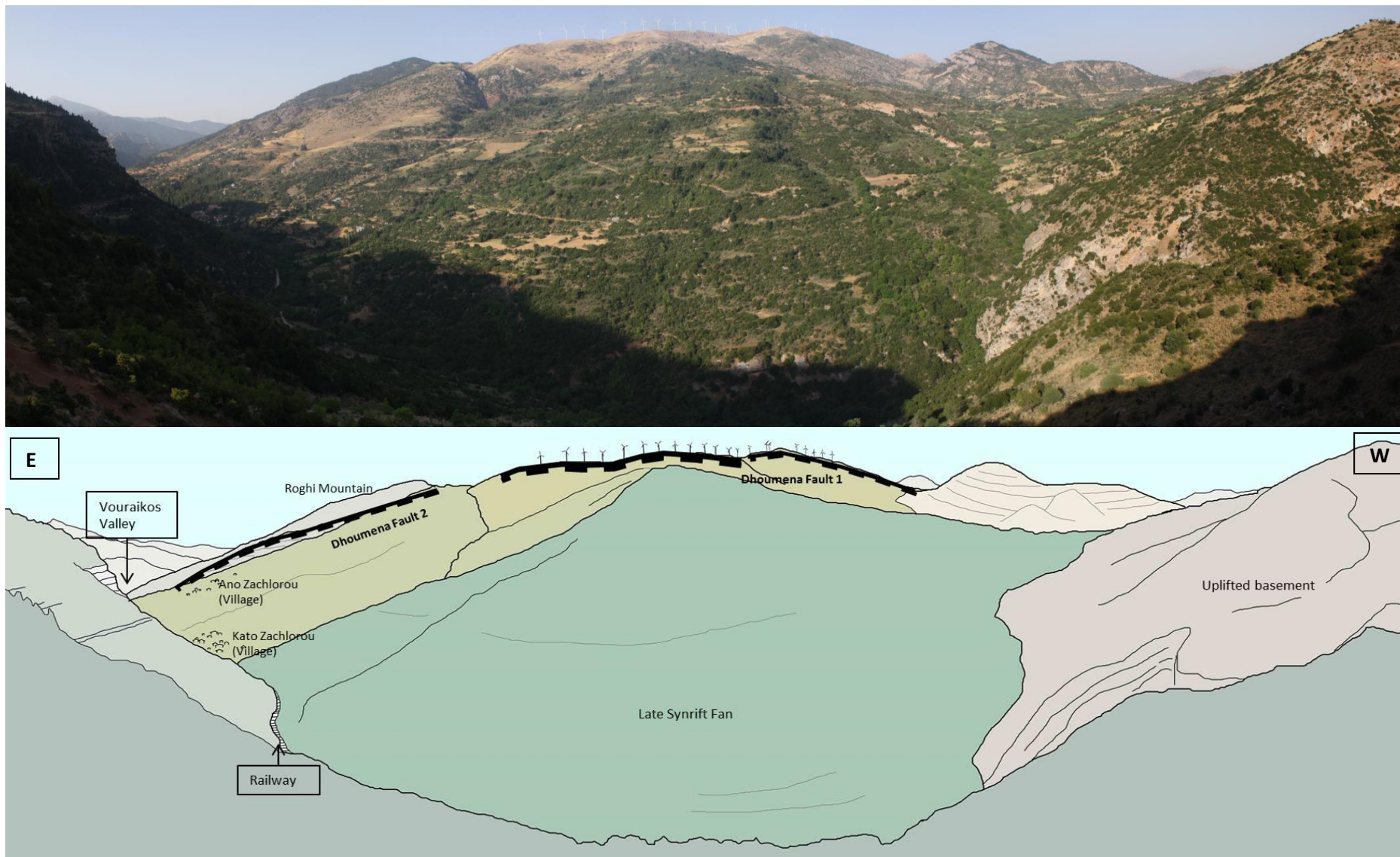


Figure 22 – Dhoumena Fault stepping in alignment with Roghi Valley in the south and the Vouraikos on the North.

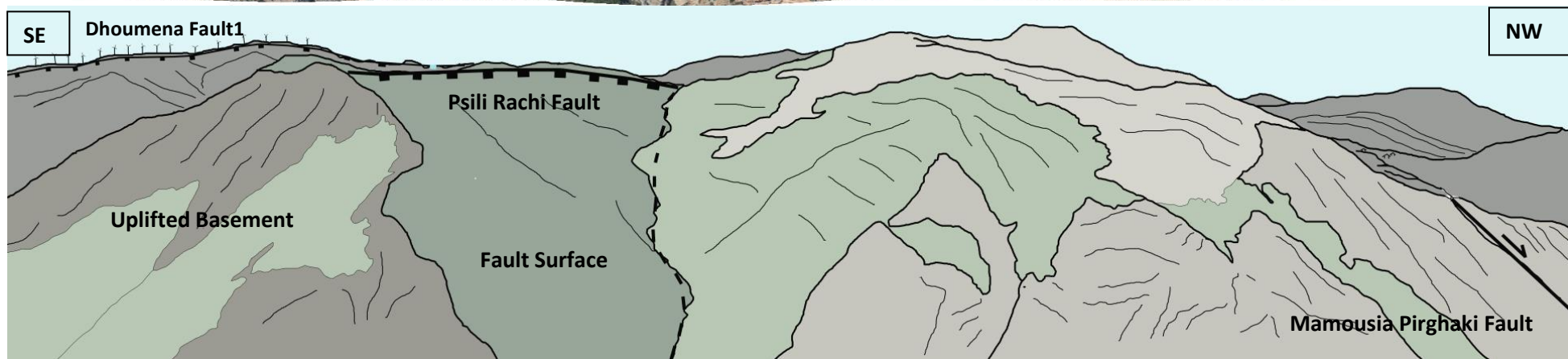


Figure 23 – Psili Rachi Fault surface is making up the uplifted basement of Dhoumena Fault Block in the background, Psili Rachi Fault is the last Fault traced before Mamousia Pirghaki in the north.

2.16 The Horst

On the immediate opposite side of Dhoumena Fault blocks in the Vouraikos, there are no structures observed that resembles the structures on the west valley side. Hence there is little to no evidence that any structure crosses the Vouraikos valley at this location, fig. 24. A horst structure to the east was observed standing on the Dhoumena fault block 2, the horst is defined between the two south dipping faults; Megha Spileo Fault 1 and 2 where the Vouraikos River bends, and the north dipping faults Portez Fault, Litha Fault, Lofos and Mamousia Pirghaki 2 (MPF2), fig. 25. The latter panoramic picture is showing an apparent view of the true dip of the south dipping faults.

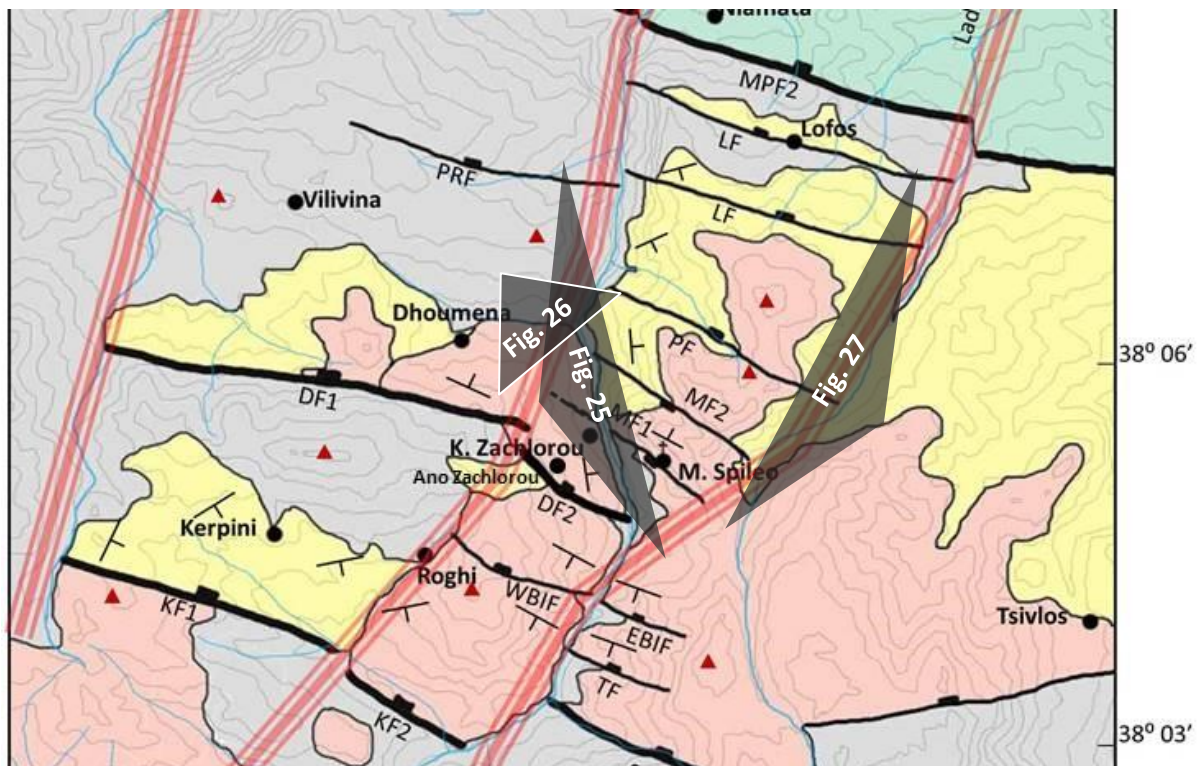


Figure 24 - Section 3 of geological map, highlighting the panoramic profiles, fig. 25, 26 and 27.

2.17 Megha Spileo Fault 1 and 2

Megha Spileo Fault 1 and 2 are the two south dipping faults with a dip of 50° and strikes 120°SE . The hangingwall of Megha Spileo Fault 1 (MF1) is a small fault block that ends in the Vouraikos Valley parallel to Dhoumena Fault 2, this may be a graben fault block, that make up the hangingwall of both Dhoumena Fault 2 and Megha Spileo 1. The view of figure 25 is close to parallel to the fault planes of the two antithetic faults, the beds seems horizontal, but they are dipping ENE, away from the view, the hangingwall of Megha Soileo 1 is displacing the marked fluvial beds on its footwall. The footwall of Dhoumena Fault 1 is making up the

fault block of Megha Spileo 2 that is displacing both the fluvial and the alluvial deposits. In addition a fallen block has succumbed into The Vouraikos Valley between the south dipping faults, fig. 25. This interpretation was made by analyzing the displacement of the pronounced thick fluvial strata.

The true dip of the south dipping faults was observed at a height close Psili Rachi Fault. From this angle the beds were no longer horizontal a clear northward dip was observed, fig. 26. The fault block of Megha Spileo Fault 1, Megha Spileo Fault 2 and the horst are structures overlain by fluvial deposits and alluvial deposits. No carbonate basement is exposed on these fault blocks, even at the base of the Vouraikos Valley, however we know that the Vouraikos is covered by recent river sediments, that may cover the carbonate basement.

The horst structure reveals different geological structures when looking from the east across the Ladhopotamos River (fig. 27, by Stuvland, 2015). No tilted fault blocks, no unconformities and no clear fault structures were observed. One thick section of conglomerates was the only thing observed on this side of the horst, however by comparing the two views of the horst structure there were discovered that the tilted basement of Portes Fault and Litha Fault stands at 800-900 m, while the very bottom of the Ladhopotamos Valley is at 900 m, that means that the only visible facies on the east profile is the late prograding alluvial fan that can be observed from the Vouraikos Valley on the top of the mountain.

By a closer look at the alluvial sediments from Ladhopotamos Valley, there were noted three dip angle change, two angular changes and one gentle dip change, fig. 27. The two angular changes matches well the strikes and location of Megha Spileo Fault 1 and 2, and the gentle dip angle change seems also to align with Portes Fault and could be the non-faulted sediments that are downlapping into the created accommodation space created in the down thrown Portes Fault Block.

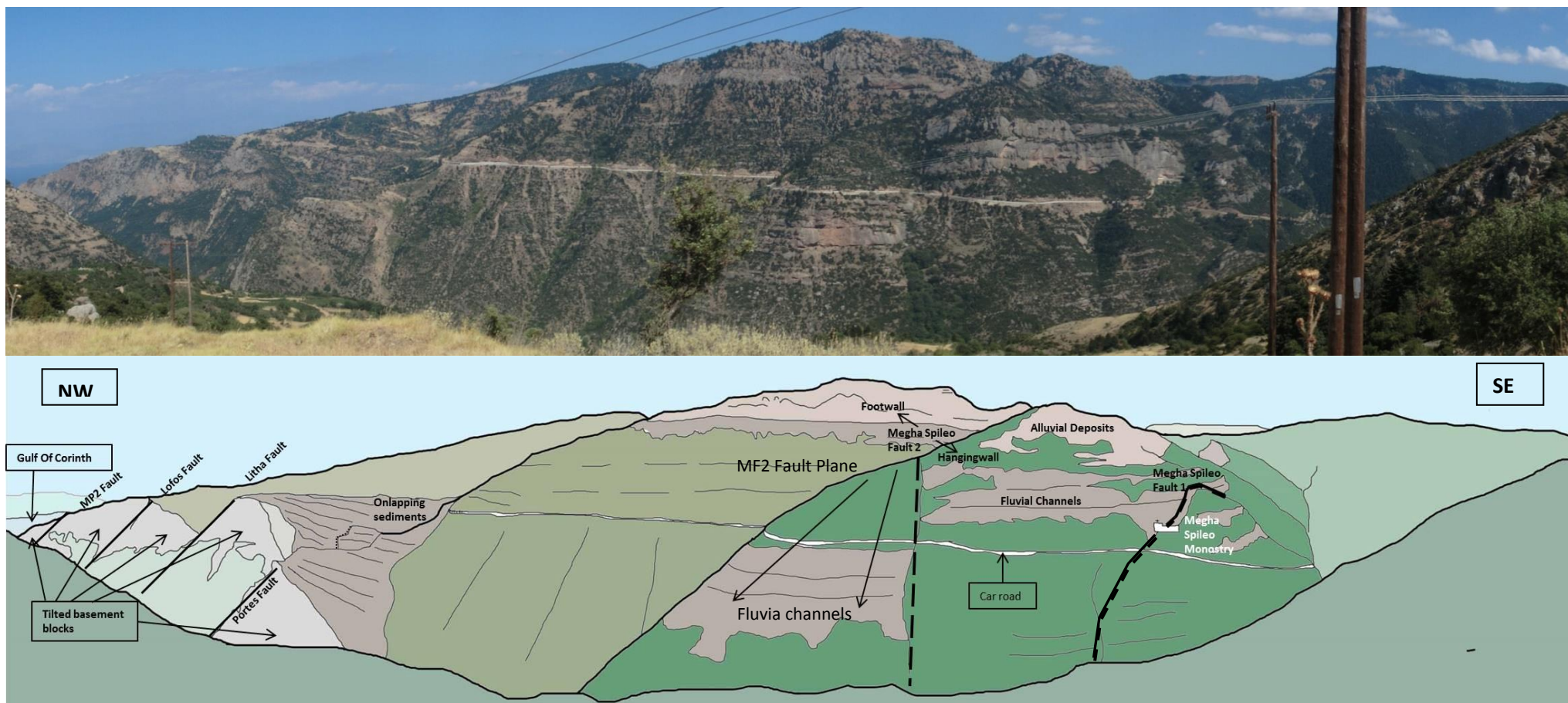


Figure 25 – The horststructure, defined by the two south dipping MF1 and 2, and the north dipping faults of Portes Fault, Litha Fault, Lofos Fault and Mamousia Pirghaki Fault 2.

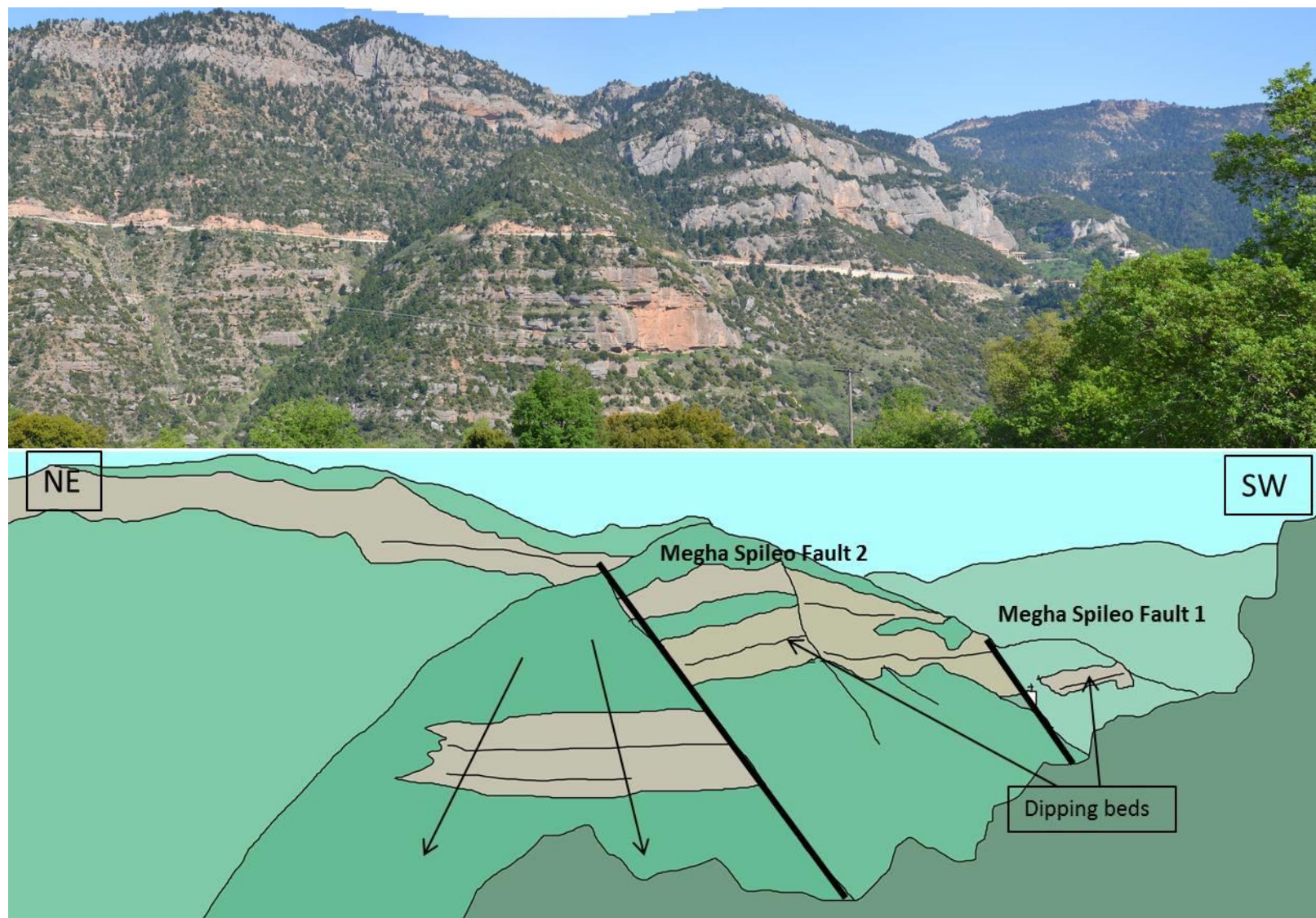


Figure 26 – True dip view of Megha Spileo Fault 1 and Megha Spileo Fault 2

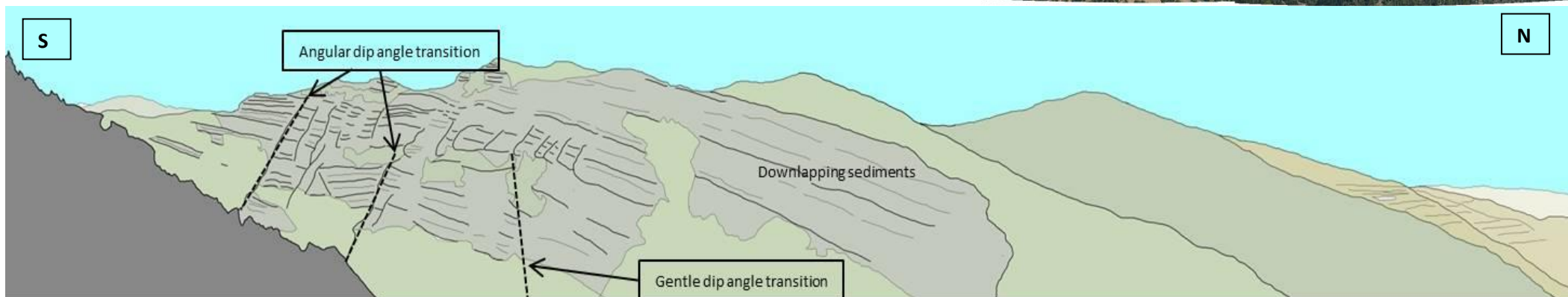


Figure 27 – The horst structure through the Ladhopotamos River Valley, with three dip angle change. The image taken by Marius Stuvland.

2.18 Tilted basement

The two profiles of each side of the north Vouraikos section before Mamousia-Pirghaki Fault (MPF) differs from each other, on the west of the Vouraikos Psili Rachi Fault Block (PRF) is the fault block following the tilted Dhoumena Fault Block and the last one before Mamousia Pirghaki Fault Bloc, fig 27a. While on the east there are far more observed fault blocks, that can not be traced across the valley. Portes Fault (PF) is terminated at the valley, Litha Fault (LTF) may be linked to Psili Rachi Fault across the valley, but the tilted basement are vertically displaced by 100 m, and finally Lofos Fault (LF) before Mamousia Pirghaki Fault, fig. 27b. All the tilted fault blocks on the east has a relative high dip angle, and has been assigned with a dip of 50° and a general strike of 110° SE, fig. 27.

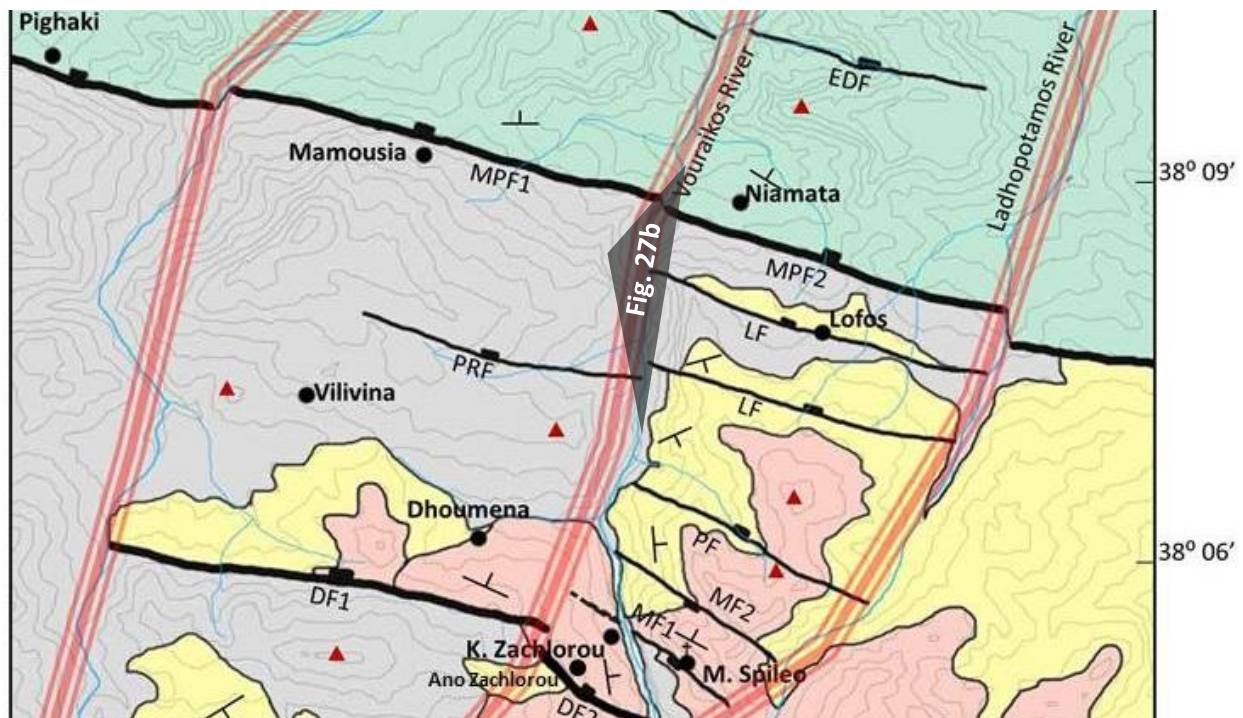


Figure 28 – Section 4 of geological map, highlighting the panoramic profile in figure 27b.

2.19 Mamousia Pirghaki Fault

Mamousia Pirghaki Fault (MPF) is a fault that comprises several fault segments, the fault has been described as 28-30 km long according to Fort et al., 2013. The fault segments are hard linked and the fault makes the steps in Kerinthis and in Ladhopotamos river valley, fig. 28. The fault has been divided into Mamousia Pirghaki 1 and 2, relative to the west and east side of the

Vouraikos Valley. There is no clear evidence that the Mamousia Pirghaki Fault is stepping in the Vouraikos river valley, however, observations indicate that the footwall of Mamousia Pirghaki 1 is higher than the footwall of the Mamousia Pirghaki 2. The Vouraikos valley width narrows dramatically down along Mamousia Pirghaki Fault strike, so fault investigation in the Vouraikos were unmanageable for this fault. Mamousia Pirghaki Fault strikes 110 SE and is dipping generally 50° , fig. 27. The entirely down thrown Mamousia Pirghaki Fault Block is consisting of an ancient Gilbert type delta; generally north dipping conglomeratic fluvial sediments, picture. 29.

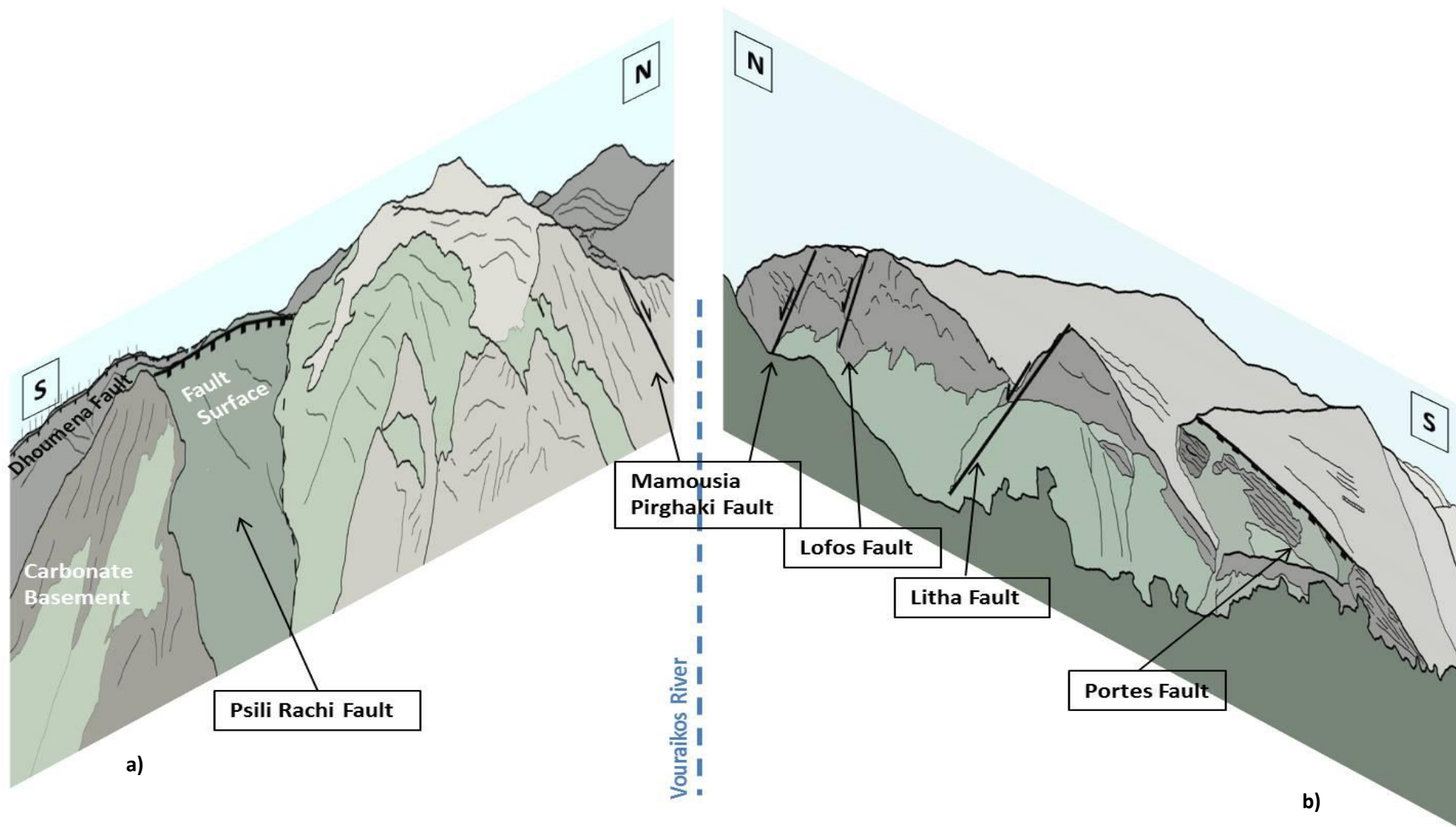


Figure 29 - Comparison of west and east Vouraikos Valley sides.

2.20 Dhervini Fault

The Vouraikos river valley widens immediately after Mamousia Pirghaki Fault, and further into the fault block, two locally perpendicular valleys to the Vouraikos cuts into the ancient delta, indicating possible fault that crosses the Vouraikos valley. This fault is referred to as Dhervini Fault, due to its location close the Dhervini village, fig. 30. The Dhervini Fault have no exposed basement, but a fault contact with same lithology was still observed in the Kerinthis River Valley; the sediments are north dipping in the footwall of Dhervini fault, while the sediments are close to horizontal in the hangingwall, fig. 31. The Dhervini Fault show no stepping in the Vouraikos Valley, however the tracing of the fault is challenging as there is no visible carbonate basement.

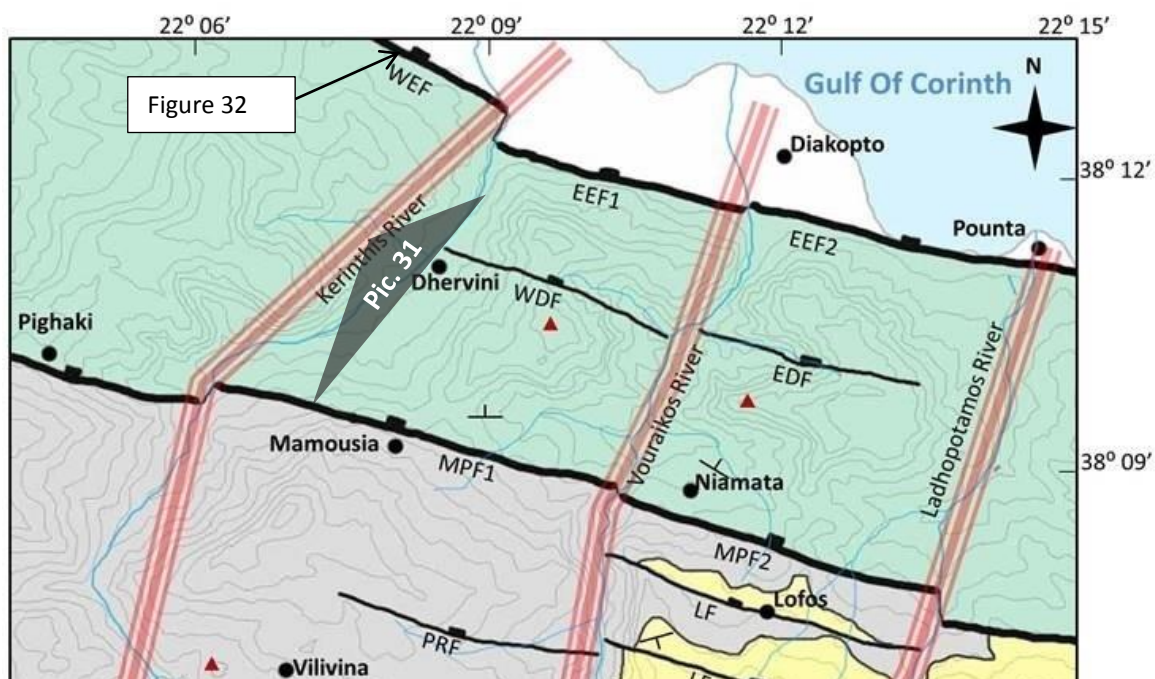


Figure 30 – Section 5 of geological map, highlighting the panoramic profile in fig. 31.

2.21 Eliki Fault

The Eliki Fault (EF) is recognized as a still active fault today, the fault left steps in the Kerinthis River, the fault segments are referred to as West Eliki Fault (WEF) and East Eliki Fault (EEF) relative to the Kerinthis River, and further divided in this study into East Eliki Fault 1 and East Eliki Fault 2 to associate the fault with the two sides of the Vouraikos Valley. The East Eliki Fault has a strike of 105SE and a dip of 45-50° N. The West Eliki Fault is uplifting the ancient deltas and down faulting the recent deltas, the fault surface can be

observed along the highway, see figure 32. The East Eliki Fault together with Dhervini Fault show no stepping in the Vouraikos, East Eliki Fault expose no basement either, the basement is interpreted to be covered by the recent deltas. This coastal fault is generally separating the uplifting of the peninsula from the subsiding Gulf of Corinth.

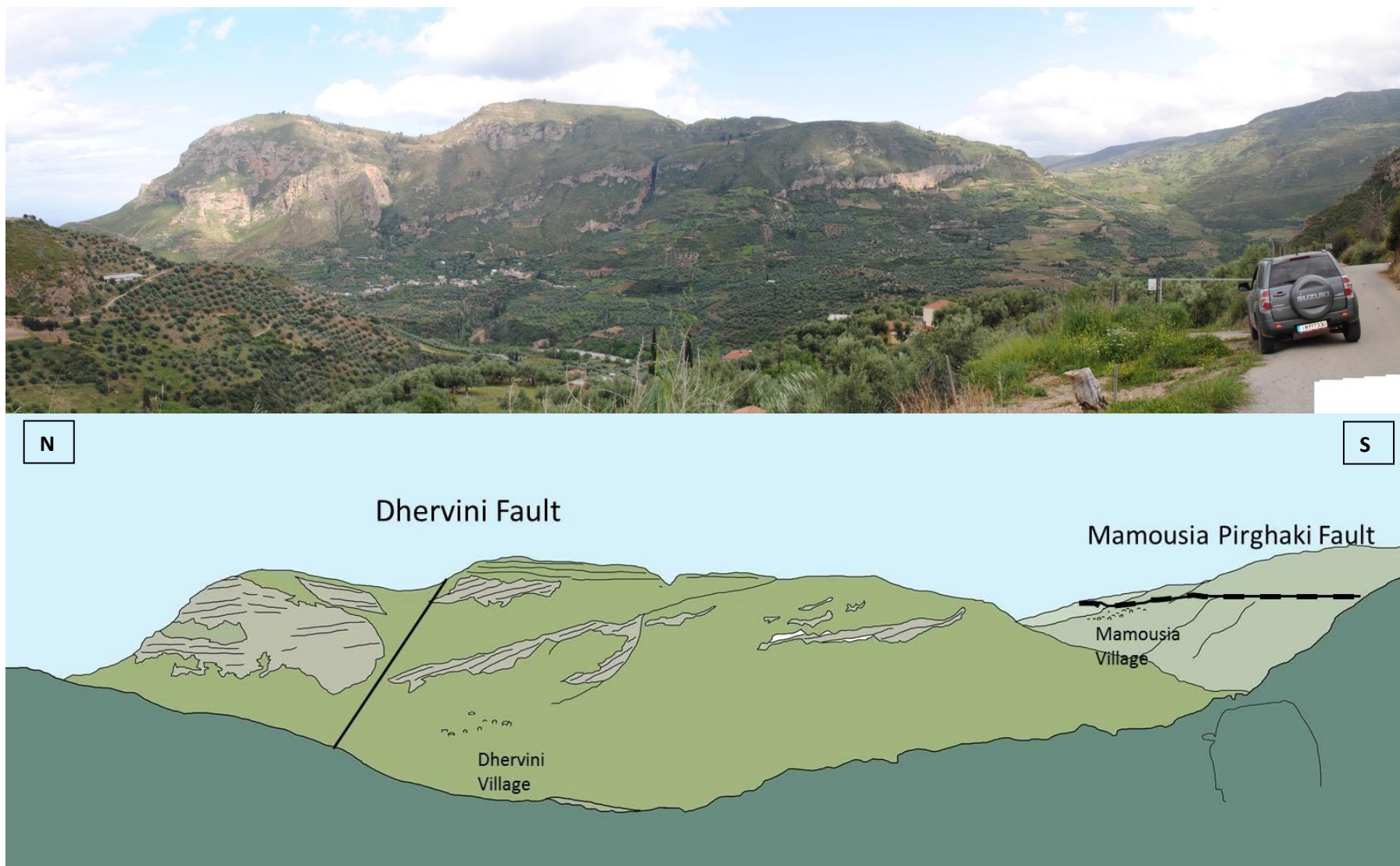


Figure 31 – Dhervini Fault and Mamousia Pirghaki Fault



Figure 32 – Fault surface of West Eliki Fault (WEF) close to the highway, east of the Kerinthis river.

CHAPTER 3

3.1 Structural Interpretation

The geological structures of the study area Kalavrita-Diakopto is dominated by north dipping normal faults, the faults has a general W-E trend and are dipping with an angle between 40-50°. There are several elements that highlight fault structures; the topographic expression, abrupt lithology changes and an interesting indicator to structural change is water drainage, from river valleys to small water streams were always present along the fault strike and along lithology changes along unconformities.

The fault dip was measured from fault planes and exposed fault contacts in the Vouraikos Valley. But an exact dip measurement is not always possible on the field, however similar fault dips of close by faults were assigned to them.

The unconformity surface between the basement and the sediments are generally south dipping as the fault blocks are back tilted. To calculate the unconformity truncation, or in other words where the unconformity meets the fault surface, basic trigonometry calculation were used, the same calculation were applied to estimate the throw or displacement of the fault, see figure 33. The result is presented as a table that reflects the fault distribution relative to each other and their position relative to the valleys and the interpreted transfer faults.

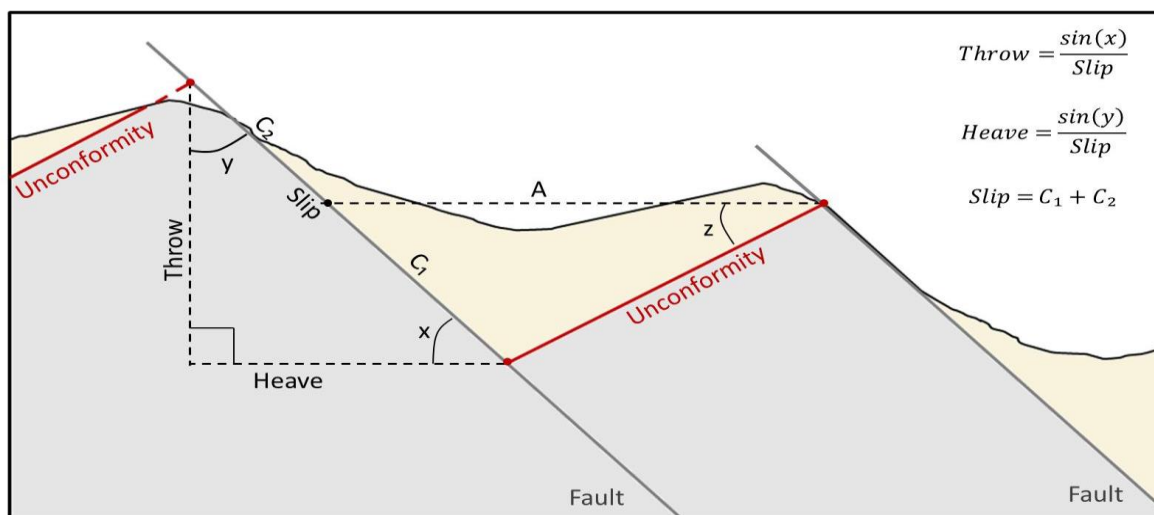


Figure 33 – Sketch showing the elements used to calculate throw and heave, basement exposure in the hanging wall and footwall.

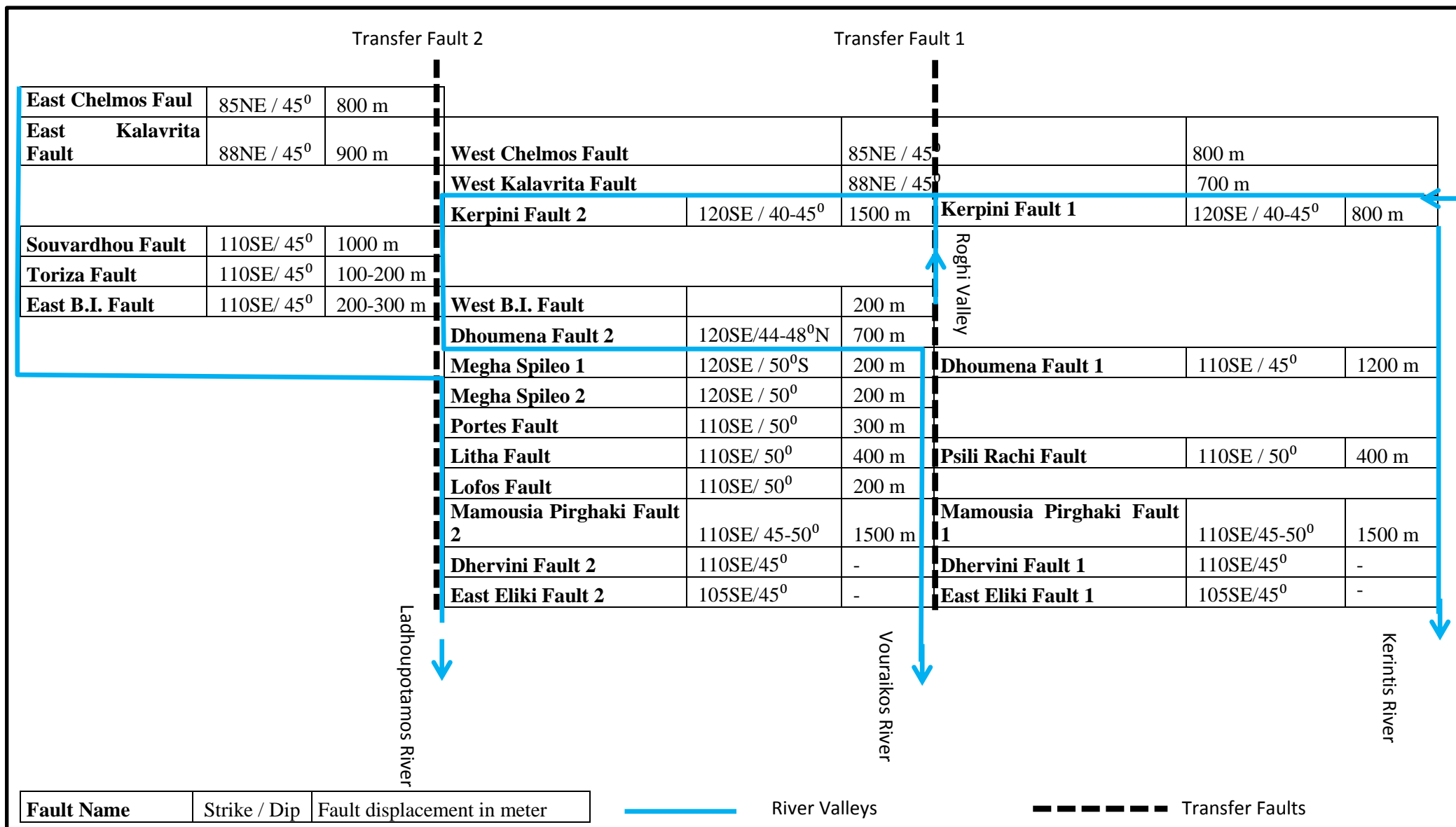


Table 1 – A table of the fault distribution and their position relative to other faults and river valleys. The faults are presented with strike/dip and their maximum displacement.

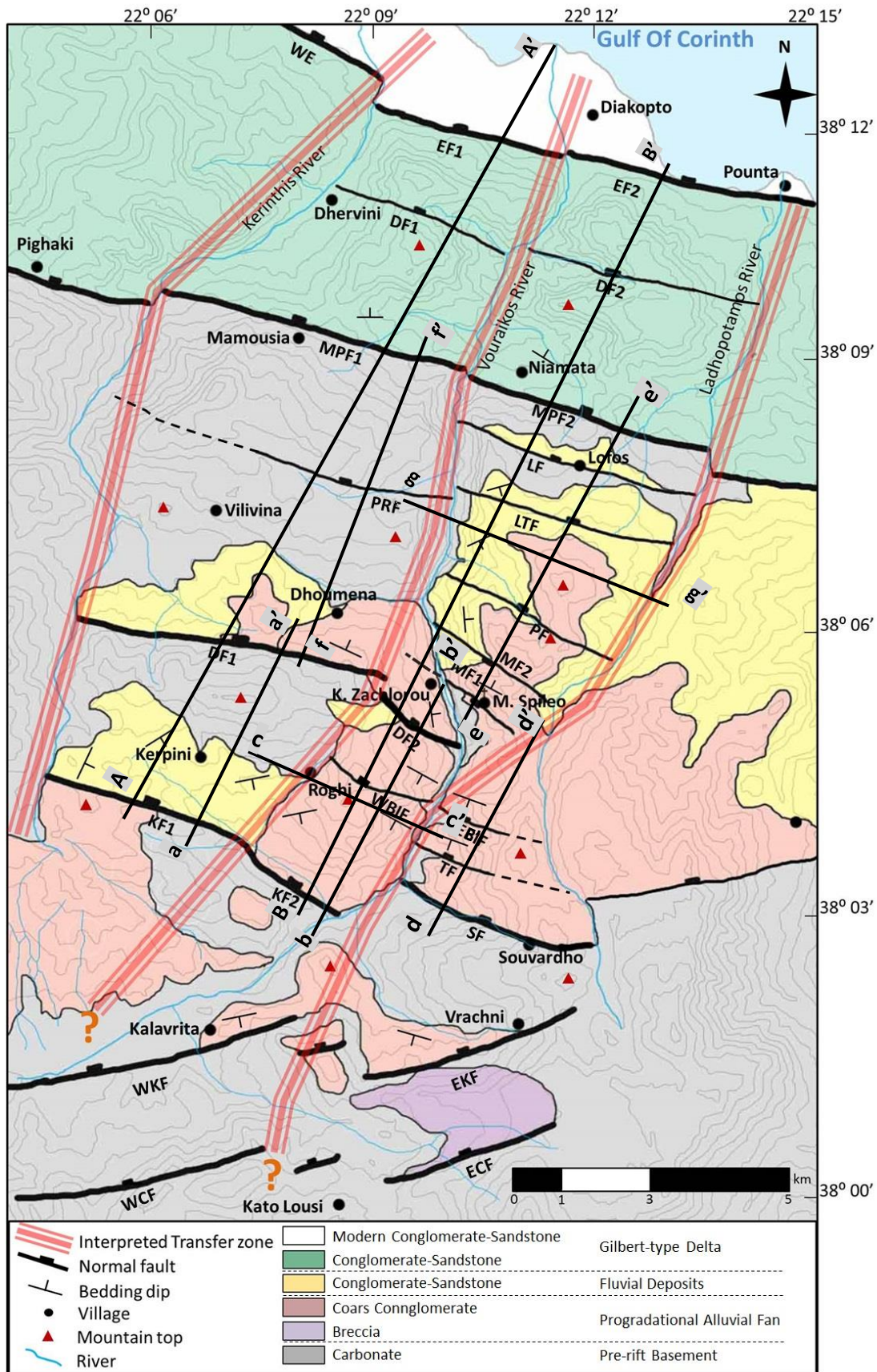


Figure 34 – Geological map with marked cross-sections.

The Kerpini fault mark a dramatic change in the topography, the carbonate basement in the footwall is tilted to about 1100m, but on the hangingwall the basement is well exposed in Kerpini fault block 1 and nearly non-visible in Kerpini fault block 2 except in some outcrops that are described earlier. The exposed basement height is increasing toward the west, or the fault displacement is decreasing, it seems like the fault might die out in the Kerinthis River with a displacement close to zero. However this is not the case towards the east, the fault displacement seems to increase all the way to the Vouraikos River. In addition there is a sharp lithology change across the Roghi Valley, suggesting a structural discontinuity caused by a fault perpendicular to the Kerpini Fault. The maximum elevated basement on the Kerpini fault block 1 is at 1300-1400 m (fig. 35) while the maximum elevated basement in the West Basement Inlier fault block and Dhoumena Fault block 2 is relatively at 700 m and 900 m (fig. 36). Dhoumena Fault 2 is right-stepping along the lineation of Roghi Valley and cannot be traced in the east of Vouraikos, this fault faces the Megha Spileo fault 1 in the bend of the Vouraikos River close to Kato Zachlouro village.

There is vertical displacement of the basement across the Vouraikos River as well, going from West basement Inlier fault block to East Basemnt Inlier Fault block there is at least a 100 m separating the uplifted basement, these elements may imply a second transfer fault in the river valleys, see figure 37.

In other studies the Souvardho Fault is referred to as East Kerpini Fault, implying that Kerpini Fault is left-stepping in the Vouraikos, however the fault steps is then stepping 1500 m and the uplifted basement in the footwall of Souvardho Fault is 200-300 m higher then Kerpini Footwall. The Souvardho Fault has a maximum displacement of approximately 1000 m. Following Souvardho fault there has been observed two outcrops exposing lithology changes of unconformity flowed by fault contact, Toriza fault and East Basement Inlier fault, these minor faults might not exceed a displacement of 200-300 m. There is a possible antithetic as an eastward continuity of Megha Spileo fault, se figure 38.

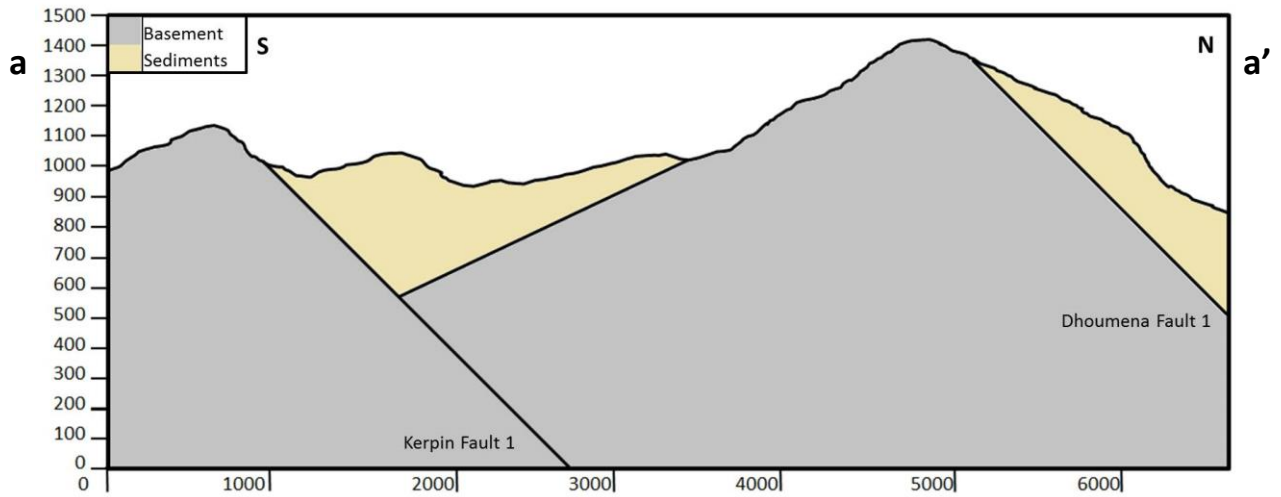


Figure 35 – Cross-section of Kerpini Fault Block 1, marked a-a' section in figure 34.

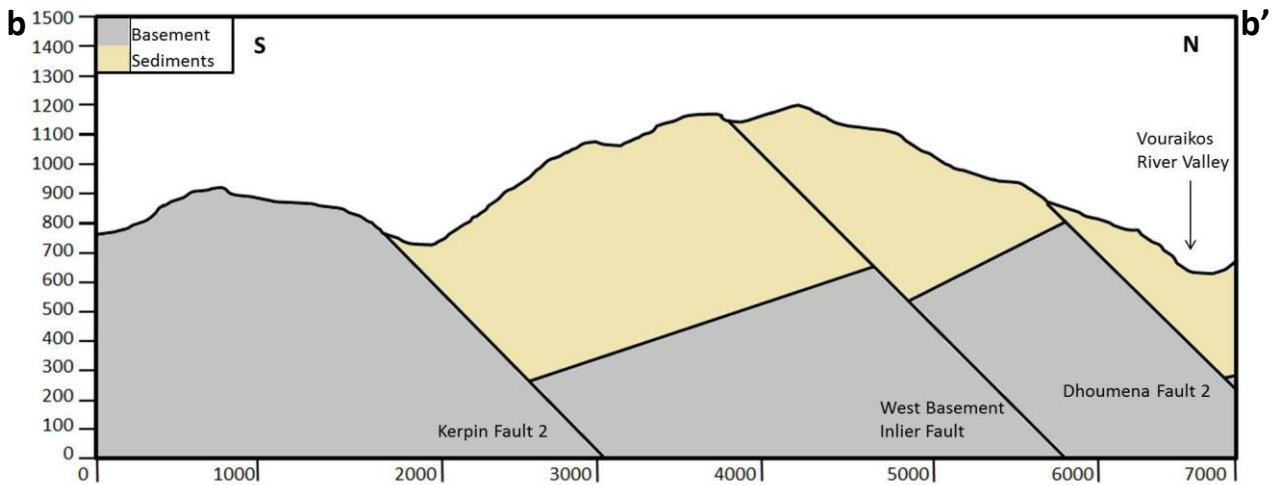


Figure 36 – Cross-section of Kerpini Fault Block 2 and West Basemnet Inlier Fault block, marked b-b' section in figure 34.

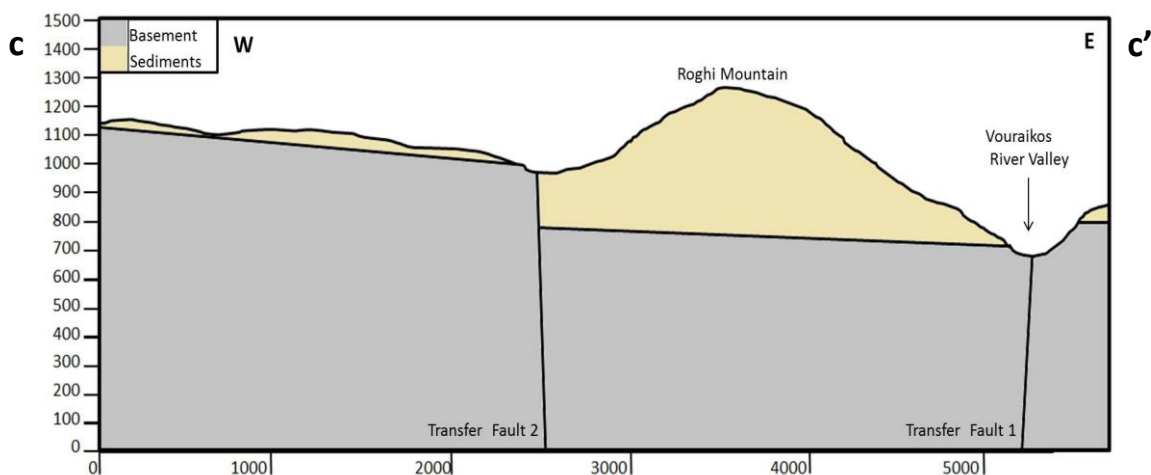


Figure 37 - Cross-section perpendicular to Roghi and Vouraikos Valleys, marked section c-c' in figure 34.

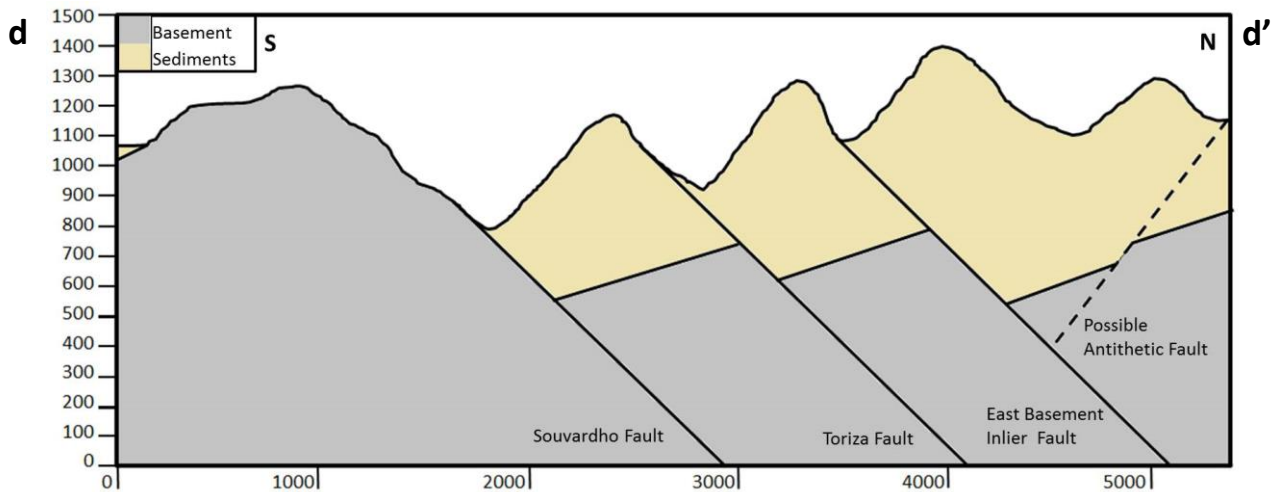


Figure 38 – Cross-section of the south east section of the Vouraikos, marked section d-d' in figure 34.

As mentioned the Megha Spileo Fault 1 seems to be facing the Dhoumena Fault 2 in the bending of the Vouraikos. Both Megha Spileo Fault 1 and 2 are two steep south-dipping faults assigned a dip of 50° , both the faults has a maximum displacement of 200 m. Megha Spileo Fault 2 terminates at the Vouraikos and Megha Spileo Fault 1 has been interpreted to terminate at the lineation of the Roghi Valley, see fig. 34. Dhoumena Fault 2 and Megha Spileo 1 are defining the graben structure between Roghi Maountain in the south and the Horst in the north. There has not been observed any basement in the horst structure before the uplifted basement in the footwall of Portes Fault, Portes Fault has a display a displacement of 300 in the Vouraikos. The two south-dipping faults seems to cut through all the sediments while the north-dipping faults are clearly overlain by onlapping sediments and overlain again by continuous alluvial fans that can be seen on the Ladhopotamos River Valley. The sedimnts stacked on the horst are interpreted as syn- to post-faulting relative to the north dipping faults, and as pre-fault relative to the south-dipping fault. The fault displacements are entirely based on calculation and assumptions that may explain the lack of basement exposure, fig. 39.

The north-west section of the Vouraikos Valley in the opposite side of the horst structure, have no trace of any structures crossing this section of the Vouraikos except Mamousia Pirghaki Faults that aligned on both sides of the valley, but might be displaced 100 m vertically. Dhoumena Fault 1 has a maximum displacement of 1200 m and is aligned with opposite dipping faults in the horst that shows in addition a far more smaller displacements, The following fault in front of Dhoumena Fault 1 is Psili Rachi Fault, this fault is almost

aligned with Litha Fault, but its uplifted basement in the footwall stands 300 m higher, fig 40 and 41.

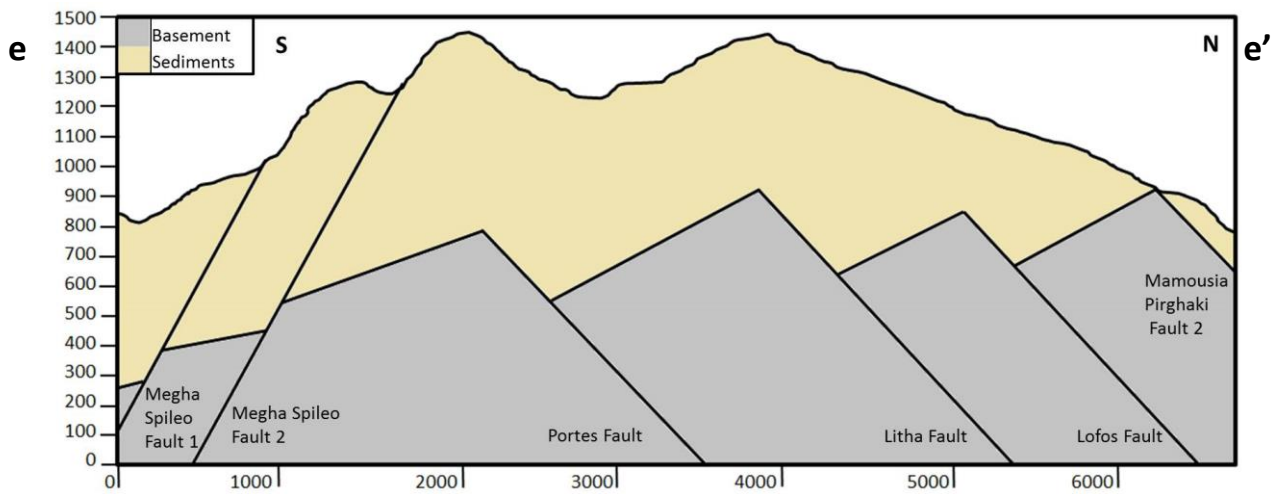


Figure 39 – Cross-section of the horst structure, marked e-e' section in figure 34.

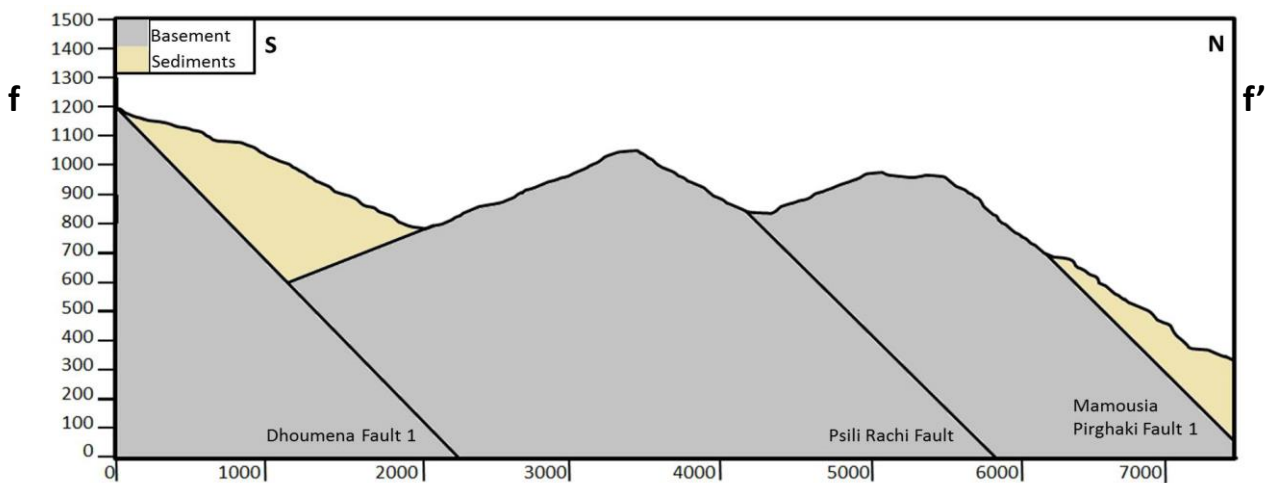


Figure 40 – Cross-section of Dhoumena Fault 1, Psili Rachi Fault and Mamousia Pirghaki Fault 1, marked section f-f' in figure 34.

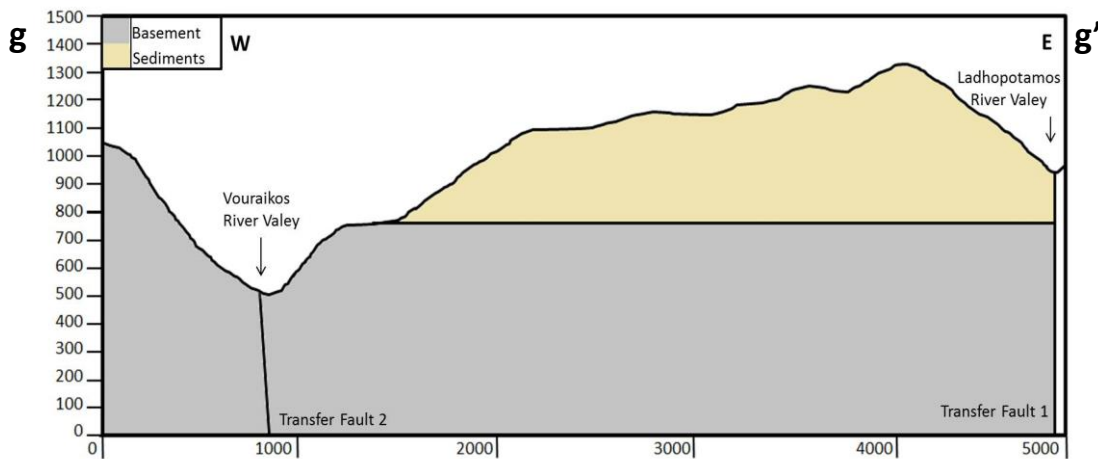


Figure 41 – Cross-section of the horst structure, perpendicular to the Vouraikos and Ladhopotamos, marked g-g' section in figure 34.

The structural investigation enforces the theory of an underlying geological structure within the N-S major river valleys that is segmenting the general W-E normal faults. The N-S valley faults have been interpreted as high angle transfer faults. The first transfer fault seems to go through the Roghi valley, continuing between Dhoumena Fault 1 and 2, through the Vouraikos valley and out through the Diakopto modern delta. The second transfer fault seems to go through the Vouraikos River and continuing through the Ladhopotamos River Valley, as shown in the geological map in figure 34 and in table 1.

By comparing two profiles (fig. 42) from each side of the interpreted transfer fault the faulting appear to be independent, at least all the way to Mamousia Pirghaki fault. There are 11 faults on the east profile and 6 on the west profile, and only three faults has similar geological features and are likely to cross the Vouraikos; Mamousia Pirghaki, Dhervini Fault and Eliki Fault.

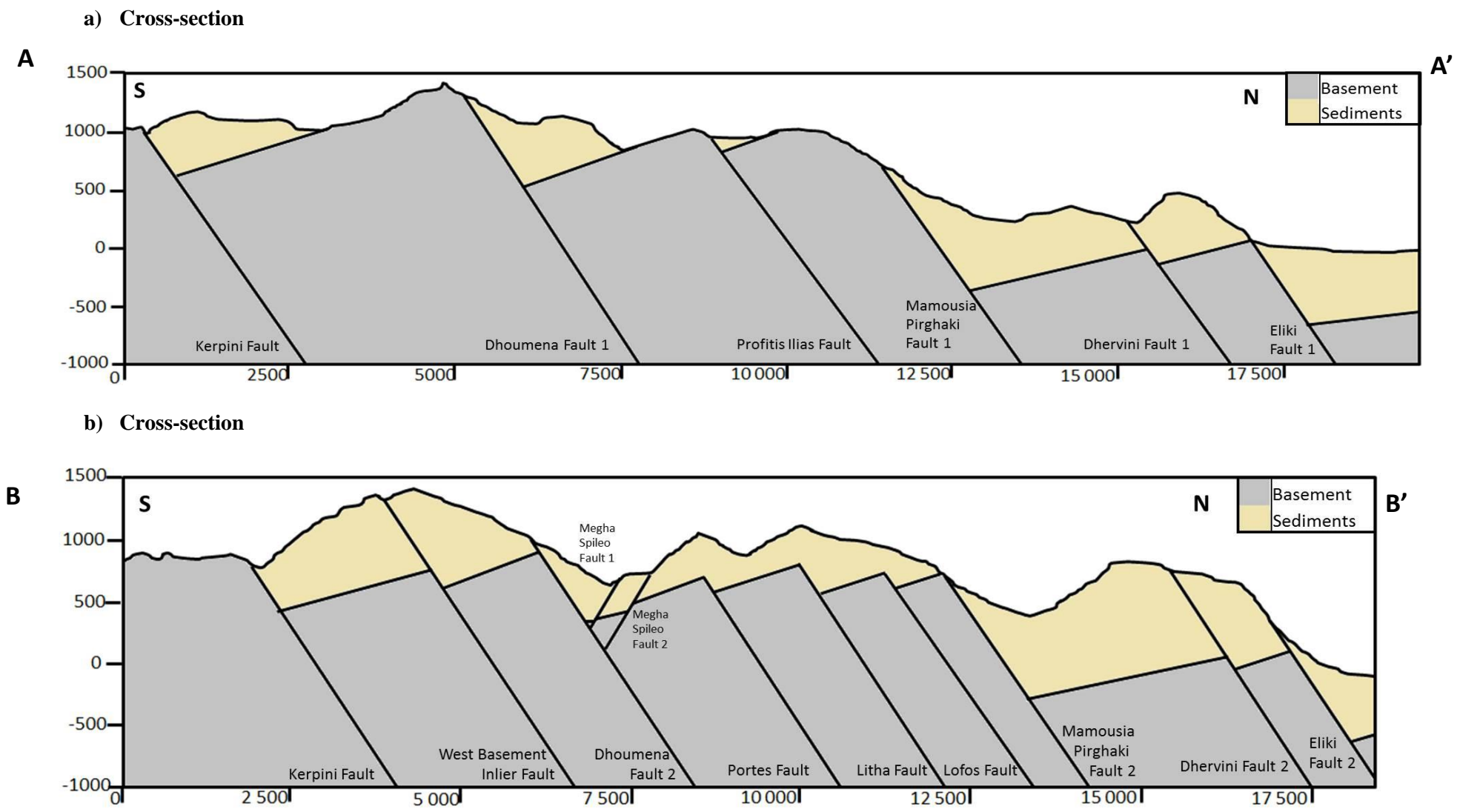


Figure 42– N-S cross-sections located in figure 34.

CHAPTER 4

4.1 3D Model Construction

All the field data were imported and applied in Petrel E&P 2014 software in order to present a spatial model of the study area. Petrel is an exploration and production software platform owned by the oil and gas company Schlumberger, the software allow the user to aggregate all the aspects related from exploration to production such as; interpretation of seismic, perform well correlation, build structural/reservoir models, volume calculation, producing maps and model simulations. The user can interact with the data directly in 3D view and control the geology of the constructed model. The spatial representation of the study area in Petrel E&P 2014 was a necessary step to gain and improve the three dimensional understanding.

The study area is mappable and above surface area, so GPS points together with digitized elevation model (DEM), which represents the true topography of the main area, was used as input data instead of seismic, figure 43. The constructed model is defined by three surfaces; the DEM Surface, Fault and Unconformity Surface and Base Surface, (fig. 44). The Fault and Unconformity Surface was constructed by joining the interpreted fault planes/surfaces together with the unconformity surface between the basement and sediments. The basal surface was set to 1000 m below sea level to limit the model. The result was a 3D model with two zones; basement zone, from Base Surface to Fault and Unconformity Surface and the second zone on top is the sediment zone restricted by Fault and Unconformity Surface and the DEM Surface, figure45.

4.2 Faults

All the faults in the model represents the faults mapped in the field, the calculation in figure 33 has been used to project fault and unconformity surfaces below the surface. Two cross-sections from the constructed model in figure 45 are represented in figure 46. The west cross-section A-A' (fig. 46a) represent a section from south to north and comprises West Chelmos Fault, West Kalavrita Fault, Kerpini Fault 1, Dhoumena Fault 1, Psili Rachi Fault, Mamousia Pirghaki Fault 1, Dhervini Fault 1 and East Eliki Fault 1.

The second cross-section, B-B' (fig. 46b) represent the east section that comprises the continuation of West Chelmos Fault and West Kalavrita Fault in section A-A', followed by

Kerpini Fault 2, West Basement Inlier Fault and Dhoumena Fault 2 that are restricted by Roghi Valley in the West and Vouraikos Valley in the east. The section B-B', crosses the Vouraikos River Valley and includes the following faults; Megha Spileo Fault 1 and 2 (antithetic faults), Portes Fault, Litha Fault, Lofos Fault, Mamousia Pirghaki Fault 2, Dhervini Fault 2 and East Eliki Fault 2.

DEM Map

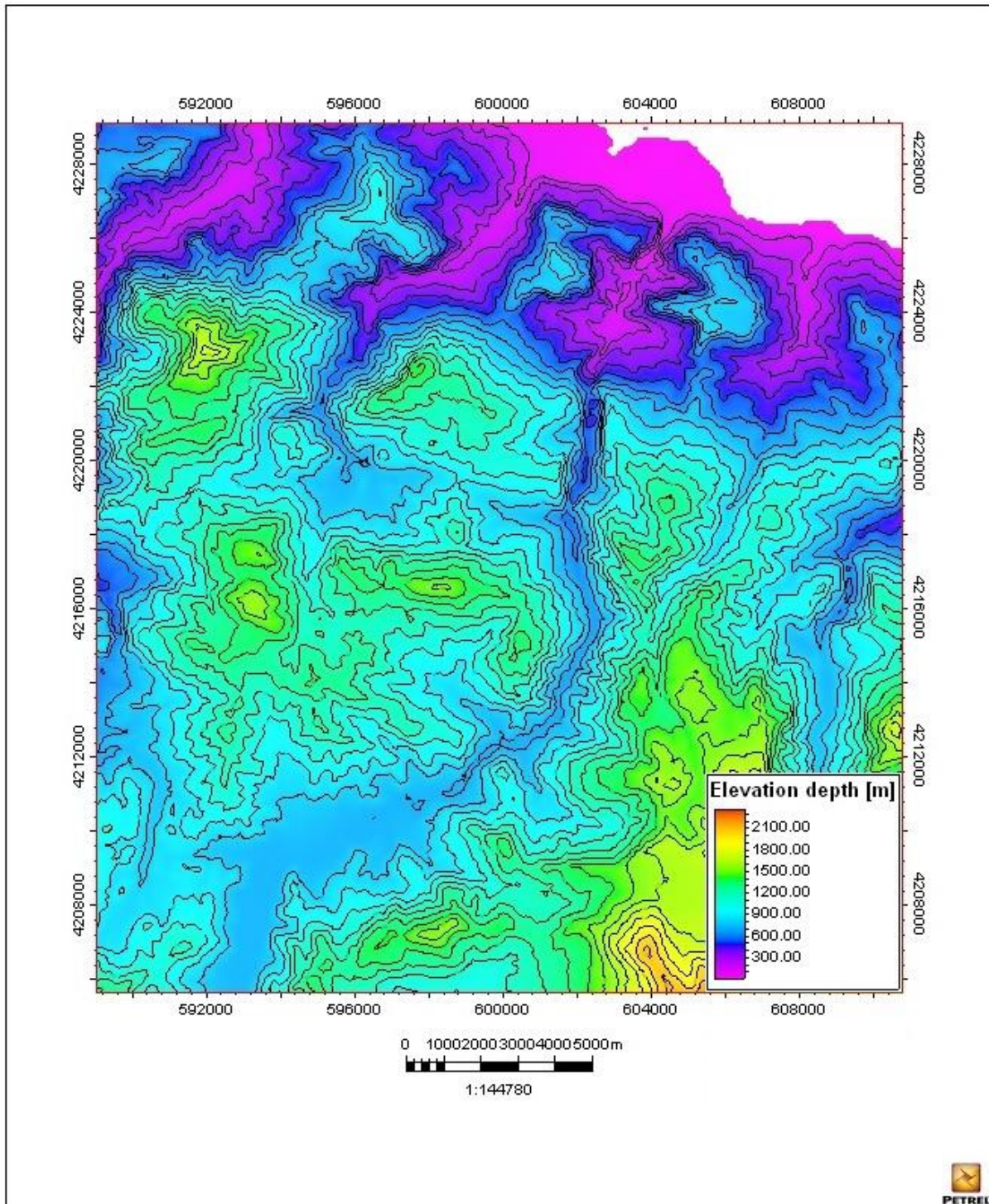


Figure 43 - Digitized Elevation Model map of the study area.

Model Surfaces

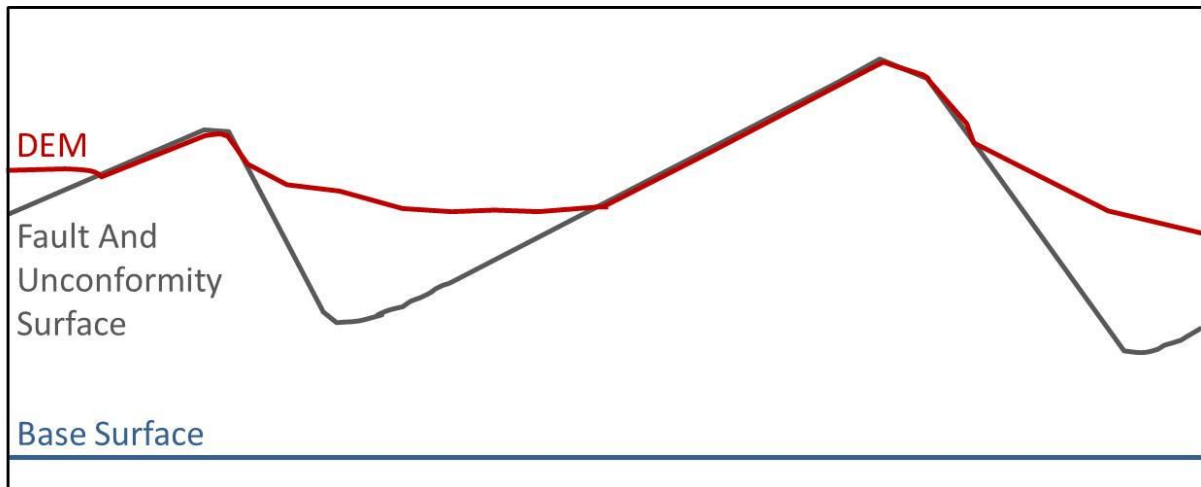


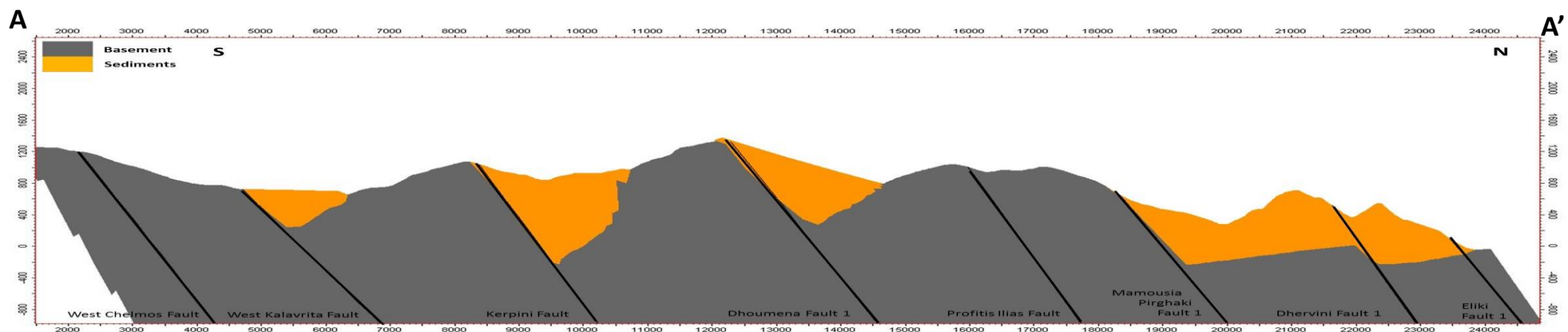
Figure 44 - The three surfaces defining the 3D model, Digitized Elevation Model (DEM), constructed fault and unconformity surface and base surface that limit the model.

3D Model



Figure 45 – 3D model representing basement (grey), sediments (orange) and the Vouraikos River (blue line), with two marked cross-sections, A and B.

a) West Section



b) East Section

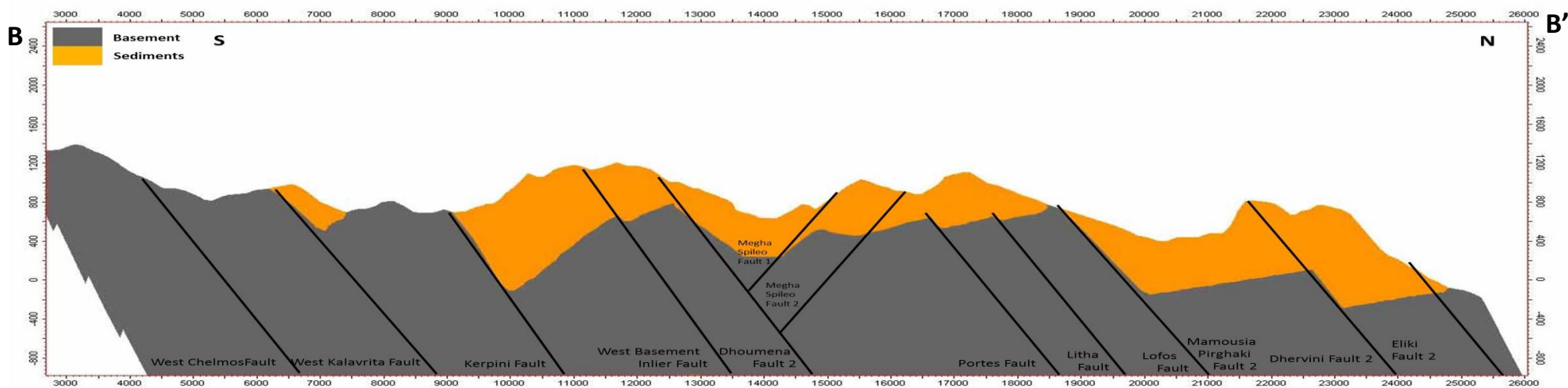


Figure 46 – N-S cross-sections located in the 3D model on figure 45.

4.3 Transfer Faults

The fault system in the area is best represented without sediments, the zone division in Petrel E&P 2014 allows us to do just that, to display the zones individually, fig 47. The fault planes represent the displacement of the faults, the unconformity plane is the eroded basement surface and separate the pre-rift basement from the syn-rift deposits. The stepping of the faults in the valleys are interpreted as NNE-SSW high angle transfer faults, Transfer Fault 1 is mapped from the stepping of Kerpini Fault in the Roghi Valley and continues underlying the north section of the Vouraikos River Valley after the bend.

Transfer Fault 2 are mapped from the stepping of Chelmos Fault, through the stepping of Kalavrita Fault and continues north along the south section of the Vouraikos River Valley, this transfer fault may continue further north, underlying the Ladhopotamos River Valley, however the latter river valley has not been mapped in this study, the transfer fault theory can only be supported in the south section of the Vouraikos, and any continuation will be an assumption.

The transfer faults were connected to all west-east trending faults; it resulted that each interpreted fault block could be displayed as a single segment in the model, fig 48. This allows each single segment to be assigned with different geological properties to obtain a better representation of the geology of the study area, for instance the fault blocks of Kerpini Fault 1, Kerpini Fault 2 and East Basement Inlier Fault are covered by different depositional systems, Kerpini Fault Block 1 is dominated by fluvial deposits, while Kerpini Fault Block 2 and East Basement Inlier Fault Block is covered by a 700 m thick package of coarse conglomeratic alluvial deposits, as mentioned in section 3.2. This was applied to each segment with the accordingly property, fig 48a. Each single segment can in addition be assigned with different number of zones; in this case Kerpini Fault Block 2 was modeled with two zones, a thin section of fluvial deposits, as a possible first event in the initiation of Kerpini Fault 2, fig 48b. The fault blocks without sediments give a better representation to the transfer fault underlying Roghi Valley and its effect on the fault steps, 48c.

4.4 Problem and Solution

The major problem of the model construction was the connection of the faults in the valleys, even by a constructed NNW-SSW transfer fault. There are 6 normal faults on the west of Transfer Fault 1, fig 46a, and 11 on the east, fig 46b, among the 11 faults are two antithetic south dipping faults that terminates parallel to Dhoumena Fault 1 in the Valley, that mean that these faults with opposite dip direction has to be connected to the transfer fault in the valley, but Petrel E&P 2014 does not allow this kind of the connection. In an attempt to solve the problem of the quantity of fault to be connected to one single transfer fault, the solution proved to solve the opposite dipping fault connection as well. Instead of one single constructed transfer fault in the valleys, two transfer faults where constructed with a gap of 1 m that acts as a single transfer fault, in this way the north dipping Dhoumena Fault 1 can be connected to one transfer fault and the south dipping Megha Spileo Fault 1 can be connected to the juxtaposed transfer fault, fig 49.

3D Model of the basement with constructed faults

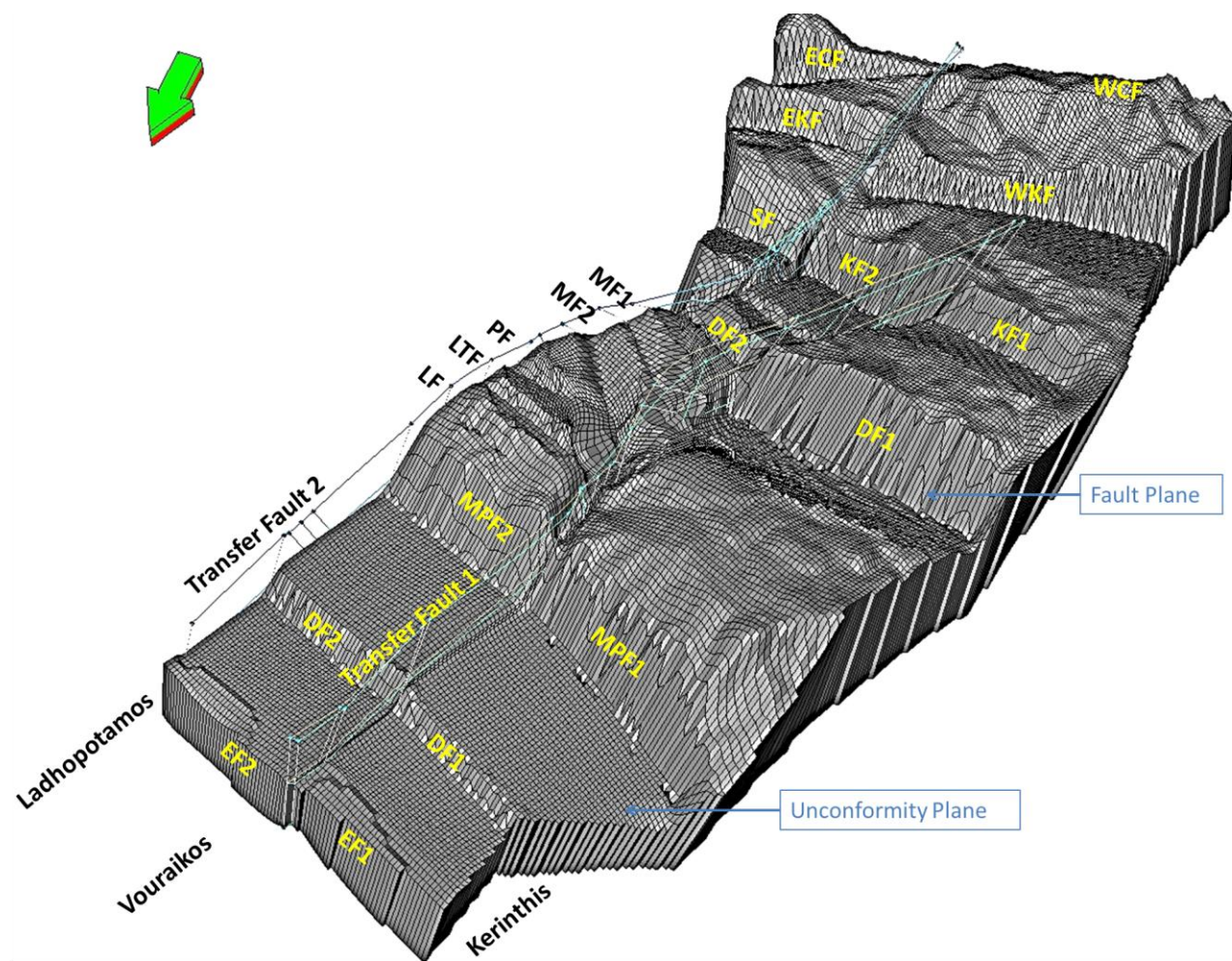


Figure 47 – 3D constructed model, displaying the basement without the sediments.

Fault blocks of KF1, KF2 and WBIF

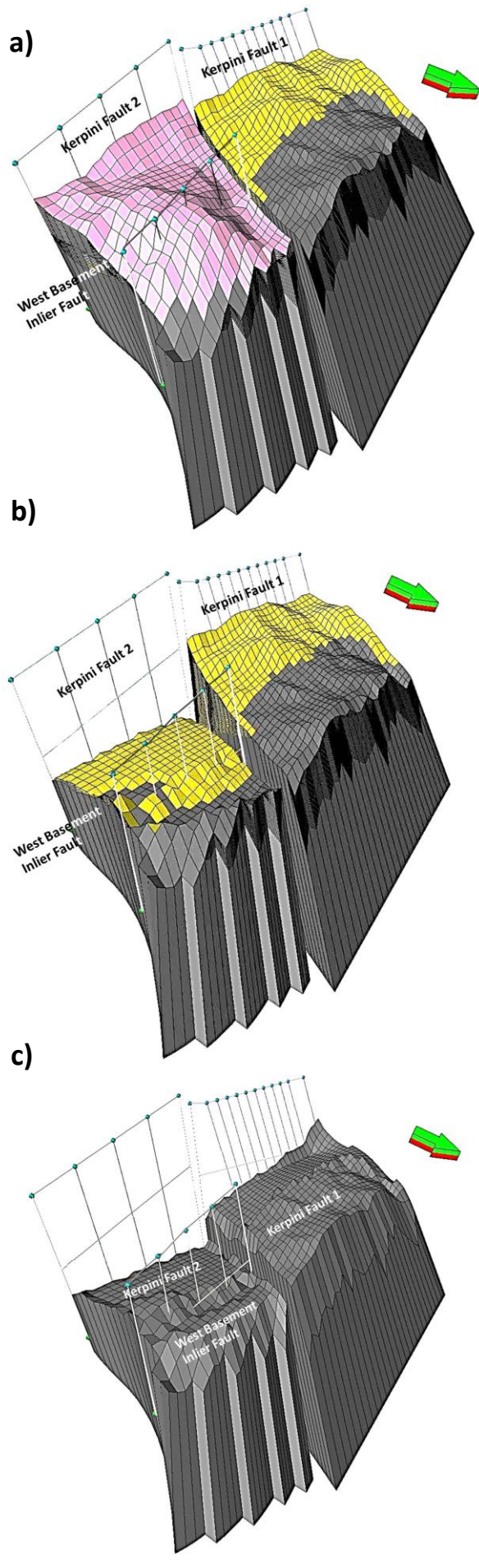


Figure 48 - Three segments from 3D model, representing the fault blocks of Kerpin Fault 1 (KF1), Kerpin Fault 2 (KF2) and West Basemnet Inlier Fault (WBIF), a) basement fault blocks overlain by sediments, b) fault blocks without the coarse sediments, c) fault blocks without sediments.



Fault construction – connecting north-dipping and south-dipping faults

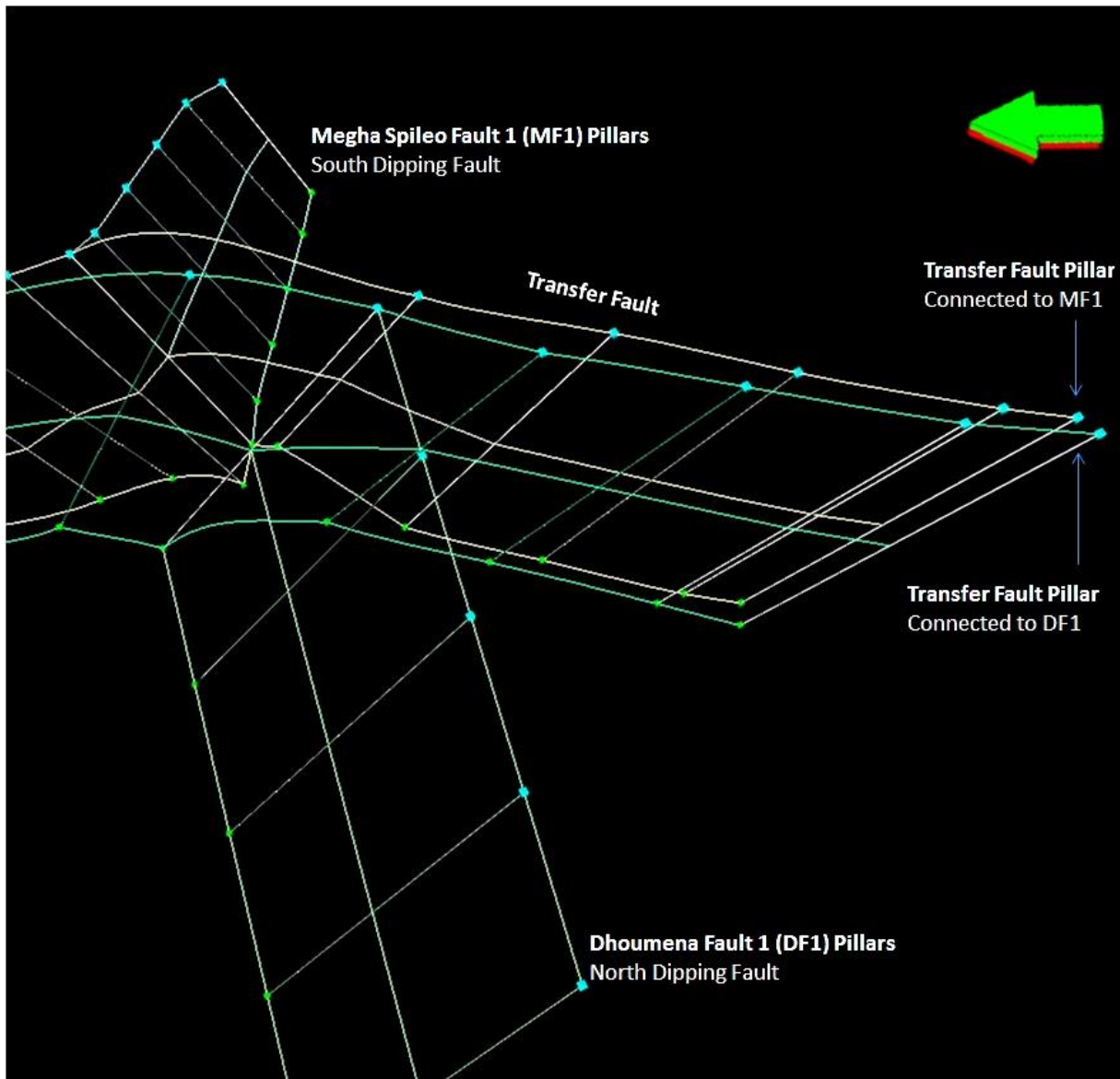


Figure 49 – North-dipping fault and south-dipping fault connected to each the transfer fault.

CHAPTER 5

5.1 Discussion

Previous work in the study area has mapped and interpreted the normal faults to be continuous across the Vouraikos Valley. An investigation through the Vouraikos valley proved that the system on the eastern side show little similarities with the western side of the valley. Kerpini and Dhoumena Fault shows several hundred meters of displacement on the west, though on the other side of the valley there is no evidence for these major faults are crossing. The Dhoumena Fault terminates in the Vouraikos River Valley and in addition defines the bending of the river; the Vouraikos changes the direction from N-NE direction at the end of the Dhoumena Fault 2 to N-NW direction that runs between Megha Spileo Fault 1 and Dhoumena Fault 2, at the termination of Megha Spileo 2 in the valley, the Vouraikos River changes back to the N-NE flow that continues all the way to the coast.

The north N-NE trending section of Vouraikos river valley aligns very well with Kerpini and Dhoumena Fault stepping in the the Roghi Valley. This section of the Vouraikos comprises both non-crossing and crossing faults. Portes Fault and Lofos Fault on the east cannot be traced on the west of the Vouraikos, Litha Fault and Psili Rachi Fault are close to aligned in the Vouraikos, but reveals 300 m of vertically separation of the basement. However the major fault of Mamousia-Pirghaki seems to cross the Vouraikos, and mark a significant change in the lithology in the study area. The area between the two major faults on the north, Mamousia-Pirghaki Fault and the coastal fault of East Eliki Fault are completely covered by deltaic sediments with no exposed basement. The Eliki Fault steps in the Kerinthis River but show no stepping through the Vouraikos River, and the minor Dhervini Fault lays between the latter two major faults, shows no clear displacement in the Vouraikos either.

The structural study in chapter 3 indicates that the basement is vertically lower on the Dhoumena Fault Block 2 and West Basement Inlier Fault Block on the east relative to Dhoumena Fault block 1. The north section of the Vouraikos reveals similar structural displacement of the basement as Roghi Valley, the uplifted basement on Litha Fault that on the east side of Vouraikos Valley is also lower than the uplifted basement on the Psili Rachi fault on the West.

The 3D structural model of the study area in Chapter 6 was generated to illustrate the structural features of the basement; how the single fault blocks may act next to each other and to present the structural role of the Vouraikos Valley. The field observation together with the

structural studies and the 3D model enforces an underlying fault in the Vouraikos River Valley, there is not a single fault underlying the Vouraikos, but the river is flowing over two high angle transfer faults, the first transfer fault is interpreted to underlay the south N-NE section of the Vouraikos Valley and this transfer fault may or may not continue under the Ladhopotamos River, further studies is needed here. The second transfer fault is interpreted to display the Kerpini Fault 1 and 2 and The Dhoumena Fault 1 and 2 in the Roghi Valley and continues north, underlying the north N-NE trending section of the Vouraikos.

5.2 Reconstruction of cross-sections

The Roghi Mountain display a far more subsided basement relative to Dhoumena Fault Block 1 and the Eastern side of Vouraikos Valley as presented in Chapter 3. The flat fluvial sediments on Roghi Mountain has a gentle south dipping angle of 5° and are overlaying alluvial deposits on West Basement Inlier Fault Block. By closing West Basement Inlier Fault and restoring the bedding to similar dip as in Kerpini Fault Block 2, the flat sediments become horizontal, implying that these fluvial sediments incised into Roghi Mountain are pre-faulting of West Basement Inlier Fault, see figure 50.

The basement subsidence in Roghi Mountain may be linked to the horst structure through transfer fault, the horst structure comprises 5 faults, and these faults may be linked to the subsidence magnitude in Roghi Mountain. We know from chapter 2 that the two south dipping fault; Megha Spileo 1 and 2 are post-impacting faults to all the sediments, similarly as the West Basement Inlier, the latter three faults could be linked to similar geological event, and may have initiated simultaneously. The remaining north dipping faults on the horst structure expose three tilted basement fault blocks; Portes, Litha and Lofos, all the fault blocks are overlain by onlapping sediments as shown in chapter 2.8. The onlapping sediments are fluvial sediments that shows syn- to post-faulting characteristics. Furthermore the basement on the footwall of Portes Fault are 100 m lower than on the hangingwall of Litha Fault and seems to display the onlapping sediments, this may imply that Portes Fault initiated after the faulting of Litha Fault, Lofos Fault is a minor fault that may have initiated due to the same event. This means the fault evolution in the horst structure started with Litha Fault followed by Portes Fault and Lofos Fault. The latter two minor faults; Portes Fault and Lofos Fault reflects a further rifting that only exists on the east side of the Vouraikos Valley, these faults occurred at an early stage and this may link to the large displacement of Kerpini Fault 2, figure 51.

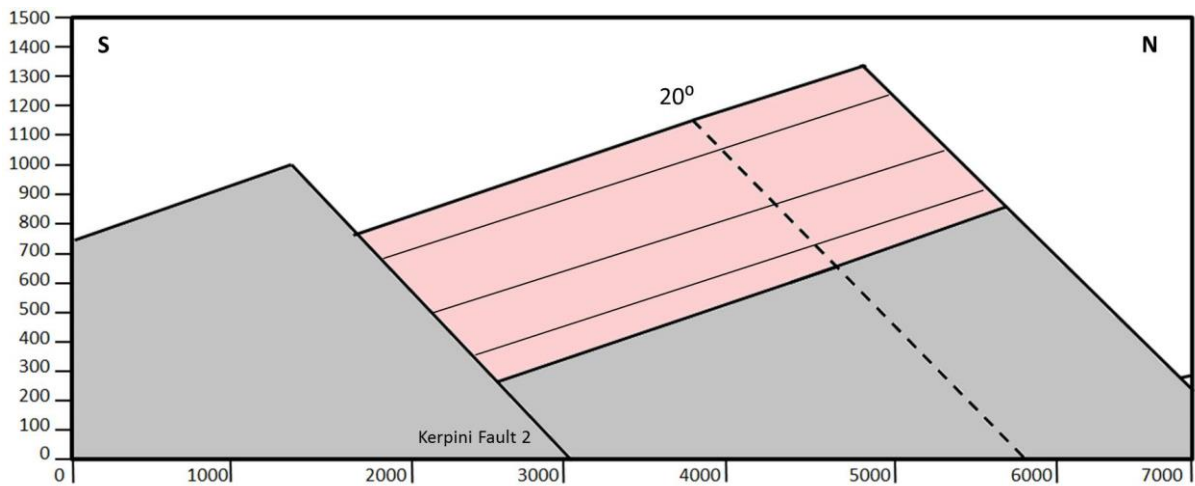
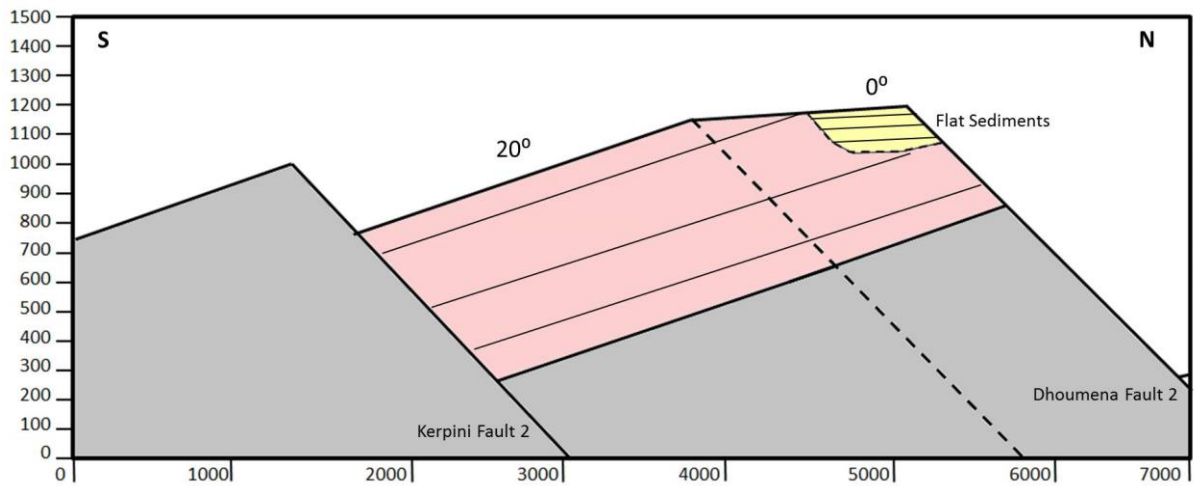
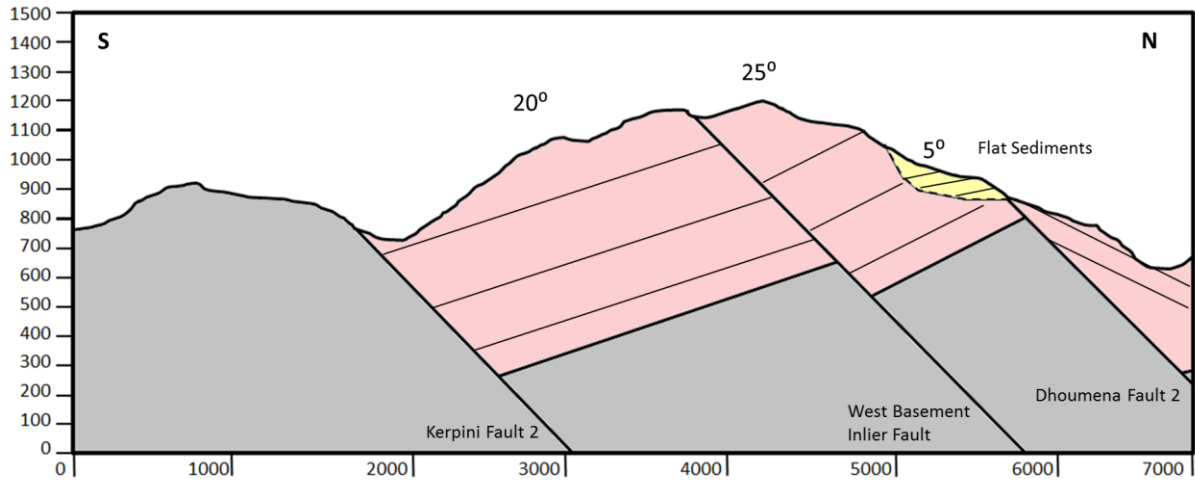


Figure 50 – Restoration of Roghi cross-section based on figure 36.

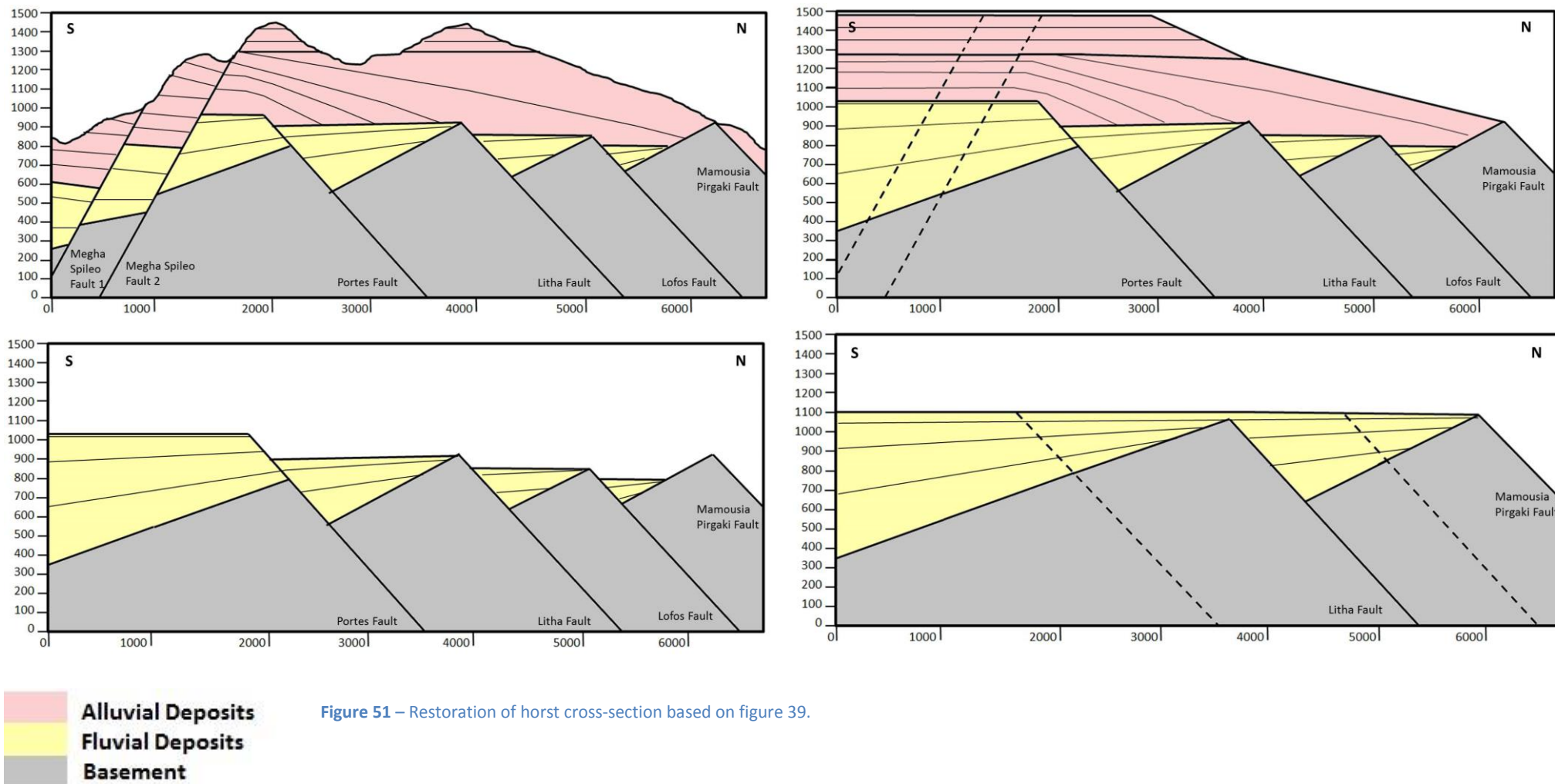


Figure 51 – Restoration of horst cross-section based on figure 39.

5.3 East Section

The above section and restoration of Roghi Mountain and the horst structure are used to construct a restoration of the fully eastern part of the study area (fig.52), presented as section A-A' in figure 34. The initiation of Kerpini Fault was followed by a coarse conglomeratic alluvial fan, as Dhoumena Fault was activated; it created a barrier for the sediments in Kerpini Fault Block, finer sediments prograded further from west to east in Dhoumena Fault Block, Litha Fault block and affected probably further north as areas (fig.52a).

Further rifting results the initiation of Portes Fault, Lofos Fault, and the further subsiding of Kerpini Fault 2. The prograding alluvial fan is revealing syn-fault characteristics on Kerpini Fault 2 and post-fault deposition on the northern faults blocks, such as Portes, Litha and Lofos. The deposition of the alluvial fan reached Kerpini Fault 2 at an active fault face (same time as the activation of Portes and Lofos Fault) and by the time the sediments covered the northern section the faults (Portes and Lofos) are already reached its maximum climax, 52b.

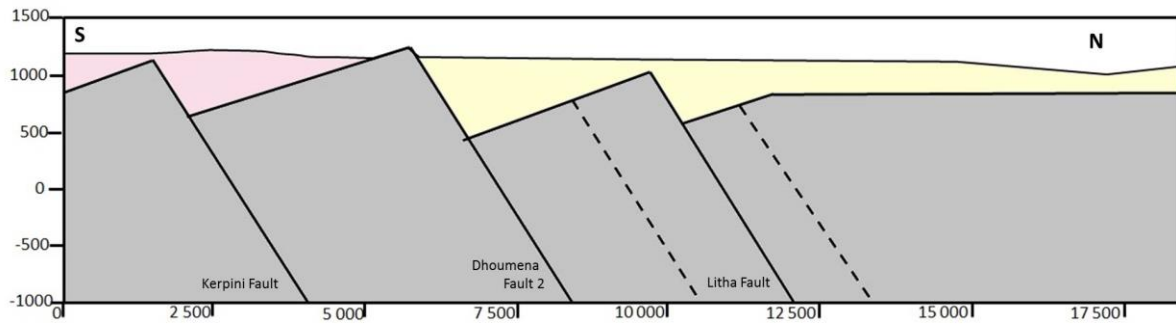
The Vouraikos River can be responsible for several major prograding sediments, but as the Mamousia Pirghaki Fault initiated the Vouraikos started feeding the delta in the new evolving Corinth, fig. 52c.

A late collapse in the Kerpini Fault block 2 (West Inlier Fault) and Dhoumena Fault 2 (Megha Spileo 1 and 2), fig. 52d.

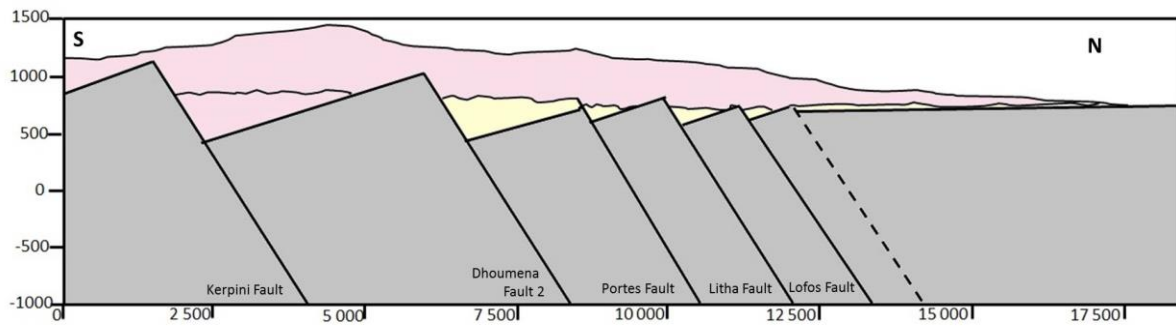
The Dhervini Fault is displacing the delta after deposition (fig. 52e) as the Vouraikos is eroding through the ancient delta to create a new delta on the subsiding East Eliki Fault, fig. 52f.

EAST CROSS-SECTION RESTORATION

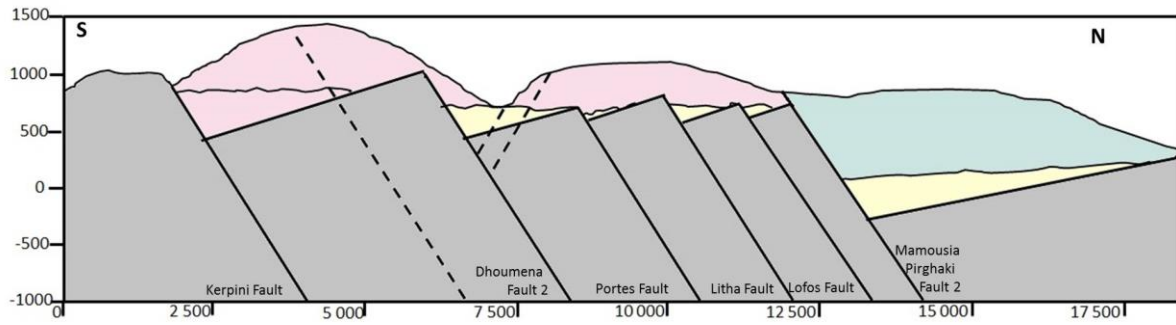
a)



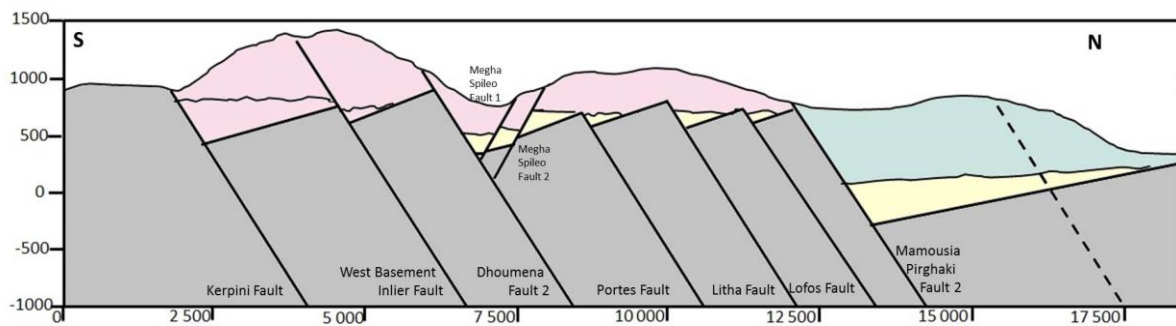
b)



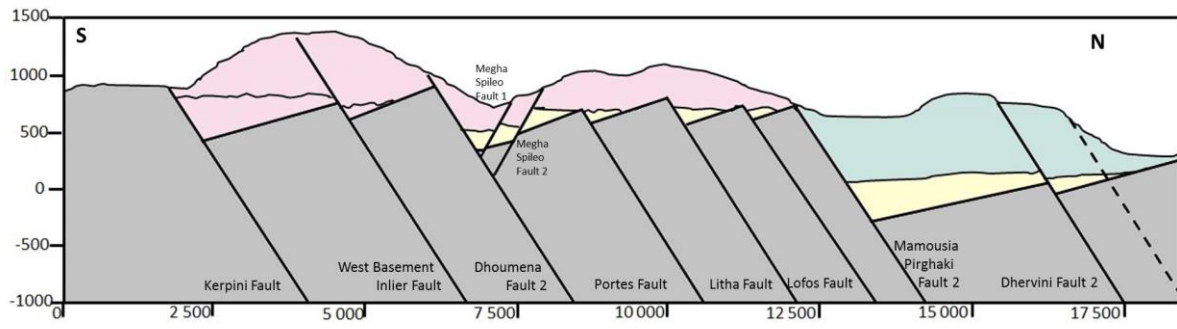
c)



d)



e)



f)

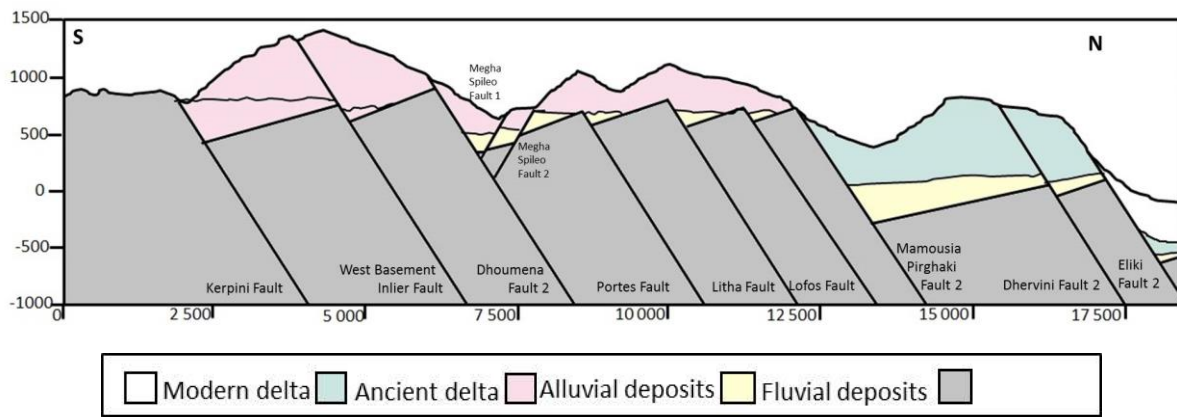


Figure 52- East section restored, based on cross-section B-B' in figure 34.

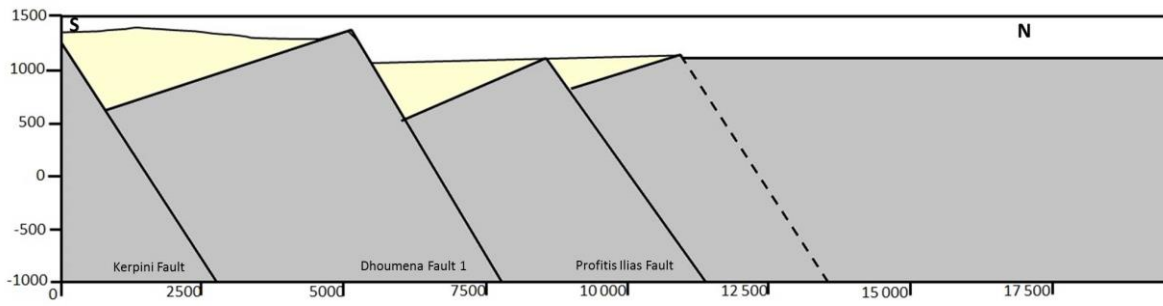
5.4 West Section

A similar restoration was constructed for the west section of the study area (fig. 53), presented as section B-B' in figure 34. The biggest displacement of Kerpini Fault is found in the Kerpini Fault 2, indicating that the fault initiated at the east and prograded to the west. Kerpini Fault 1 steps 200-300 m in the Roghi Valley, and initiated first in the west section. The Kerpini Fault Block is overlain by mostly alluvial deposits that deposited after the deposition of the alluvial fan in Roghi Mountain. Following the Kerpini Fault is the faulting of Dhoumena Fault followed by Psili Rachi, fig. 53a. The Faults may have been balanced on the both side of the Vouraikos at a certain time, see figure 52a and 53a.

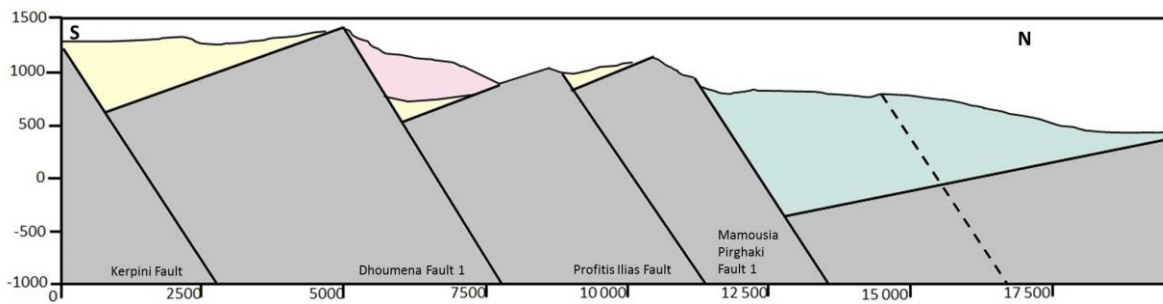
The ancient delta was fed by the Vouraikos River and is covering the entire fault block of Mamousia Pirghaki, fig. 53b. The Dhervini Fault is affecting the delta on both sides of the Vouraikos, the Dhervini fault is minor fault that collapsed as the Mamousia Pirghaki Fault Block was tilted, fig. 53c. The last fault to the north is East Eliki Fault 1, separating the uplifted peninsula from the subsiding Corinth, fig. 53d.

WEST CROSS-SECTION RESTORATION

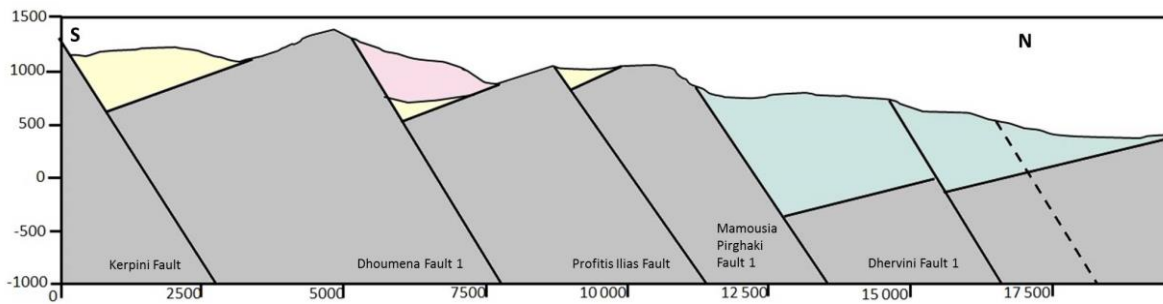
a)



b)



c)



d)

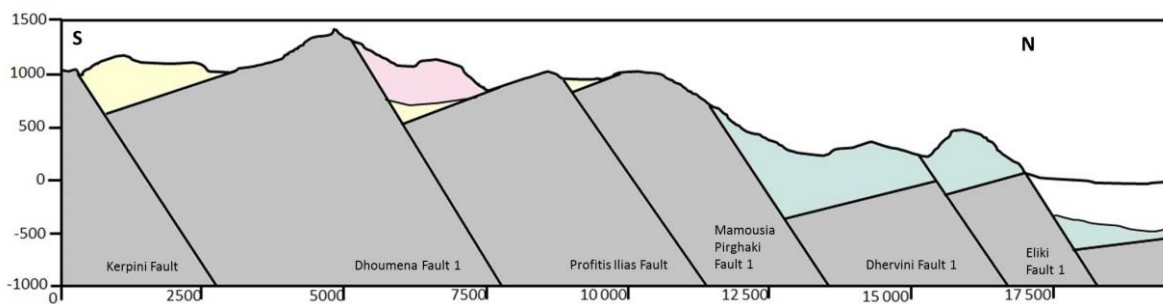


Figure 53- West crss-section restored based on A-A' section in figure 34.

5.5 Evolution History of the Study Area

The Kerpini Fault initiated in the east and prograded to the west, the fault steps in the Roghi Valley underlain by a transfer fault that allow the extension to be transferred from Kerpini Fault 2 to Kerpini Fault 1, the transfer fault are presented as extensional strike slip fault with a high angle fault plane. The alluvial fan in Kerpini Fault Block 2 created a barrier for the west-east flowing rivers, but the fluvial deposits incise the top of Roghi. The transfer fault transferred Dhoumena Fault, and at a later stage transferred Litha and Psili Rachi Faults, west-east flowing rivers filled the accommodation space, fig. 55.

The pronounced difference in extensional accommodation space between east and west section are due to the development of the transfer fault, a further extension and subsidence in the east section caused the collapse of Portes and Lofos Fault within Dhoumena Fault Block 2 and Litha Fault Block, this created accommodation space for the north-south prograding alluvial fan that covered the east section, these sediments are only deposited in the east, on the west section debris-flow fans are deposited at the footwall of Dhouena Fault, fig. 56.

The major Mamousia Pirghaki Fault created a great subsidence in the basement and space for the Vouraikos fed delta in the new evolving Gulf of Corinth, fig. 57. A further collapse in the east section in Kerpini Fault Block 2 and Dhoumena Fault Block 2 creates a graben structure that defines the present shape of the Vouraikos River Valley, fig 58. The delta has been uplifted and faulted twice, by Dhervini Fault (fig.58), and at a later state uplifted and faulted by East Eliki Fault, the Vouraikos Valley cut through the ancient delta and created the modern delta on the hangingwall of the East Eliki Fault. Fans are deposited into the Vouraikos as the valley is eroded deeper, especially in the north Roghi part, fig. 59.

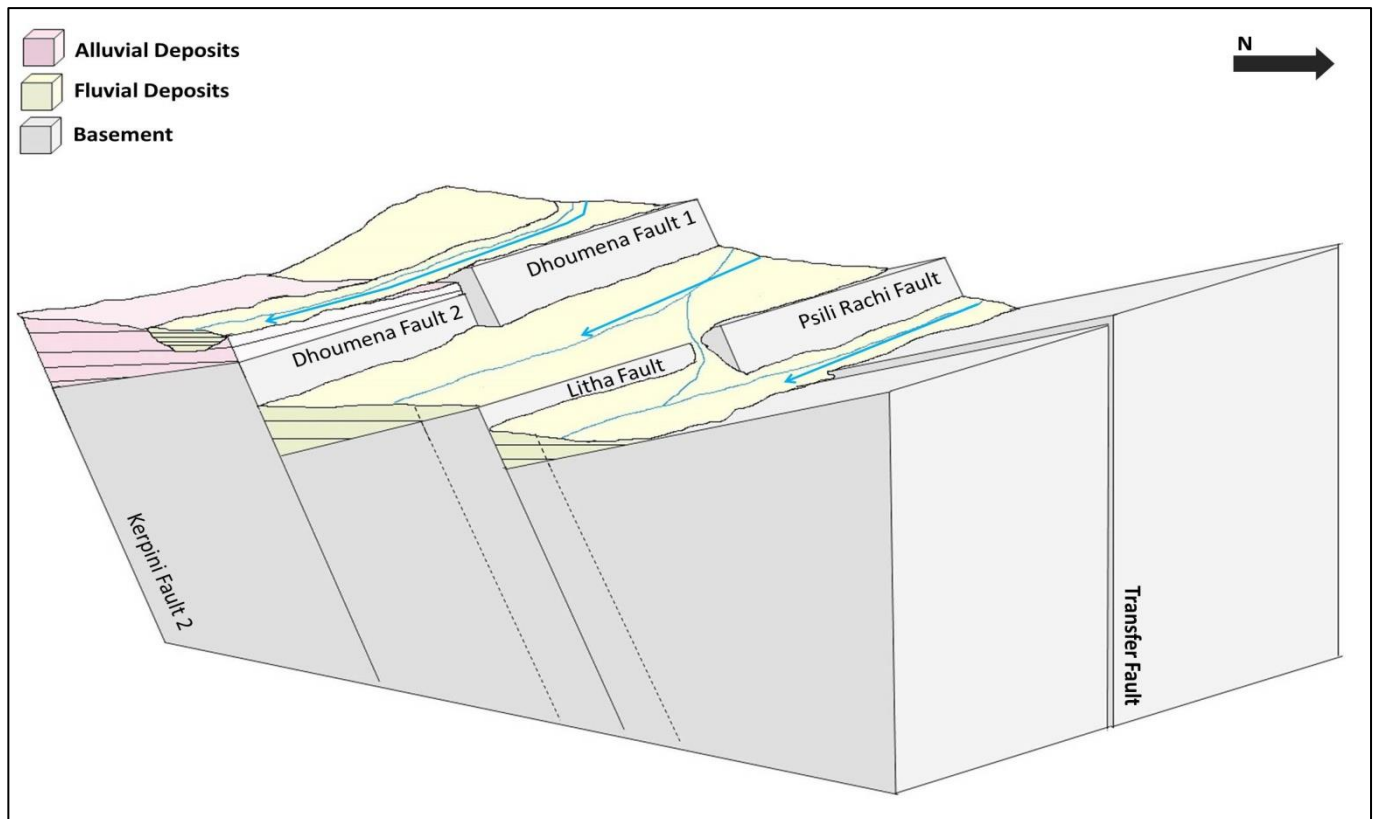


Figure 54 – Sketched 3D model of the study area at an early stat: Kerpini -, Dhoumena-, Litha- and Psili Rachi Fault are faulted, and Portes Fault and Lofos Fault has initiated.

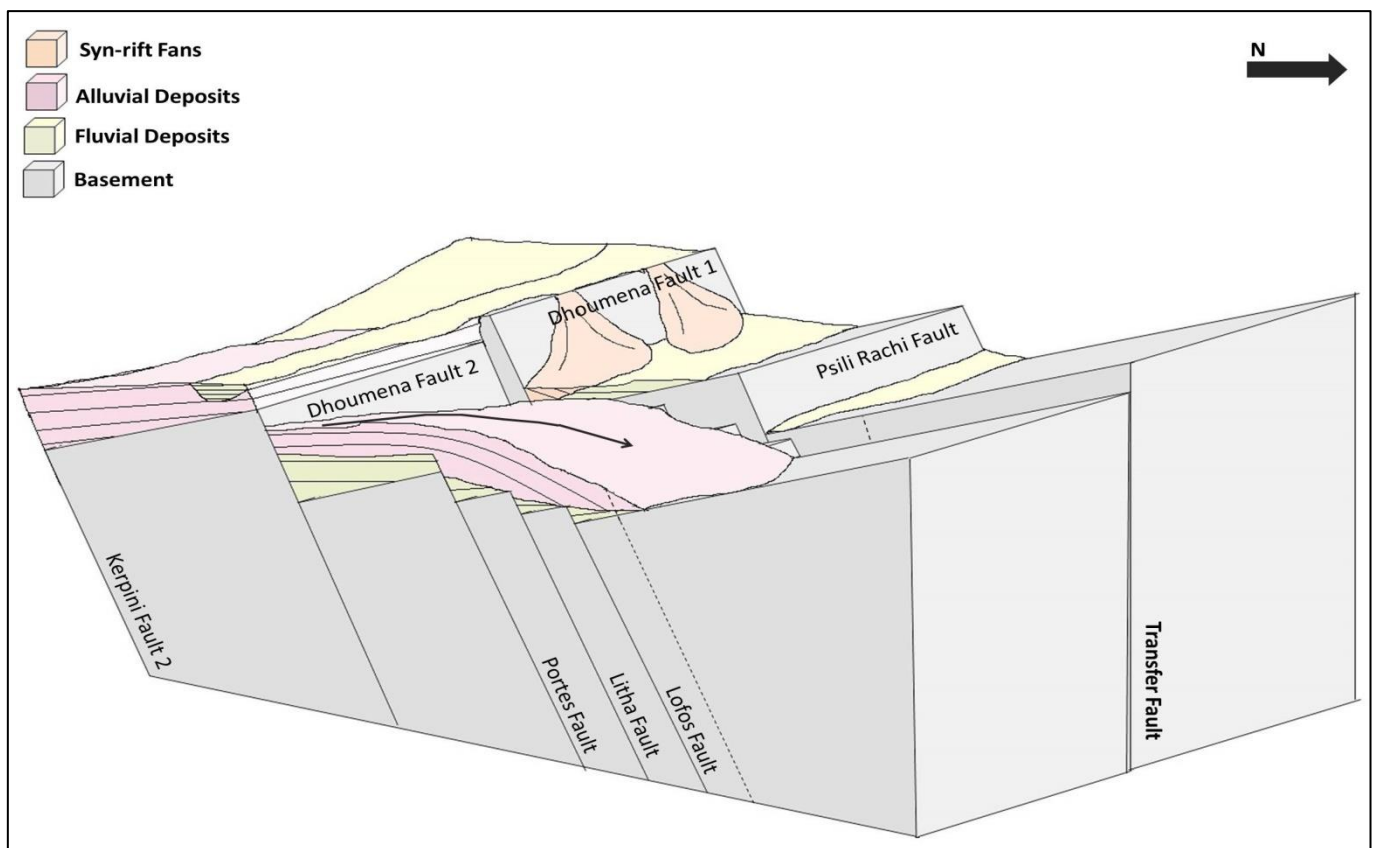


Figure 55 – Sketched 3D model of the study area after the deposition of the S-N propogation of alluvial fan, Mamousia Pirghaki has initiated.

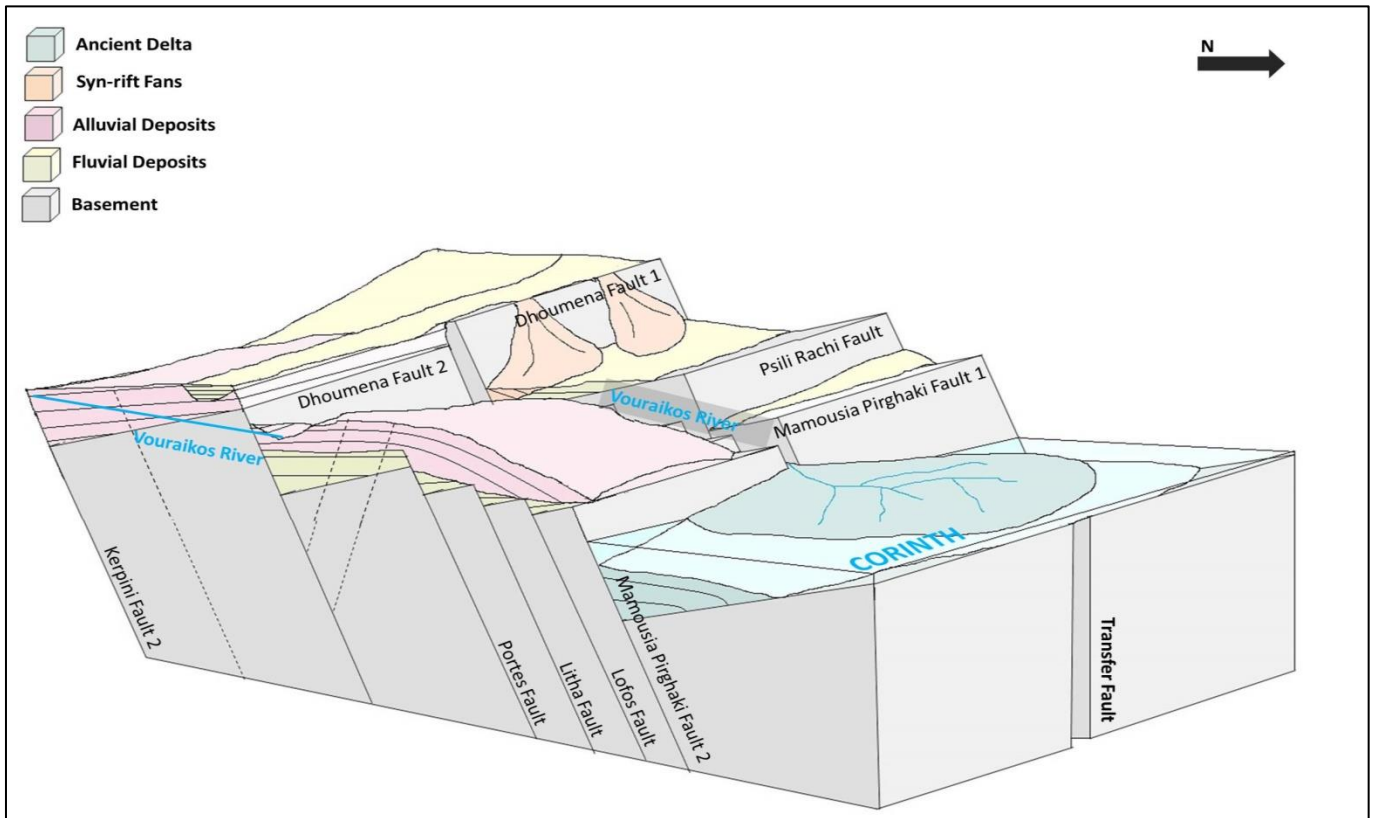


Figure 56 – Sketched 3D model of the study area, the Vouraikos is feeding the delta in the new evolving Gulf of Corinth, failure in the Kerpini Fault Block 2 and Dhoumena Fault Block 2.

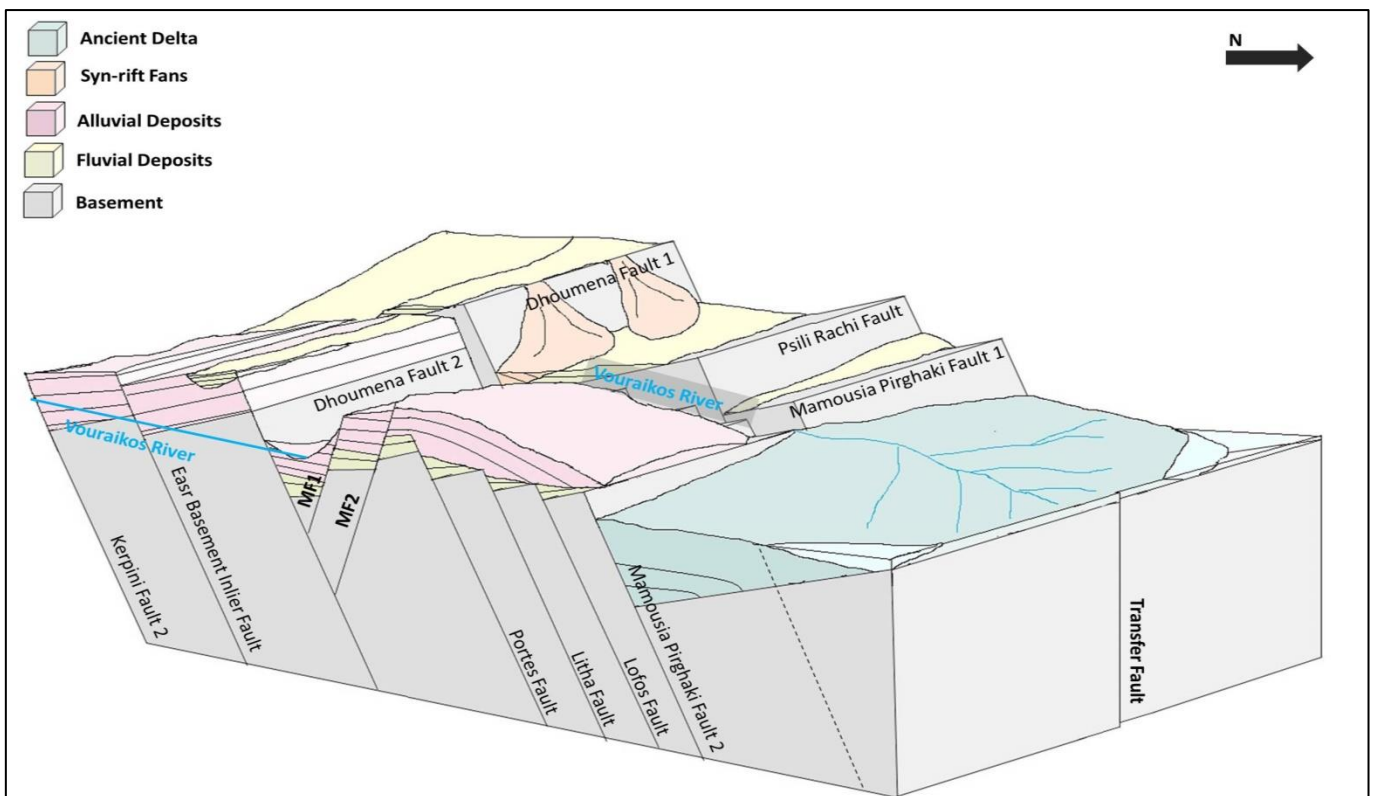


Figure 57 – Sketched 3D model of the study area, graben structures are created in the Dhoumena Fault Block 2 by 2 south dipping faults, the West basement Inlier has also collapsed, the delta is being uplifted and the Dhervini Fault has initiated.

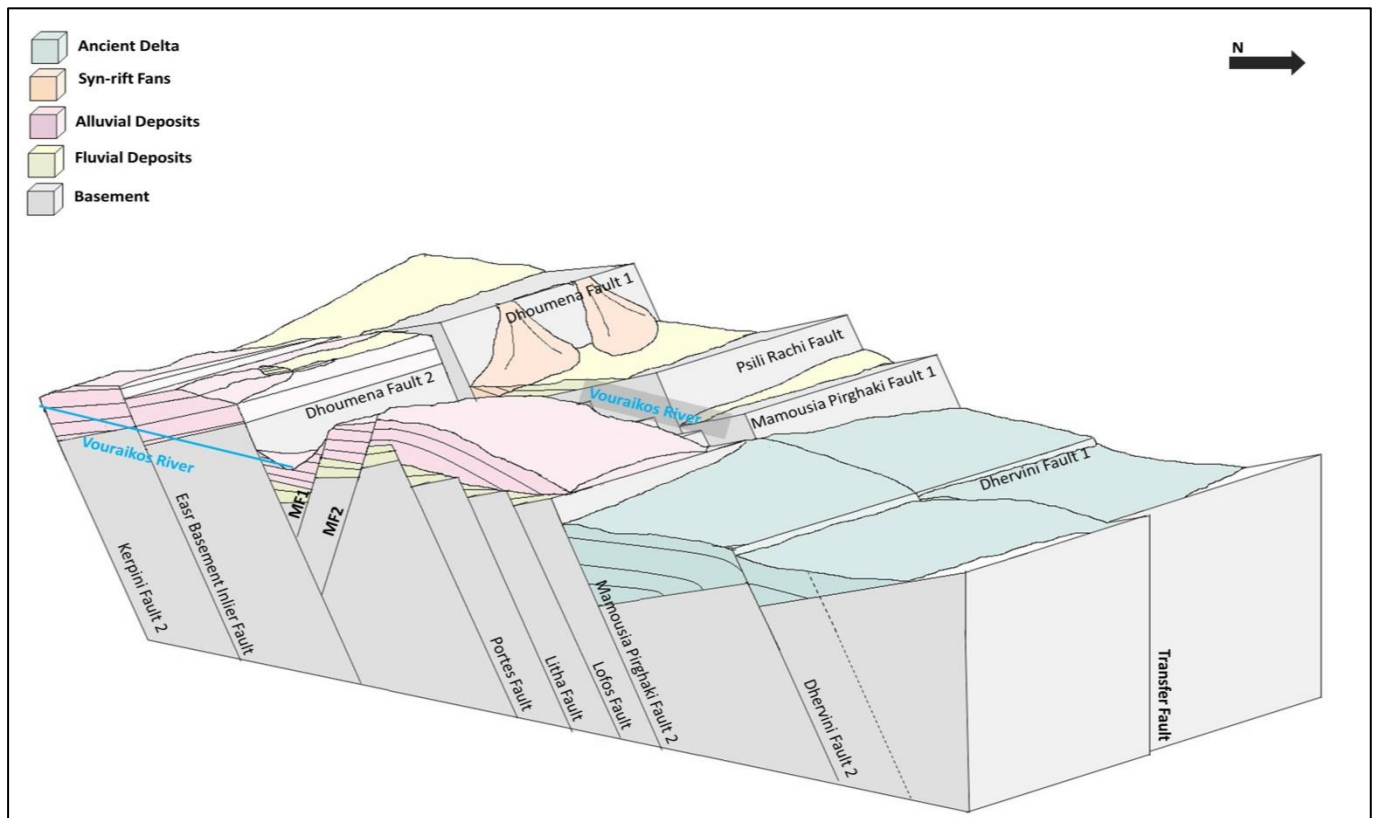


Figure 58 – The Vouraikos is cutting through the ancient delta and the East Eliki Fault is initiating in the uplifted Dhervini Fault block.

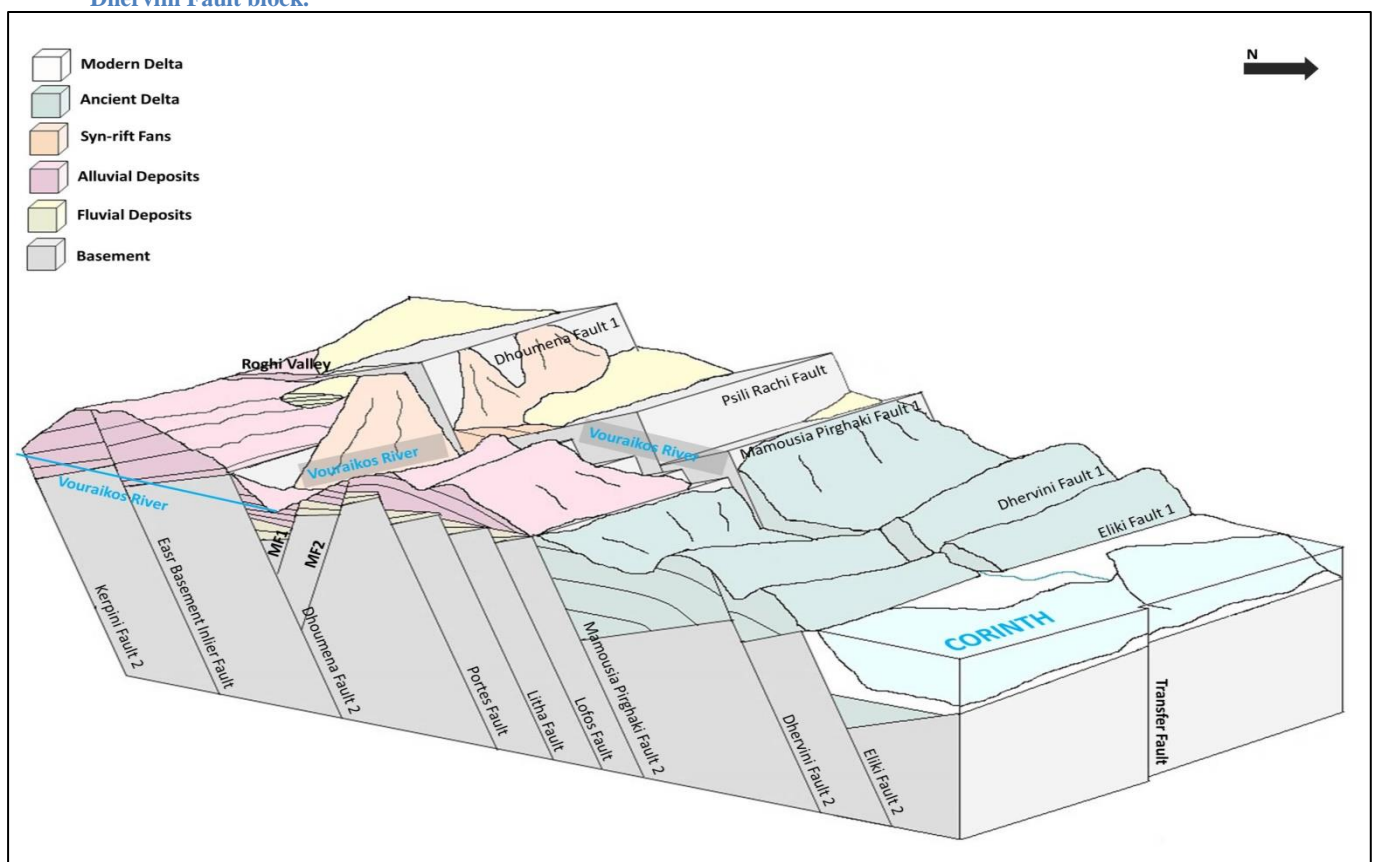


Figure 59 – Sketched 3D model of the study area of the current situation, the still active East Eliki Fault is separating the uplifted peninsula from the subsiding gulf.

CHAPTER 6

6.1 Conclusion

The onshore stratigraphies show that the study area has undergone several rifting stages that may be due to the increase of the extensional rate as proposed by Ford et al., (2013). The rift stages are separated by three general depositional systems:

- Coarse alluvial fans due to the uplift and erosion of the footwalls of the early inactive faults; Chelmos- , Kalavrita- and Kerpini Fault.
- General west-east directed fluvial deposits, forced by the barriers of the uplifted footwalls, this event filled and covered the early Dhoumena Fault Block, and is preserved below the alluvial fans in Dhoumena Fault 1 and in the horst structure.
- The upper section is a major south-north progradational alluvial fan that may be linked to the initiation of Mamousia-Pirghaki Fault and the feeding of the delta in the new evolving Gulf.

All the faults and lithology properties indicate an underlying high angle SSW-NNE transfer fault in the valleys, the transfer fault transferred two adjacent faults that experienced different displacement and strain as we see in Kerpini Fault Blocks 1 and 2. However the north faults of Mamousia-Pirghaki, Dhervini and East Eliki do not show any clear stepping in the Vouraikos Valley, but any fault correlation in this valley section is very challenging, as there is no exposed pre-rift basement. In this case it's inconclusive if a transfer fault is underlying the north Vouraikos River Valley. However the total fault displacement of the east section exceed the west section with 1300 m (table 1, chapter 3), and the distance between Kerpini Fault 2 and East Eliki Fault 2 compared with the distance between Kerpini Fault 1 and East Eliki Fault 1 is approximately 1000 m longer, suggestion that the east section has undergone more rifting, and this theory can be supported by the overall higher exposed basement on the west. So the carbonate basement may be vertically displaced below the ancient delta and/or is experiencing different strain and rifting, that could result different displacement in the different fault blocks in the future when the active faults have reached an inactive state.

References

- Armijo, R., Meyer, B., Hubert, A. & Barka, A.** (1999) Westward propagation of the north Anatolian into the northern Aegean: timing and kinematics. *Geology*, 27, 267–270.
- Avallone, A., Briole, P., Agatza-Balodimou, A.M., Billiris, H., Charade, O., Mitsakaki, C., Nercessian, A., Papazissi, K., Paradissis, D. & Veis, G.** (2004) Analysis of eleven years of deformation measured by GPS in the Corinth Rift Laboratory area. *C.R. Geosciences*, 336, 301–311.
- Bell, R., McNeill, L., Henstock, T. & Bull, J.** (2011) Comparing extension on multiple time and depth scales in the Corinth rift, central Greece. *Geophys. J. Int.*, 186, 463–470, doi: 10.1111/j.1365-246X.2011.05077.
- Bernard, P., Lyon-Caen, H., Briole, P., Deschamps, A., Boudin, F., Makrourpoulos, K., Papadimitriou, P., Lemeille, F., Patau, G., Billiris, H., Paradissis, D., Papazissi, P., Castarede, H., Charade, O., Nercessian, A., Avallone, D., Pachiani, F., Zahradnik, J., Sacks, S. & Linde, A.** (2006) Seismicity, deformation and hazard in the western rift of Corinth: New insights from the Corinth Rift Laboratory (CRL). *Tectonophysics*, 426, 7–30.
- Bozkurt, E.** (2001) Neotectonics of Turkey – a synthesis. *Geodinamica Acta*, 14, 3-30.
- Briole, P., Rigo, A., Lyon-Caen, H., Ruegg, J., Papazissi, K., Mistakaki, C., Balodimou, A., Veis, G., Hatzfeld, D. & Deschamps, A.** (2000) Active deformation of the Gulf of Korinthos, Greece: results from repeated GPS surveys between 1990 and 1995. *J. Geophys. Res.*, 105, 25605–25625.
- Brun, J.P.**, (2014) *Tectonics – Extension Systems*, 76-79.
- Collier, R. and Jones, G.** (2004) Rift Sequences of the Southern Margin of the Gulf of Corinth (Greece) as Exploration / Production Analogues. *Search and Discovery*, 50007.
- Collier, R.E.L. & Dart, C.J.** (1991) Neogene to Quaternary rifting, sedimentation and uplift in the Corinth Basin, Greece. *J. Geol. Soc., London*, 148, 1049–1065.
- Collier, R.E.L., Leeder, M.R., Rowe, P.J. & Atkinson, T.C.** (1992) Rates of tectonic uplift in the Corinth and Megara Basins, central Greece. *Tectonics*, 11, 1159–1167.
- Clarke, P., Davies, R., England, P., Parsons, B., Billiris, H., Paradissis, D., Veis, G., Cross, P., Denys, P., Ashkenazi, V., Bingley, R., Kahle, H.-G., Müller, M.V. & Briole, P.** (1998) Crustal strain in Central Greece from repeated GPS measurements in the interval 1989–1997. *Geophys. J. Int.*, 134, 195–214.
- Dart, C.J., Collier, R.E.L., Gawthorpe, R.L., Keller, J.V.A. & Nichols, G.** (1994) Sequence stratigraphy of (?)Pliocene- Quaternary synrift, Gilbert-type fan deltas, northern Peloponnesos, Greece. *Mar. Petrol. Geol.*, 11, 545–560.
- Davies, R., England, P., Parsons, B., Billiris, H., Paradissis, D. & Veis, G.** (1997) Geodetic strain of Greece in the interval 1892–1992. *J. Geophys. Res.*, 102 (B11), 24571–24588.

Dawers, N.H., Anders., M.H., (1995) Displacement-length scaling and fault-linkage. *Journal of Structural Geology* 17, 607-614.

Ebinger, C.J., Deino, A.L., Drake, R.E., Tesha, A.L., (1989) Chronology of volcanism and rift basin propagation: Rungwe Volcanic Province, East Africa. *Journal of Geophysical Research* 94, 15785-15803

Doutsos, T. and Piper, D.J.W. (1990) Listric faulting, sedimentation, and morphological evolution of the Quaternary eastern Corinth rift, Greece: First stages of continental rifting. *Geological Society of America Bulletin*, 102, 812-829.

Doutsos, T. & Poulimenos, G. (1992) Geometry and kinematics of active faults and their seismotectonic significance in the western Corinth-Patras rift (Greece). *J. Struct. Geol.*, 14, 689–699.

Doutsos, T., Kontopoulos, N. & Poulimenos, G. (1988) The Corinth-Patras rift as the initial stage of continental fragmentation behind an active island arc (Greece). *Basin Res.*, 1, 177–190.

Ferintinos, G. and Brooks, M. (1984) Tectonics and Sedimentation in the Gulf of Corinth and the Zakynthos and Keffalinia channels, western Greece. *Tectonophysics*, 110, 25-54.

Flotté, N., Sorel, D., Müller, C. & Tensi, J. (2005) Along strike changes in the structural evolution over a brittle detachment fault: Example of the Pleistocene Corinth-Patras rift (Greece). *Tectonophysics*, 403, 77–94.

Flotté, N. and Sorel, D. (2001) Structural cross-sections through the Corinth–Patras detachment fault-system in northern Peloponnesus (Aegean arc Greece). *Bulletin Geological Society Greece*, **XXVI**, 235-241.

Ford, M., Rohais, S., Williams, E.A., Bourlange, S., Jouselin, D., Backert, N. and Malartre, F. (2013) Tectono-sedimentary evolution of the western Corinth rift (Central Greece). *Basin Research*, **25**, 3-25.

Jackson, J.A., Gagnepain, J., Houseman, G., King, G.C.P., Papadimitriou, P., Soufleuris, C. & Virieux, J. (1982) Seismicity, normal faulting and the geomorphological development of the Gulf of Corinth (Greece): the Corinth earthquakes of February and March 1981. *Earth Planet. Sci. Lett.*, 57, 377–397.

Jolivet, L. (2001) A comparison of geodetic and finite strain pattern in the Aegean, geodynamic implications. *Earth Planet. Sci. Lett.*, 187, 95–104.

Koukouvelas, I.K., Asimakopoulos, M. & Doutsos, T.T. (1999) Fractal characteristics of active normal faults: an example of the eastern Gulf of Corinth, Greece. *Tectonophysics*, 308, 263–274.

Leeder, M.R., Mack, G.H., Brasier, A.T., Parrish, R.R., McIntosh, W.C., Andrews, J.E. and Duermeijer, C.E. (2008) Late-Pliocene timing of Corinth (Greece) rift-margin fault migration. *Earth and Planetary Science Letters*, **274**, 132-141.

- Lyon-Caen, H., Papadimitrion, P., Deschamps, A., Bernard, P., Makropoulos, K., Pacchiani, F. & Patau, G.** (2004) First results of CRLN seismic array in the western Corinth rift: evidence for old fault reactivation. *C.R. Geosciences*, 336, 343–352.
- Moretti, I., Sakellariou, D., Lykousis, V. and Micarelli, L.** (2003) The Gulf of Corinth: an active half graben? *Journal of Geodynamics*, 36, 323-340.
- Mack, G.H., Seager, W.R.,** (1995) Transfer zone in the southern Rio Grande Rift. *Journal of the Geological Society, London* 152, 551-560.
- Macdonald, K. C., Fox, P.J.,** (1983) Overlapping spreading centers: new accretion geometry on the East Pacific Rise. *Nature* 302, 55-58.
- McKenzie, D.,** (1972) Active Tectonics of the Mediterranean Region: *Geophysical Journal of the Royal Astronomical Society*, v. 30, no. 2, p. 109-185.
- Martinod, J., Hatzfeld, D., Brun, J.P., Davy, P., and Gautier, P.** (2000) Continental collision, gravity spreading, and kinematics of Aegea and Anatolia. *Tectonics*, 19, 2, 290-299.
- Milani, E.J., Davison, I.,** (1988) Basement control and transfer tectonics in the Reconcavo–Tucano–Jatoba rift, Northeast Brazil. *Tectonophysics* 154, 41–70.
- Morley, C.K.,** (1988) Variable extension in Lake Tanganyika. *Tectonics* 7, 785–801
- Morley, C.K., Nelson, R.A., Patton, T.L., Munn, S.G.,** (1990) Transfer zones in the East African Rift System and their relevance to hydrocarbon exploration in rifts. *American Association of Petroleum Geology* 74, 1234–1253.
- Moustafa, A.R.** (1996) Internal structure and deformation of an accommodation zone in the northern part of the Suez rift. *Journal of Structural Geology* 18, 93–107
- Nelson, R.A., Patton, T.L., Morley, C.K.** (1992) Rift–segment interaction and its relation to hydrocarbon exploration in continental rift systems. *American Association of Petroleum Geology Bulletin* 76, 1153–1169.
- Ori, G.G.** (1989) Geologic history of the extensional basin of the Gulf of Corinth (Miocene–Pleistocene), Greece. *Geology*, 17, 918-921.
- Peacock, D. C. P., and Sanderson, D. J.** (1991) Displacements, segment linkage and relay ramps in normal fault zones: *Journal of Structural Geology*, v. 13, no. 6, p. 721-733.

Pirazzoli, P.A., Stiros, S.C., Fontugne, M. & Arnold, M. (2004) Holocene and Quaternary uplift in the central part of the southern coast of the Corinth Gulf (Greece). *Mar. Geol.*, 212, 35–44.

Pollard, D.D., Aydin, A. (1988) Progress in understanding jointing over the past century. *Geological Society of America Bulletin* 100, 1181–1204.

Rohais, S., Joannin, S., Colin, J.P., Suc, J.P., Guillocheau, F. & Eechard, R. (2007b) Age and environmental evolution of the syn-rift fill of the southern coast of the gulf of Corinth (Akrata-Derveni region, Greece). *Bull. Soc. Geol. France*, 178, 231–243.

Sherman, S.I. (1978) Faults of the Baikal rift zone. *Tectonophysics* 45, 31–39

Sorel, D. (2000) A Pleistocene and still-active detachment fault and the origin of the Corinth-Patras rift, Greece. *Geology*, 28, 83-86.

Stefatos, A., Papatheodorou, G., Ferentinos, G., Leeder, M., and Collier, R. (2002) Seismic reflection imaging of active offshore faults in the Gulf of Corinth: their seismotectonic significance: *Basin Research*, v. 14, no. 4, p. 487-502.

Walsh, J.J., Watterson, J. (1991) Geometric and kinematic coherence and scale effects in normal fault systems, in: Roberts, A.M., Yelding, G., Freeman, B. (Eds.), *The Geometry of Normal Faults Geological Society of London Special Publication*, 56, pp. 193–206.

Westaway, R. (2002) The Quaternary evolution of the Gulf of Corinth, central Greece: coupling between surface processes and flow in the lower continental crust.

Yaltrak, C., Alpar, B., and Yüce, H. (1998) Tectonic elements controlling the evolution of the Gulf of Saros (northeastern Aegean Sea, Turkey). *Tectonophysics*, 300, 227–248.